DISTAL RENAL TUBULAR ACIDOSIS DEVELOPMENTS IN ITS DIAGNOSIS AND PATHOPHYSIOLOGY

by

Stephen Benedict Walsh

A Thesis submitted for the degree of Doctor of Philosophy

July 2009

Nephrology and Physiology
University College London

Dedication

To my dear friend

Rosalind Wedgwood.

We all miss you so very much.

Abstract

This thesis describes two groups of experiments, both relating to the condition of distal renal tubular acidosis (dRTA).

In the first, an alternative diagnostic test of dRTA to the 'gold standard' short ammonium chloride (NH_4Cl) test was assessed. This was achieved by the simultaneous oral administration of the diuretic furosemide and the mineralocorticoid fludrocortisone to increase distal sodium delivery and α-intercalated cell proton secretion. I evaluated 11 control subjects and 10 patients with known dRTA by giving oral NH_4Cl or furosemide/fludrocortisone in random order on separate days. 3 subjects were unable to complete the study due to vomiting after the NH_4Cl, however there were no adverse effects with furosemide/fludrocortisone administration. The urine pH decreased to less than 5.3 in the controls with both tests, whereas no patients were able to lower their urine pH below 5.3 with either test. The simultaneous administration of furosemide/fludrocortisone proved to be an easy, effective and well-tolerated alternative to the standard NH_4Cl test for the diagnosis of dRTA.

The second group were laboratory-based molecular physiology experiments. Anion exchanger 1 (AE1) mediates electroneutral anion exchange across cell membranes. It is the most abundant protein in the red cell membrane, but is also found in the basolateral membrane of renal α-intercalated cells, where it is required for urinary acidification. Point mutations have been described that convert the red cell AE1 into a cation conductance. AE1 mutations can also cause hereditary dRTA. I investigated the properties of four dRTA associated AE1 mutations (R586H, G609R, S613F and G701D) by heterologous expression in *Xenopus Laevis* oocytes. These mutants proved to be functional anion exchangers, unlike the red cell mutants, but also demonstrated a cation 'leak'. I found a very large leak property in the G701D mutant, which is prevalent in SE Asia. I hypothesised that this property might confer a

survival advantage. I characterised three other AR dRTA-associated AE1 mutants found in SE Asia, S773P, Δ850 and A858D via similar transport experiments in AE1-expressing Xenopus oocytes. These three SE Asian mutants also had cation leaks of similar magnitude to that seen in G701D, a property that distinguishes them as a discrete group. The clustering of these cation-leaky AE1 mutations to malarious areas of SE Asia suggests that they may confer malaria resistance.

Acknowledgements

Firstly, I should like to thank my supervisor, Professor Robert Unwin, for his unwavering support when all hope of starting research seemed to be flickering out, for his vision, his patient guidance and not least for his bright idea of sending me to the south of France for two years.

I would also like to thank my good friends and supervisors in Nice, Franck Borgese and Helene Guizouarn, for patiently teaching me pretty much everything I know about laboratory physiology specifically and laboratory science generally. The practical help of Nicole 'Chef' Gabillat (in all matters) was absolutely invaluable. The general help and good cheer of the physiology group in the *Laboratoire de Physiologie des Membranes Cellulaires* in the Universitié de Nice, especially Dr Olivier Soriani, will be sorely missed, particularly at lunchtime.

The advice that David Shirley provided for the scholarly and statistical work on urinary acidification was detailed, relentless and delivered with wit and brio. It proved absolutely crucial and we all hope that he makes a full and speedy recovery in order to start terrorising the Bishops Castle tennis club once more.

Thanks must also go to Ashley Toye, for his interest and support in the AE1 work, his kind gifts of a number of antibodies and his detailed 'scientific' tour of Bristol.

The ERA/EDTA awarded my European research fellowship, which was very much appreciated and enabled me to carry out this work.

Special thanks to Professor John Cunningham, whose help and interest ensured that I was able to complete this wonderful period of research at all and to Professor Oliver Wrong, for all his detailed advice, whose work has loomed large over this entire field, and who is an inspiration to us all.

Abbreviations

AE1	Anion exchanger 1
ATP	Adenosine triphosphate
BMA	Biotin maleimide
CA2	Carbonic anhydrase 2
CCD	Cortical collecting duct
DEPC	Diethyl pyrocarbonate
DIDS	4,4-diisothiocyano-2,2-disulfonic stilbene
DNDS	4,4-dinitrostilbene-2,2-disulfonate
dRTA	Distal renal tubular acidosis
eAE1	Erythrocyte AE1 isoform
ECM	Extracellular matrix
EDTA	Ethylene diamide tetraacetic acid
EMA	Eosinyl-5-malemide
ENaC	Epithelial sodium (Na) channel
ER	Endoplasmic reticulum
G6PD deficiency	Glucose-6-phosphate dehydrogenase deficiency
GFR	Glomerular filtration rate
GPA	Glycophorin A
GPB	Glycophorin B
GPC	Glycophorin C
H2DIDS	4,4-diisothiocyanodihydrostilbene-2,2-disulfonic acid
HbE disease	Haemoglobin E disease
HEK-293 cells	Human embryonic kidney 293 cells
HEPES	4-(2-hydroxyethyl)-1-piperazineethanesulfonic acid
HS	Hereditary spherocytosis
HSt	Hereditary stomatocytosis
IMCD cells	Inner medullary collecting duct cells
kAE1	Kidney AE1 isoform
LLC-PK1 cells	LLC-porcine kidney 1 cells
LYIA	Lucifer yellow iodoacetamide
MBS	Modified Barth's solution

MDCK cells	Madin Darby canine kidney cells
MOPS	3-(N-morpholino) propanesulphonic acid
MSTEA	2-(aminoethyl)-methanethiosulphonate
MTSES	2-(sulphonatoethyl)-methanethiosulphonate
NEM	N-ethylmalemide
NMDG	N-methyl-D glucamine
NPP	New permeabilty pathway
NPPB	5-nitro2-(3-phenylpropylamino) benzoic acid
pCMBS	p-chloromercurybenzene sulphonate
PCR	Polymerase chain reaction
PNG	Papua New Guinea
pRTA	Proximal renal tubular acidosis
RCV	Relative cell volume
RhAG	Rhesus-associated glycoprotein
RVD	Regulatory volume decrease
SAO	Southeast Asian ovalocytosis
SDS	Sodium dodecyl sulfate
SDS-PAGE	Sodium dodecyl sulfate polyacramide gel electrophoresis
SITS	4-acetomido-4'isothiocyanato-stilbene-2,2'disulfonic acid
SNP	Single nucleotide polymorphism
tAE1	Trout AE1
TBE buffer	Tris-borate-EDTA buffer
TCC	Transport-related conformation change
TM segments	Transmembrane segments
v H+ATPase	Vacuolar H+ATPase
W-B treatment	WRK and borohydride treatment
Wrb antibodies	Anti-Wright b antibodies
WRK	Woodward's reagent K
α-IC	α-intercalated cell

Publications

Simultaneous Furosemide And Fludrocortisone: An Alternative To Ammonium Chloride Assessment Of Urinary Acidification.
Stephen Walsh; David Shirley; Oliver Wrong; Robert Unwin
Kidney International 2007 Jun;71 (12):1310-6.

Cation transport activity of anion exchanger 1 (AE1) mutations found in inherited distal renal tubular acidosis (dRTA): structure-function implications for AE1
Stephen B Walsh, Franck Borgese, Nicole Gabillat, Robert John Unwin, and Helene Guizouarn
Am J Physiol Renal Physiol 2008 Jun; 295 (2): F343-F350

Southeast Asian AE1 associated renal tubular acidosis: Cation leak is a class effect
Stephen Walsh, Franck Borgese, Nicole Gabillat, Helene Guizouarn
Biochem. Biophys. Res. Commun 2009 15 May; 382 (4): 668-72

Contents

1. Introduction 18
1.1 Scope of the Introduction 18
1.2 History and nomenclature of RTA 19
1.2.1 Definition 19
1.2.1.1 Distal renal tubular acidosis (dRTA, type 1 RTA), ... 19
1.2.1.2 Proximal renal tubular acidosis (pRTA, type 2 RTA) 20
1.2.1.3 Type 3 RTA 21
1.2.1.4 Type 4 RTA 22
1.2.2 History 22
1.2.3 Conclusion 24
1.3 Testing for dRTA 25
1.3.1 History 25
1.3.1.1 Early acid load testing 25
1.3.1.2 The short ammonium chloride test 25
1.3.1.3 Sodium sulfate testing 26
1.3.1.4 Urinary pCO2 26
1.3.1.5 Furosemide testing 26
1.3.2 Conclusions 27
1.4 Potassium wasting and dRTA 27
1.4.1 Association 27
1.4.2 Theories 28
1.4.3 Conclusions 30
1.5 The α-intercalated cell 31
1.5.1 Control of pH in the Collecting Duct 31
1.5.2 The intercalated cells 31
1.5.2.1 vH^+ATPases 32
1.5.2.2 Anion Exchangers-AE1 32
1.5.2.3 Anion Exchangers-Pendrin 33
1.5.3 Intercalated cell plasticity and Hensin 34
1.5.4 Conclusions 35
1.6 AE1 structure and function 36
1.6.1 AE1 Functions 36
1.6.1.1 Anion exchange 36

1.6.1.2 Anion Proton Cotransport 37
1.6.1.3 Red Cell Membrane Structure 37
1.6.1.4 Metabolon with carbonic anhydrase 2 40
1.6.1.5 Red Cell Senescence 40
1.6.2 Structure 40
1.6.2.1 Secondary Structure 40
1.6.2.1.1 The N-terminal cytoplasmic domain 41
1.6.2.1.2 Topology of the AE1 membrane domain 43
1.6.2.1.3 The First Eight TM Segments 44
1.6.2.1.4 The Remaining TM Segments 46
1.6.3 Structure/Function 48
1.6.3.1 Proton binding sites 48
1.6.3.2 Eosinyl-5-malemide probing 50
1.6.3.3 Histidine modification 51
1.6.3.4 Evidence for anion access channels in AE1 52
1.6.3.4.1 External Access Channel 52
1.6.3.4.2 Cytoplasmic Access Channel 54
1.6.4 Conclusions 54
1.7 AE1 and the α-intercalated cell 56
1.7.1 AE1 and the intercalated cell 57
1.7.1.1 AE1 regions important for intracellular targeting (the C-terminal tail) 57
1.7.2 Autosomal dominant dRTA 58
1.7.3 Autosomal recessive dRTA 59
1.7.4 Molecular mechanisms of AD dRTA 60
1.7.5 Molecular Mechanisms of AR dRTA 63
1.7.6 Conclusions 64
1.8 AE1 and the red cell 64
1.8.1 AE1 and the red cell 64
1.8.2 AE1 interaction with Glycophorin A 65
1.8.3 Haemoglobin 66
1.8.4 Membrane skeletal proteins 67
1.8.5 The Rh Complex 67
1.8.6 AE1 and red cell disease 71

1.8.6.1 Hereditary Spherocytosis 71
1.8.6.2 Hereditary Stomatocytosis 72
1.8.6.3 Southeast Asian Ovalocytosis 74
1.8.7 Conclusions 77
1.9 AE1 and the cation leak 78
1.9.1 AE1 channel permeability and cell volume regulation 78
1.9.2 AE1 channel activity in humans 81
1.9.3 Conclusions 83
1.10 Hypothesis 83
2. General Methods 85
2.1 Introduction 85
2.2 DNA synthesis 85
2.3 Agarose gel electrophoresis 86
2.4 Buffer solutions 86
2.5 Xenopus oocyte harvesting 86
2.6 Oocyte injection 87
2.7 Western blot of oocyte membrane proteins 87
2.8 Intracellular Cation Measurements 88
2.9 Intracellular pH measurements 88
3. Novel Clinical Assessment of Urinary Acidification 91
3.1 Introduction 91
3.2 Aims 94
3.3 Methods and Materials 95
3.3.1 Subject selection 95
3.3.2 The NH_4Cl protocol 95
3.3.3 The furosemide/fludrocortisone protocol 95
3.3.4 Urine collection and measurement 96
3.3.5 Ethical approval 96
3.3.6 Statistical analysis 96
3.4 Results 97
3.4.1 Urinary acidification 98
3.4.2 Ammonium excretion 98
3.4.3 Titratable acidity 99
3.4.4 Urine flow rate and electrolyte excretion 103

3.5 Conclusion 106
3.5.1 Efficacy 106
3.5.2 Physiological parameters 106
3.5.3 Adverse effects 108
3.5.4 Convenience 108
3.5.5 Physiologic basis 108
3.5.6 Conclusion 109
4. The Cation Leak Activity of dRTA Associated AE1 Mutants 111
4.1 Introduction 111
4.2 Aims 113
4.3 Methods and materials 113
4.3.1 Xenopus oocyte harvesting 113
4.3.2 Oocyte injection 113
4.3.3 Plasmid and DNA construction 114
4.3.4 Western blot 114
4.3.5 Chloride influx experiments 114
4.3.6 Intracellular pH measurements 115
4.3.7 Rubidium influx experiments 115
4.3.8 Intracellular cation measurements 116
4.3.9 Electrophysiology experiments 116
4.3.10 Chemicals 119
4.4 Results 120
4.4.1 Western blot results 120
4.4.2 Chloride influx experiments 120
4.4.3 Intracellular pH measurements 120
4.4.4 Rubidium uptake experiments 121
4.4.5 Pharmacological blockade 124
4.4.6 Intracellular cations 124
4.4.7 Oocyte electrophysiology 126
4.4.8 Oocytes co-expressing AE1 and wildtype AE1 131
4.5 Conclusions 133
4.5.1 Structure function implications 133
4.5.2 Cation leak behaviour and the erythrocyte in AE1-associated dRTA 137

4.5.3 Cation leaky AE1 in the α-intercalated cell in dRTA 137
4.5.4 Hypokalaemia 138
4.5.5 Disease distribution 138
5. The Cation Leak Activity of Other Southeast dRTA Associated AE1 mutants 140
5.1 Introduction 140
5.2 Aims 141
5.3 Methods and materials 142
5.3.1 Xenopus oocyte harvesting 142
5.3.2 Oocyte injection 142
5.3.3 Plasmid and DNA construction 142
5.3.4 Western blot 143
5.3.5 Lithium influx 143
5.3.6 Intracellular cation measurements 143
5.3.7 Intracellular pH measurements 144
5.3.8 Chemicals 144
5.4 Results 145
5.4.1 Western Blot 145
5.4.2 Anion Transport; 145
5.4.2.1 Intracellular pH recordings 145
5.4.3 Cation Transport; 148
5.4.3.1 Lithium influx 148
5.4.3.2 Intracellular cation contents 148
5.5 Conclusions 151
5.5.1 Structure function implications 151
5.5.2 Large cation leak a class effect of SE Asian dRTA-associated AE1 154
6. Discussion 156
6.1 Testing Urinary Acidification 156
6.1.1 How good is it? 156
6.1.1.1 Walter 156
6.1.1.2 Viljoen 156
6.1.1.3 Audit 157
6.1.1.4 Potassium excretion in AE1-associated dRTA 160

6.2 Molecular structure/function implications 160
6.2.1 Phylogeny 160
6.2.2 Evidence for wt AE1 acting as a cation transporter 163
6.3 Malaria resistance hypothesis 165
6.3.1 Epidemiology 165
6.3.1.1 Malaria in Thailand 165
6.3.1.2 Lao-thai ethnic distribution 166
6.3.1.3 HbE and Thalassemia in Thailand 168
6.3.1.4 Endemic dRTA in NE Thailand 169
6.3.2 Founder effect 169
6.3.3 Similarity to SAO 169
6.3.4 Red cell cation leaks in Thalassaemias and Haemoglobinopathies 170
6.3.5 Hypothesis - Do red cell cation leaks protect against severe malaria? 170
6.4 Alternative speculative mechanisms 175
6.4.1 Accelerated Red Cell 'Apoptosis' 175
6.4.2 ATP depletion 176
6.4.3 Low intra-erythrocytic potassium inhibiting parasite growth 177
6.5 High sodium/low potassium erythrocyte 177
6.5.1.1 Animal resistance 177
6.5.1.2 Babesia 178
6.5.2 Possible further avenues of investigation 178
7. Appendix 1: Further experience with the Furosemide and Fludrocortisone test 179
7.1 Protocol for the furosemide and fludrocortisone test 180
8. Appendix 2: Potassium Excretion in AE1 and non-AE1 dRTA patients 182
9. References 184

Figures

Figure 1-1 A cartoon of the alpha-intercalated cell.....39
Figure 1-2 Schematic representation of the secondary structure of AE1. 42
Figure 1-3 3D map of the dimeric transport domain of the Band 3 protein.....45
Figure 1-4 A cartoon of the Rhesus complex, showing ankyrin binding to the spectrin skeleton and supporting the AE1 dimer/oligomer. 70
Figure 1-5 A blood film from a patient with hereditary stomatocytosis. 73
Figure 1-6 Blood films from three of the original family described with SAO by Honig et al in 1971. 76
Figure 2-1 An example intracellular pH trace for an oocyte expressing wt AE1. 90
Figure 3-1 A cartoon of the mechanism of action of the furosemide and fludrocortisone test. 93
Figure 3-2 Time-course of changes in urine pH after the NH_4Cl and furosemide/fludrocortisone tests 100
Figure 3-3 Baseline to minimum urinary pH achieved in individual subjects undergoing the NH_4Cl and furosemide/fludrocortisone tests. 101
Figure 3-4 Individual sequential urine pH measurements in control subjects. 102
Figure 3-5 Electrolyte excretion and urine flow rate 104
Figure 3-6 Ammonium and titratable acid excretion. 105
Figure 4-1 A representative western-blot of an oocyte plasma membrane probed with anti-AE1 antibodies (BRIC170). 122
Figure 4-2 Composite figure of anion transport experiments 123
Figure 4-3 Composite figure of $^{86}Rb^{+}$ uptake experiments. 128
Figure 4-4 Intracellular cation contents. 129
Figure 4-5 Composite figure of electrophysiology experiments. 130
Figure 4-6 Further $^{86}Rb^{+}$ uptake in G701D expressing oocytes with and without GPA. 132
Figure 4-7 Helical wheel model of the hypothetical α-helix extending from the bottom of TM9 to residue 692. 136
Figure 5-1 A representative western blot of an oocyte membrane probed with anti-AE1 antibodies (BRIC170). 146

Figure 5-2 Composite figure of intracellular pH data. 147
Figure 5-3 Representative experiment of ouabain- and bumetanide-resistant Li influx 149
Figure 5-4 Composite figure of intracellular cation content measurements. 150
Figure 5-5 Distribution of AE1 mutations in SE Asia. 153
Figure 6-1 Schematic showing minimum pHs of individuals undergoing urinary acidification with control/sham, ammonium chloride, furosemide alone and furosemide and fludrocortisone 158
Figure 6-2 Paired pre-test and nadir urine pH values. 159
Figure 6-3 Unrooted phylogenetic tree of Cl/HCO_3^- exchangers 162
Figure 6-4 Map of Thailand, showing Isan (northeast Thailand) in red. 167
Figure 6-5 Predicted changes in selected homeostatic variables of P falciparum–infected red cells during the asexual reproduction cycle of the parasite. 173
Figure 6-6 A cartoon of the proposed events in malarial asexual reproduction in infected erythrocytes 174
Figure 7-1 Composite graph of urinary pH data for patients routinely receiving urinary acidification testing 181
Figure 8-1 Graphs showing potassium excretion. 183

Tables

Table 3-1 Biochemical parameters for patients with dRTA who completed the study 97
Table 4-1 Intracellular cation content after incubation in NMDG 125
Table 4-2 Measurements of resting membrane potential as a function of the ionic composition of the extracellular medium 127

1. Introduction

1.1 Scope of the Introduction

Broadly speaking this thesis could be said to address the physiology and pathophysiology of distal sodium and potassium handling in the syndrome of distal renal tubular acidosis (dRTA).

From its inception the project set out to address these subjects in specific and very different ways, with quite different approaches and goals.

The specific questions that I sought to answer were;

1) “Can increased delivery of sodium to the distal nephron be used to reliably assess distal urinary acidification in dRTA and health?”

2) “Can the urinary potassium wasting observed in inherited dRTA be attributed, in part, to a property of the mutated transport protein that causes it?”

During the course of my studies, the second question supplied the most interesting data, and my work focussed more on the transport protein in question, the Anion Exchanger 1 (AE1 or band 3) its ability to function as a cation channel like transporter when mutated and on an evolving hypothesis about the possible positive advantage this may have conferred to heterozygotes with these mutations.

My introduction attempts to set the scene for this work at the time that it was started. Unfortunately this involves reviewing a number of fairly disparate subjects, which are all somewhat esoteric. Firstly I’ll review the renal tubular acidoses, the history of their characterisation and classification and define dRTA and the syndrome of incomplete dRTA. I will then review the various techniques used to test distal urinary acidification in order to confirm incomplete dRTA. As this relates directly to sodium wasting in dRTA, I will

then outline the models and theories of sodium and potassium loss in dRTA. I will next review the important work relating to the pH regulatory function of the cortical collecting duct, and the intercalated cells in particular. This will be followed by a detailed examination of the work concerning the structure function relationship of AE1, AE1 function and trafficking in the α-intercalated cell and in the erythrocyte, and finally the work elucidating the cation leak property of wildtype and mutant AE1.
The three experimental chapters will include discussions of my findings in relation to current literature and in the discussion I will attempt to draw these together and outline where I think this work leads to.

1.2 History and nomenclature of RTA

1.2.1 Definition

The renal tubular acidoses are a collection of syndromes characterised by impairment of the ability of the renal tubules to acidify the urine, which is not due to an impairment of glomerular function.

1.2.1.1 Distal renal tubular acidosis (dRTA, type 1 RTA),

Distal renal tubular acidosis the focus of this thesis, is the classical and commonest form, and involves a failure of acid secretion in the distal nephron, more specifically by the acid secreting α-intercalated cells of the distal convoluted tubule and the cortical collecting duct.

It is characterised by:

- An inability to acidify the urine to a pH of less than 5.3

Which can lead to:

- Variable metabolic acidosis
- Osteomalacia and/or bone demineralisation subsequent to the acidosis

- Nephrocalcinosis (calcium salt deposition in renal parenchyma) and/or renal calculi due to high calcium, low citrate, alkaline urine
- Variable hypokalemia due to urinary potassium wasting
- Variable salt-losing nephropathy due to urinary sodium wasting

It has a number of causes, primary and secondary:
Primary:

- Mutations of the anion exchanger AE1, normally present on the basolateral surface of the α-intercalated cell[1].
- Mutations of the a4 or B1 subunit of the v H^+ATPase, normally present on the apical surface of the α-intercalated cell [2].

Secondary:

- In association with autoimmune disease, notably Sjögren's syndrome [3], but also systemic lupus erythematosus [4], rheumatoid arthritis [5], autoimmune thyroid disease [6], primary biliary cirrhosis [7] and hypergammaglobulinemia [8]
- Due to a number of toxins, such as ifosphamide [9], toluene [10], lithium carbonate [11] and amphotericin B [12]
- Nephrocalcinosis [13](which can cause, as well as be caused by dRTA, presumably by mechanical disruption of the cortical collecting tubule)
- Sickle cell disease [14]
- Renal transplantation [15] (probably a toxic effect of calcineurin inhibitors [16])
- Chronic urinary tract obstruction [17]
- Liver cirrhosis [18]

1.2.1.2 Proximal renal tubular acidosis (pRTA, type 2 RTA)

Proximal renal tubular acidosis is a defect of the proximal nephron, characterised by impairment of the ability of the proximal tubule to absorb

bicarbonate from the tubular lumen. It almost always accompanies the so-called Fanconi syndrome of proximal tubular dysfunction characterised by aminoaciduria, phosphaturia, glycosuria, uricosuria and tubular proteinuria. As the defect is one of bicarbonate reabsorbtion, there will be bicarbonaturia, and if untreated, as the plasma bicarbonate falls, it will eventually meet the lowered bicarbonate reabsorbtion threshold, and then the bicarbonate will all be reabsorbed, and the urine will acidify normally again. It is associated with bone demineralisation, due to the acidosis and urinary phosphate wasting.

Causes include inherited and acquired causes.

Inherited:

- Cystinosis [19]
- Galactosemia [20]
- Hereditary fructose intolerance [21]
- Lowe syndrome [22]
- Tyrosinemia
- Type 1 glycogen storage disease (von Gierke's disease) [23]
- Wilson’s disease [24]

Acquired:

- Amyloid [25]
- Myeloma [26]
- Paroxysmal nocturnal hemoglobinuria
- Toxins, such as nucleotide and nucleoside analogues (especially adefovir) and reverse transcriptase inhibitors [27] used for HIV, ifosphamide [28], lead and cadmium [29].

1.2.1.3 Type 3 RTA

Type 3 RTA originally described a mixed distal and proximal RTA of infancy, which may, in retrospect, have been a severe dRTA (q.v.). Now Type 3 RTA,

if used at all, is used to describe a hereditary defect in Carbonic Anhydrase 2, which is found in distal nephron α-intercalated cells, proximal tubular cells and bone. As a result it causes both proximal and distal RTA, as well as osteopetrosis and cerebral calcification with subsequent mental impairment [30, 31]. Approximately 70% of cases are found in the Magreb region of North Africa, probably due to high rates of consanguinity there [32].

1.2.1.4 Type 4 RTA

Type 4 RTA is characterised by hyperkalemia, due either to hypoaldosteronism, or resistance to aldosterone. There is probably a defect in ammonium excretion in the inner medulla [33], but measured urinary pH is usually normal. The commonest cause is in moderate renal impairment, usually secondary to diabetic nephropathy.

1.2.2 History

The first description of what would later be termed renal tubular acidosis was by an English paediatrician, Reginald Lightwood, whose report was an abstract from a meeting [34] in 1936 that did not mention acidosis, but a “calcium infarction of the kidneys” in infants who died of a dehydrating, salt-wasting disease.

Later the same year, Butler, Wilson and Farber of the Massachusetts General Hospital described "Dehydration and acidosis with calcification of renal tubules" [13]. The paper was chiefly concerned with infants, but the appendices described two adults, one of whom had recently had a parathyroid adenoma removed for primary hyperparathyroidism, the first report of RTA and nephrocalcinosis secondary to hypercalcaemic renal damage.

Subsequently, Lightwood, Payne and Black added acidosis and a urinary acidification defect to the syndrome suffered by the sick infants with

Nephrocalcinosis [35]. In this paper, and others appearing at the same time, including those from Stapleton [36, 37] ,it was acknowledged that hypercalciuria was often a feature of these patients.

New cases of the so-called ‘Lightwood syndrome’ failed to appear through the 1950s-1960s, and it was also reported that the urinary acidification defect tended to disappear, as affected children grew older [38]. This finding raised the possibility that its cause had been removed from the environment, vitamin D or calcium excess, or mercury in teething powders were suggested. The Lightwood syndrome came to be regarded as an unexplained historic accident of the forties that no longer existed, and the interest of tubular physicians tended to shift more to older children, where renal acidosis with a urinary acidification defect seemed to be a commoner and more persistent problem.

Albright, a colleague of Butler’s at the Massachusetts General Hospital described clearly what we would now term ‘distal renal tubular acidosis’ in his book with Reifenstein [39], detailing the resultant bone disease and nephrocalcinosis and the role of alkali treatment, and labelling it as a form of "tubular insufficiency without glomerular insufficiency"; he attributed the acidosis to renal tubular inability to make ammonia and an acid urine.

Albright did not use the term ‘renal tubular acidosis’, the term was probably first used by Pines and Mudge [40] in 1951 (although one of the adults that they reported had a ureterocolic anastomosis, and so a tubular defect was an unlikely explanation for their acidosis).

Wrong and Davies introduced the concept of an acidification defect in the absence of a systemic acidosis, the so-called ‘incomplete syndrome’, and also quantified the threshold pH that patients with a distal renal tubular acidosis were unable to acidify their urine below; 5.3 [41].

Although acidosis was recognised in the Fanconi syndrome, it was not initially described as a form of renal tubular acidosis, as it was rare and features other than the acidosis dominated the clinical picture. The acidosis was attributed to

a loss of base in the urine, either bicarbonate, or a base that would have been converted to bicarbonate if it were retained. The terms ‘proximal renal tubular acidosis’ and ‘distal renal tubular acidosis’ were coined by Rodriguez-Soriano and colleagues in their classification published in 1969 [42].

The nomenclature was confused somewhat when Curtis Morris introduced a numerical system for their classification [43]. Morris labelled distal or classical RTA as "Type1" RTA, proximal RTA as "Type 2", and designated "Type 3"as a paediatric form of RTA that was a mixture of Types 1 and 2, which most nephrologists regarded as a severe form of Type 1, requiring rather more alkali than most Type 1 patients.

Morris’ ‘Type 3’ disappeared from the clinical spectrum, later to be replaced by the different carbonic anhydrase deficiency (see above), but its existence meant that hyperkalemic renal tubular acidosis had to be designated ‘Type 4’.

As this is due to hyperaldosteronism, the urine pH drops appropriately in response to an acid load and renal insufficiency is a notable feature of the condition, thus there is a good argument to be made that it shouldn’t have been classified as a renal tubular acidosis at all.

1.2.3 Conclusion

- Distal RTA (dRTA) is a syndrome comprising an inability to acidify the urine to a pH of less than 5.3, variable metabolic acidosis, nephrocalcinosis/renal stone formation, osteomalacia and variable hypokalemia and salt wasting.

- The numeric classification of the renal tubular acidoses is confusing and unhelpful.

1.3 Testing for dRTA

1.3.1 History

In those patients with a metabolic acidosis and near normal GFR, a diagnosis of dRTA can be made when urine pH is consistently >5.3 [41].

There is a diagnostic difficulty if the acidification defect is not sufficient to provoke a systemic acidosis, the so-called 'incomplete syndrome of RTA', (described by Wrong and Davies [41]) leaving the clinician unable to tell whether a measured alkaline urine is appropriate or not. This conundrum required a test of urinary acidification, to demonstrate the ability, or not, of the kidney to acidify the urine in the face of an appropriate stressor.

1.3.1.1 Early acid load testing

Early studies using hydrochloric acid or ammonium chloride, as an acid load to examine the renal response to an acidifying stimulus had been done [44-47], but these had lasted five or more days, and were clearly too time consuming for routine use.

1.3.1.2 The short ammonium chloride test

Wrong and Davies, who described the 'incomplete syndrome' of dRTA in 1959, published an account in the same paper, of the short ammonium chloride test, in which oral ammonium chloride (NH_4Cl) was administered and serial urinary pHs measured, in order to provoke a systemic acidosis, and thus reveal a previously obscured acidification defect [41]. The authors demonstrated consistent lowering of plasma pH and total CO_2 with this protocol, in normal subjects, and a failure to acidify urine below a pH of 5.3 in those with dRTA. It has subsequently been adopted internationally as the 'gold standard' diagnostic test for dRTA. However, although the test lasts only 8 hours and does not require blood testing, it can be unpleasant for some patients; because gastric irritation, nausea and vomiting are common.

1.3.1.3 Sodium sulfate testing

In 1955, Schwartz *et al* [48] had described urinary acidification in response to intravenous infusion of pH-neutral sodium sulfate. The mechanism was believed to be indirect and crucially different from the provocation of a systemic acidosis by NH_4Cl, as it involved an increase in the delivery of a non-reabsorbed anion to the distal nephron, where it was thought to increase the lumen-negative electrical gradient favouring increased proton (H^+) secretion. It produced a very acid urine, as low as 4.0 [49], whether it produces a lower urinary pH than a systemic acidosis does in dRTA has not been established, but there is a suggestion that it might [50, 51]. This uncertainty, and the inconvenience of having to administer sodium sulfate intravenously, has meant that it is used infrequently, if at all.

1.3.1.4 Urinary pCO2

In 1974, Halperin et al [52], in a work extending earlier observations by Pak Poy and Wrong [53], described the use of the urine pCO_2 tension to test for dRTA, noting that the urine pCO_2 tension was greater in the urine than the blood in normal subjects (ie the Urine-Blood pCO_2 ratio, or U-B pCO_2 was high), but approximately similar in those with dRTA. Concerns were voiced about the specificity of the low urinary pCO_2 for dRTA, as low pCO_2 tensions had been observed in pRTA with Fanconi's syndrome [53] as well as with advanced renal failure [54].

1.3.1.5 Furosemide testing

In 1986, Batlle [55] described a variation of the sodium sulfate test using oral furosemide to increase distal nephron sodium delivery and enhance sodium reabsorbtion, thus increasing lumen negativity and stimulating H^+ secretion. Urine pH changes in response to an increased distal delivery of sodium have been reported to be greater in normal subjects when they are sodium depleted [56] or following prior administration of a mineralocorticoid [57]. Clinical experience with furosemide alone or with mineralocorticoid the night before proved it to be not as specific as hoped, later empiric studies underlined this [58].

1.3.2 Conclusions

- Testing urinary acidification is only necessary to exclude or confirm incomplete dRTA.
- The direct provocation of a systemic acidosis with oral ammonium chloride remains the gold standard test, but it is unpleasant and time consuming to perform.
- Measurement of the urine/blood ratio of pCO_2 is probably unreliable.
- Increasing the distal sodium delivery, with intravenous sodium sulfate or oral furosemide, may be invasive and is also unreliable.

1.4 Potassium wasting and dRTA

1.4.1 Association

That hypokalaemia occurs in dRTA secondary to urinary potassium wasting, is an observation that was made early in the description of the disease [39, 40, 59, 60]. The inference was made that the hypokalemia was a reversible consequence of the acidification defect, based on the observation that the correction of the systemic acidosis with alkali therapy leads to a reduction in the urinary potassium loss and therefore a resolution of the hypokalaemia [39, 40, 61].

Hypokalaemia can be observed in both dRTA and proximal RTA (pRTA) [59], but it is a cardinal feature of dRTA. However even in dRTA, the severity of hypokalaemia is not constant. Wrong et al showed that the hypokalaemia of immune related dRTA (chiefly related to Sjögren's syndrome) was significantly more severe than that found in hereditary dRTA from the UK [62].

Hypokalaemia is also a prominent feature of Southeast Asian AE1 associated dRTA, Bruce et al found that the mean serum potassium at presentation in hereditary SE Asian AE1 associated dRTA was 2.7 ± 0.6 mmol/L, compared with an average serum potassium at presentation of 3.6 ± 0.6 mmol/L in patients with occidental hereditary dRTA. Indeed, two of the studied patients presented with hypokalaemic paralysis [63].

1.4.2 Theories

Sartorius and co-workers examined the effect of the prolonged administration of an acid load on renal ion excretion, by the intermittent administration of large amounts of ammonium chloride over the course of 15 days to healthy adult males. They found that the provocation of a systemic acidosis stimulated renal potassium excretion throughout the period of acidosis and also stimulated sodium excretion, which decreased in a stepwise fashion after the first day of acidosis [64]. This was evidence that an acidosis *per se* could cause renal potassium and sodium wasting in healthy kidneys.

Gill et al measured the renal losses of sodium and potassium in 5 patients with dRTA. They found that with dietary sodium deprivation, the dRTA patients were unable to conserve sodium renally and thus became sodium deplete. All the patients had negative potassium balances even with average potassium intakes; these balances persisted during sodium restriction, when aldosterone levels rose, presumably reflecting volume contraction and contributing to urinary potassium loss. However, they found that potassium losses were not dependent on aldosterone, as two patients did not have raised aldosterone levels, and rapid volume expansion with 2 litres of intravenous normal saline did not abolish the potassium loss. Administration of sodium bicarbonate or disodium phosphate reduced the negative potassium balance and abolished hypokalemia. The authors concluded that renal potassium losses in dRTA were due to a failure of H^+ secretion and (as they assumed that H^+ and potassium shared a common permeability) thus potassium losses were increased by an absence of competing protons. [61]

This was compounded by sodium wasting and subsequent secondary hyperaldosteronism, which increases potassium losses by increasing apical cortical collecting duct permeabilities to potassium as well as increasing the basolateral sodium/potassium exchanger.[65]

Sebastian and co-workers however, showed that in two patients with dRTA, correction of their metabolic acidosis did not terminate their urinary potassium losses, which remained abnormally high (>80 mEq/day) despite ongoing hypokalemia. Urinary aldosterone was high in one dRTA subject; normal range in the other, measured plasma volume (determined by ^{181}I albumin dilution) was normal in both cases.[66]

The same authors later studied ten subjects with dRTA, in whom they administered potassium bicarbonate to correct their acidosis, and then sodium restricted them, to reveal any underlying sodium wasting tendency. Half of the patients had impaired sodium conservation; the remainder appeared to have intact sodium conservation. Six patients had an induced water diuresis, all had inappropriately high minimum urinary sodium concentrations and the sodium excretion rates of sodium were flow-dependent. These data suggested strongly that the renal sodium wasting was not exclusively due to impaired Na^+/H^+ exchange in the cortical collecting duct, and nor could it apparently be ascribed just to generalised tubular damage from nephrocalcinosis, as not all of the sodium wasting patients had (radiographically evident) nephrocalcinosis.[67]

A defect in apical proton excretion coupled with urinary potassium losses suggested the apical H^+/K^+-ATPase as a possible candidate for dysfunction, to several authors.[68, 69] This seemed to be supported by the finding of hypokalemic endemic dRTA in Northeast Thailand, which has high environmental levels of vanadium, a H^+/K^+-ATPase inhibitor, and the finding that vanadate could induce an acidification defect in a rat model.[70] However, H^+/K^+-ATPase appears to be far less common in the human distal nephron than in the rat or rabbit [71], and a H^+/K^+-ATPase mutation causing dRTA has yet to be described, unlike AE1 and v H^+-ATPase mutations [72].

1.4.3 Conclusions

- Urinary potassium wasting with subsequent hypokalaemia in dRTA is variable, with some causes being associated with more severe hypokalemia.

- Chronic acidosis can cause healthy kidneys to lose potassium and sodium.

- Sodium depletion and hyperaldosteronism may contribute to urinary potassium wasting but cannot account for all of it. It persists in dRTA after volume correction and normalisation of aldosterone levels.

- Urinary potassium wasting also persists after correction of chronic acidosis.

- No direct evidence has been offered to support the theory that defective proton secretion into the CCD lumen drives potassium into the lumen down an electrochemical gradient.

- H^+/K^+-ATPase deficiency (functional or absolute) remains unlikely, for reasons of its apparent scarcity in the human nephron and the lack of any data showing H^+/K^+-ATPase deficiency causing dRTA in humans.

1.5 The α-intercalated cell

Intercalated cells in the kidney are found alongside the principal cell (the other segment-specific cell type) in the distal convoluted tubule, the connecting tubule and the collecting duct. This section will deal with the evidence concerning their gross structure and function.

1.5.1 Control of pH in the Collecting Duct

Early observations were made that when mammals are administered acidifying salts (e.g. NH_4Cl) they produce acid urine, which is almost free of bicarbonate [73]; but when they are given bicarbonate ($NaHCO_3$), the urine is alkaline and bicarbonate-rich [73-75]. However, fluid collected from the late distal convoluted tubules of either alkalotic or acidotic animals is neither acidic nor alkaline, and does not have an excess or deficit of bicarbonate [73, 75]. Thus, the collecting ducts were implicated in pH and bicarbonate regulation of the urine.

This was confirmed when McKinney *et al* found that rabbits fed NH_4Cl (as an oral acid) had acidic urine and that their isolated cortical collecting ducts, when studied *in vitro*, absorbed bicarbonate. Conversely, animals fed $NaHCO_3$ had alkaline urine and their isolated cortical collecting ducts secreted bicarbonate [76].

The outer medullary collecting duct reabsorbs, but does not secrete, bicarbonate; moreover, reabsorbtion in this nephron segment is unaffected by acid-base status [77-79]. Thus, acid-base responsiveness, and bicarbonate secretion, appears to be confined to the cortical collecting duct.

1.5.2 The intercalated cells

The two major subtypes of mitochondria-rich cells in the turtle bladder, which are ultrastructurally and embryologically equivalent to mammalian intercalated cells, were designated α and β cells by Stetson and Steinmetz [80, 81]. Intercalated cells were identified in mammals, ultrastructurally distinguished

by their high mitochondrial density, dark cytoplasm, cytoplasmic tubulovescicular structures and apical microprojections [82, 83]. These intercalated cells were designated A and B in the rat [83], and α and β in the rabbit [84].

The α-intercalated cell is abundant in the outer medullary collecting duct and is also present in the cortical collecting duct. The β-intercalated cell, by contrast is present only in the cortical collecting duct.

There was, therefore, reason to suspect that α-intercalated cells were responsible for bicarbonate reabsorbtion, and β-intercalated cells for bicarbonate secretion.

1.5.2.1 vH^+ATPases

Expression of vacuolar H^+ATPase (vH^+ATPase) is characteristic of intercalated cells and one isoform of the 56-kd subunit is specific for the intercalated cell [85]. A subset of intercalated cells in the cortical collecting duct and the outer medullary collecting duct of the rat show apical staining for vH^+ATPase (i.e. α-intercalated cells), and another distinct subset show basolateral staining (i.e. β-intercalated cells) [86-89]; although other intermediate staining patterns are seen [86]. Rabbits do not have such well defined basal staining on their β-intercalated cells, although vH^+ATPase has been detected there by ultrastructural immunocytochemistry[90].

Functional studies using the vH^+ATPase inhibitor N-ethylmaleimide (NEM) are consistent with this picture, proton extrusion by rabbit α-intercalated cells is inhibited by apical, though not basolateral, NEM [91].

1.5.2.2 Anion Exchangers-AE1

It was shown that rabbit α-intercalated cells required basolateral chloride/bicarbonate exchange to achieve acidification in isolated perfused tubules, whereas removal of chloride from the perfusing bath inhibited

acidification [92]. Chloride-bicarbonate exchange (studied by measuring intracellular pH) in α-intercalated cells is also inhibited by the disulfonic stilbene anion exchange inhibitor DIDS (4,4-diisothiocyano-2,2-disulfonic stilbene) [92, 93], and the affinity of DIDS binding to these cells is similar to DIDS binding to erythrocytes [94].

Antibodies against the anion exchanger 1 (AE1, the erythrocyte band 3, SLC4A1) molecule show strong immunoreactivity against the basolateral surface of α-intercalated cells, but not at all to β-intercalated cells [86]. I will discuss α-intercalated cell and erythrocyte AE1 expression in more detail in subsequent sections.

1.5.2.3 Anion Exchangers-Pendrin

Schwartz first reported the functional presence of an apical Cl^-/HCO_3 exchanger [95], which was not AE1. It differed in several ways, not least by engaging in Cl^--Cl^- exchange [84] and its resistance to inhibition by luminal stilbenes [96, 97].

Pendrin, or SLC26A4, is an anion exchanger encoded by the gene *pds*, and mutations of which can cause the genetic disorder Pendred syndrome, which is associated with deafness and goitre. Royaux and co-workers found that pendrin was strongly expressed in rat kidney (as well as in the inner ear and thyroid gland), and localised pendrin's expression to those vH^+ATPase-expressing cells present in the cortical collecting duct devoid of AE1 at their basolateral membrane, that is, β-intercalated cells. *pds* knockout mice had no pendrin detectable in their kidneys; while tubules isolated from alkali-loaded wildtype mice secreted bicarbonate, those from alkali-loaded *pds* knockout mice failed to secrete bicarbonate[98]. Solemani *et al* found that pendrin mRNA was also abundant in proximal tubule suspensions from kidney cortex, and that when expressed in HEK-293 cells, pendrin functioned as a Cl^-/HCO_3 exchanger, a Cl^-/OH exchanger and a Cl^-/formate exchanger[99]. This evidence strongly suggested that the β-intercalated cell apical anion exchanger is pendrin. Kim and co-workers found that pendrin is also strongly

expressed at the apical surface of so-called “non-A-non-B” cells in the cortical collecting duct, which are intercalated cells expressing apical vH^+ATPase, but not basolateral AE1 [100].

1.5.3 Intercalated cell plasticity and Hensin

Schwartz and co-workers suggested in their seminal 1985 paper that intercalated cells may be able to reverse their (functional) polarity in adapting to systemic acid-base changes: metabolic acidosis converting β-intercalated cells to α-intercalated cells [95].

Some support for this concept came from the primary culture of rabbit cortical collecting duct cells, immunodissected and sorted into principal or β-intercalated cells. Principal cells remained unchanged in primary culture, whilst cells seeded as 98% β-intercalated cells became (with new generations of cell division) a mixture of α and β-intercalated cells, and principal cells[101, 102]. DNA replication was highest in those cultures seeded with sorted β-intercalated cells, suggesting that they were dividing rapidly and giving rise to other cell types; indeed, surface markers allowed the identification of a single cell dividing mitotically into daughter principal and intercalated cells[101, 102].

Furthermore, in rabbit cortical collecting ducts incubated in acid media, β-intercalated cells displayed reversal of polarity of their H^+ pumps and Cl^-/HCO_3^- exchangers, an effect apparently mediated by an extracellular matrix (ECM) protein termed hensin; anti-hensin antibodies blocked the effect (as did the microtubule inhibitor colchicine), and acid-loading increased hensin deposition in the ECM beneath adapting β-intercalated cells [103].

However, these data need to be interpreted with some caution, as the defining feature of α-intercalated cells, namely basolateral AE1, has not been identified on any of the cells that have developed basolateral Cl^-/HCO_3^- exchange. Weiner and Hamm published data consistent with a Cl^-/HCO_3^- exchanger on the basolateral membrane of rabbit cortical collecting duct β-intercalated cells[104]. Emmons *et al* showed that the majority of rabbit cortical collecting

duct intercalated cells have stilbene insensitive Cl^-/HCO_3^- exchangers on both apical and basolateral surfaces, and that these were the so called γ-intercalated cells (i.e., “non-A-non-B” cells) [96]. It is possible that the effects of hensin and pH adaptation seen by Schwartz, Al-Awqati and co-workers could be the result of recruitment of basolateral Cl^-/HCO_3^- exchangers to the basolateral membrane in γ-intercalated cells; it is difficult to see how this can be refuted without demonstrable immunoreactive AE1 at the basolateral membrane of a hensin-transformed cell.

1.5.4 Conclusions

- Acid responsiveness and bicarbonate secretion is a function of the cortical collecting duct.
- There are two types of intercalated cell in the distal nephron. The α-intercalated cell is found in the outer medullary collecting duct and cortical collecting duct. The β-intercalated cell is only found in the cortical collecting duct.
- α-intercalated cells have apical vH^+ATPase and basolateral AE1.
- β-intercalated cells have basolateral vH^+ATPase and apical pendrin. They have no AE1.
- Some workers have suggested that β-intercalated cells can convert into α-intercalated cells in response to systemic acid base changes. According to their work, β-intercalated cells appear to be able to reverse their polarity, to an extent, but the defining characteristic of α-intercalated cells, namely AE1, has not been detected. Thus conversion of β-intercalated cells to α-intercalated cells remains unproven.

1.6 AE1 structure and function

The anion exchanger 1 protein, or band 3 was discovered on the electrophoretic separation of human red cell plasma membrane proteins, the position on the sodium dodecyl sulphate gel (the third band) giving it its original name, band 3. It was noted at this time that it is the most abundant protein in the cell membrane, comprising approximately 25% of the membrane protein, with about 1.2 x 10^6 copies per cell [105].
It was subsequently found that stilbene disulphonates that specifically inhibit red cell anion exchange covalently labelled the band 3 molecule [106].

The amino acid sequence of murine AE1 was deduced from cDNA in 1985 [107], and the full 911 amino acid sequence of the human erythrocyte AE1 was similarly deduced by Tanner et al in 1988 [108].

This 911 amino acid version of human AE1 is found primarily in red blood cells (but not exclusively, it is also found in atrial tumour cells, for example [109]), a truncated form, known as kAE1, produced by an alternative splicing of the same gene *SLC4A1*, is found in the kidney, at the basolateral membrane of α-intercalated cells in the cortical collecting duct [110, 111]. This form is truncated by 65 amino acid residues from the N-terminal end of the protein.

1.6.1 AE1 Functions

1.6.1.1 Anion exchange

AE1 mediates the electroneutral 1:1 exchange of chloride for bicarbonate at the cell membrane. In the red cell this permits bicarbonate, formed from CO_2 in the peripheral circulatory system by the intra-erythrocytic enzyme carbonic anhydrase 2, to leave the cell in exchange for chloride. This effectively stores CO_2 in the plasma in the form of dissolved bicarbonate, significantly

increasing the CO_2 carrying capacity of the circulation. Although this process is very important, it is evidently not essential for life, as animals can survive either near complete inhibition of it by disulphonic stilbenes [112], or knockout of the gene for this protein [113].

In the intercalated cell, this permits the extrusion of bicarbonate from the basolateral membrane to the systemic circulation in return for the exchange of a chloride ion. This allows the continued hydration of CO_2 inside the cell, catalysed by carbonic anhydrase 2, to produce more hydrogen ions for extrusion by the apical vH^+ATPase to acidify the urine [114]. (See Figure 1-1)

1.6.1.2 Anion Proton Cotransport

AE1 normally electroneutrally exchanges two monovalent anions, however, protonation of AE1 may allow it to carry a divalent anion, such as sulphate. This results in sulphate and hydrogen ion symport [115], in exchange for chloride.

1.6.1.3 Red Cell Membrane Structure

eAE1, through its cytoplasmic N-terminal domain, plays an important structural role in providing a site for membrane attachment for elements of the red cell cytoskeleton. Conditions which lead to less AE1 being present in the red cell membrane result in alterations of the red cell shape and decreased mechanical stability of the membrane, as is seen in AE1 knockout mice [113, 116], and hereditary hematological diseases such as hereditary Spherocytosis [117] and Southeast Asian ovalocytosis (SAO) [118].

It's protein ligands include ankyrin [119-121], protein 4.1 [122, 123], protein 4.2 [124, 125], glyceraldehydes-3-phosphate dehydrogenase (GAPDH) [126], phosphofructokinase [127], aldolase [128], haemoglobin [129], hemichromes [130] and tyrosine kinase [131]. Perhaps unsurprisingly, each of these interactions plays an important function of the functioning of the red cell, from

the control of the cell flexibility and shape [121], regulation of glucose metabolism [132], ion transport [133] and cell lifespan [134].

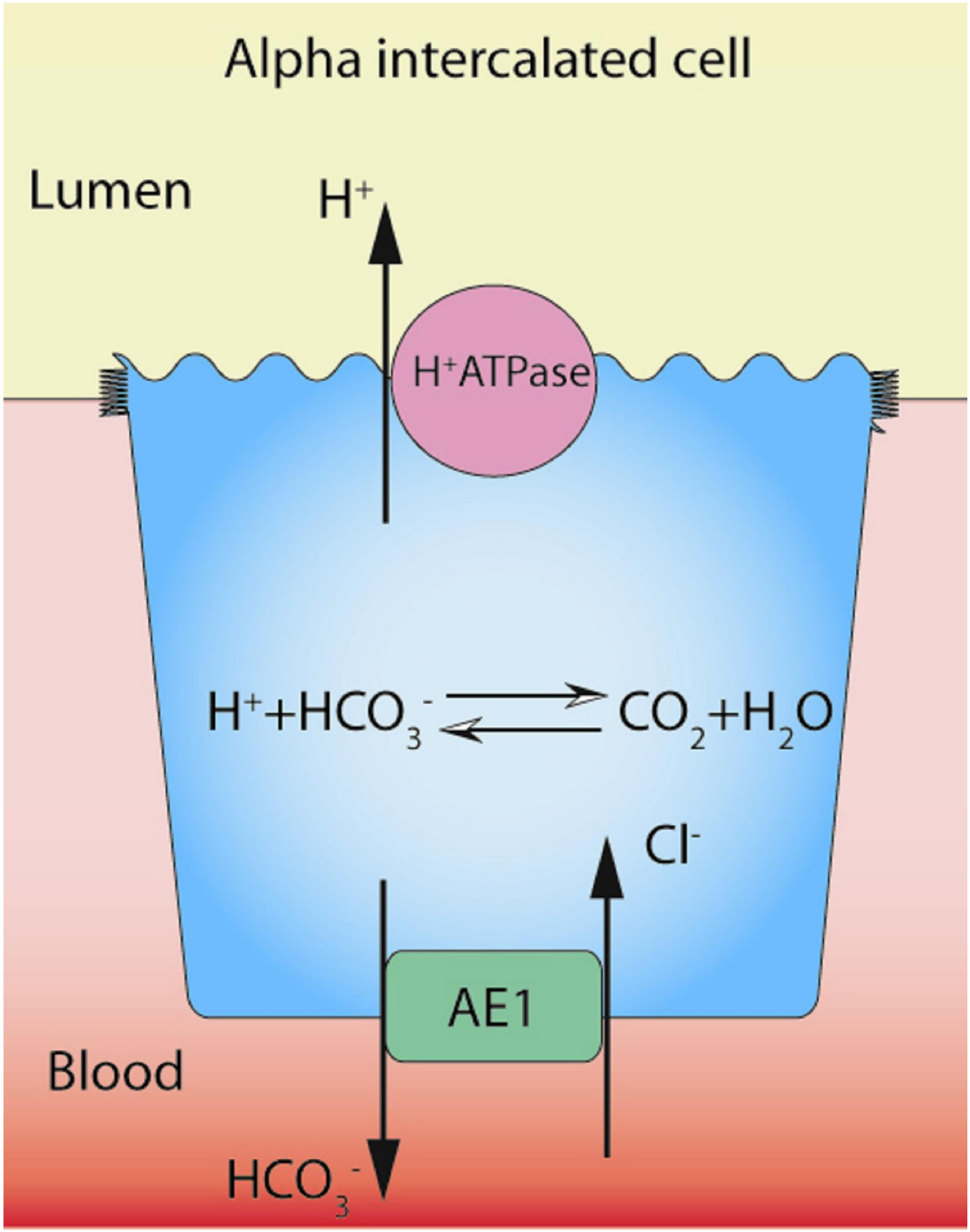

Figure 1-1 A cartoon of the alpha-intercalated cell

Showing the hydration of carbon dioxide in the cell interior, producing bicarbonate and a proton, which are extruded basolaterally by the anion exchanger and apically by the proton pump respectively.

1.6.1.4 Metabolon with carbonic anhydrase 2

The C-terminal cytoplasmic domain binds to carbonic anhydrase 2, under physiological conditions, in a unit termed the ‘metabolon’, with the effect of greatly increasing the efficiency of bicarbonate generation and extrusion [135, 136].

1.6.1.5 Red Cell Senescence

AE1 is also involved with signalling the chronological age of the red cell and contributing to it being cleared at the end of its natural lifespan, hemoglobin degradation products bind to AE1 and, presumably via a conformational change, cause circulating anti-AE1 antibodies to attach to it, activating complement and ultimately phagocytosis of the red cell [134, 137, 138].

1.6.2 Structure

As mentioned above, Kopito and Lodish deduced the primary structure of human eAE1 from human AE1 cDNA [107].

1.6.2.1 Secondary Structure

Proteolysis and gene sequencing studies have demonstrated that AE1 consists of 2 distinct structural and functional domains, divided by sites for cytoplasmic trypsin (Lys360) and chymotrypsin (Trp359) cleavage.
The N-terminal domain (1-360) is cytoplasmic and has sites for hemoglobin, glycolytic enzyme and cytoskeleton binding [120]. The membrane spanning C-terminal domain (361-911) is necessary for anion exchange, and able to do so alone [107]. (see Figure 1-2)

1.6.2.1.1 The N-terminal cytoplasmic domain

As stated above, the cytoplasmic domain acts as an anchor for the membrane to be attached to various cytoskeletal proteins, stabilising the membrane against mechanical stress.

A study of the 2.6 angstrom resolution crystal structure of this domain was reported in 2000 [139], that defined most of the domain (1-356), which forms a dimer. However, this AE1 domain crystallised at an unphysiological pH of 4.8, and it seems likely that the structure is unrepresentative in important ways from that at physiologic pH [140]. This crystal is nonetheless useful in that it shows the interaction of the two monomers in the dimer, particularly noteworthy being the near 2-fold symmetry around an axis in the dimer interface.

The relationship of the cytoplasmic domain to the membrane is also unclear, although the region of the domain that was crystallised was 1-379, the segment 357-379 were not resolved, possibly because this region is flexible. Hydropathy analysis suggests that the protein does not enter the membrane until approximately residue 405, this region appears to be important, as the mutation that causes SAO causes a deletion of residues 400-408 [141].

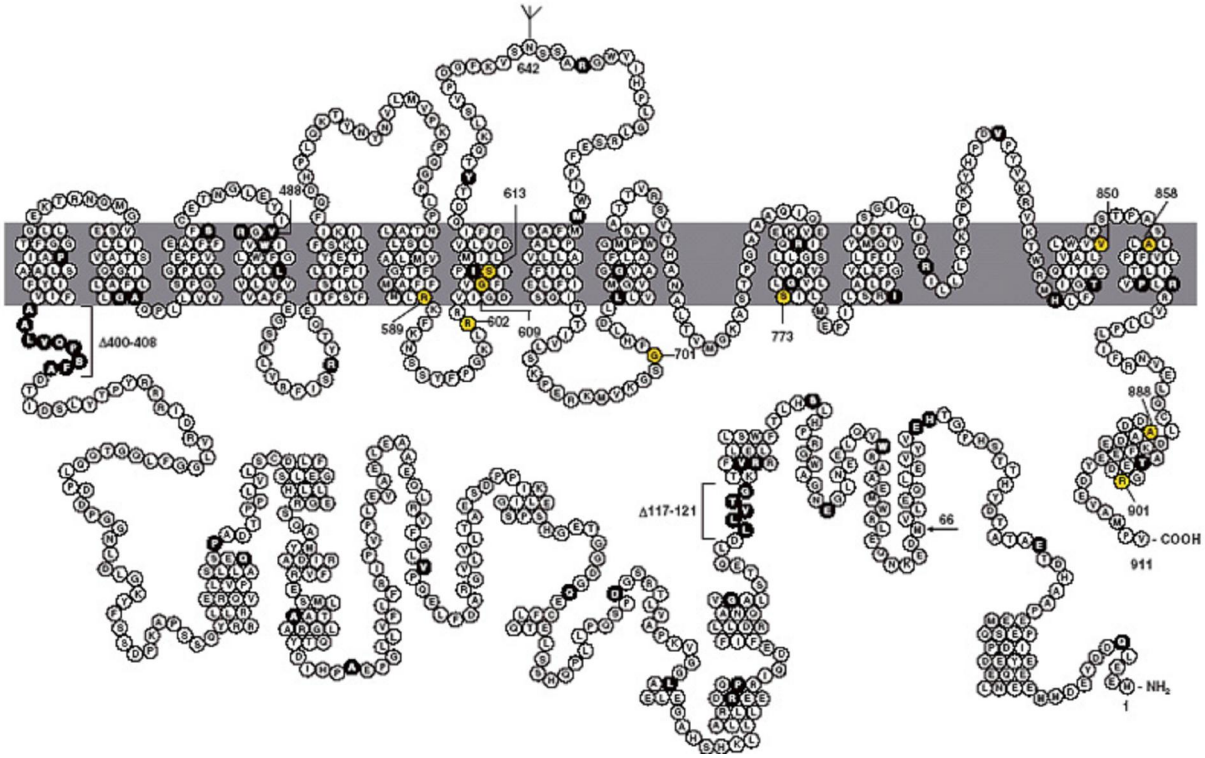

Figure 1-2 Schematic representation of the secondary structure of AE1.

Yellow residues mark the sites of known point mutations that cause hereditary dRTA. Black marked residues signify other point mutations or deletions that cause red cell disease. The shaded zone represents the lipid bilayer of the cell membrane, with the area above it representing the cell exterior. (after Shayakul and Alper, Clin Exp Nephrology 2004)

1.6.2.1.2 Topology of the AE1 membrane domain

A high-resolution structure of the membrane-spanning domain of AE1 has proved elusive because of the difficulties in getting well ordered crystals from detergent micelles.
Low resolution images were obtained via two dimensional crystals studied by electron microscopy and reconstituted into a 3D construct with a very low resolution of 20 angstroms [142-144]. At this resolution, structures such as α-helices were not observed; the size of the dimer was 100 x 60 x 80 angstroms. It had two protrusions, probably on the cytosolic side of the membrane, between which was a stain filled 'canyon' at the dimer interface- which was proposed as the anion access channel [142]. (Figure 1-3)

In the absence of a high-resolution crystal structure of AE1, studies have been undertaken to try and elide the topology of the membrane-spanning region by hydropathy plots, vectorial chemical labelling, proteolysis and molecular biological techniques.

Studies using a series of unique single cysteine AE1 mutants expressed in HEK cells and observed the accessibility of each mutated cysteine to biotin maleimide (BMA). Only cysteines outside the membrane bilayer are able to react with BMA [145]. External agents that are membrane impermeant, such as Lucifer Yellow Iodoacetamide (LYIA), were used to block the BMA reaction, thus distinguishing extracellular from intracellular residues [146, 147]. The same authors used a scanning N-glycosylation method by inserting a consensus sequence for N-glycosylation (or a part of the (extracellular 4) loop containing the endogenous N-glycosylation site) into various putative loop regions of the protein. This enabled the degree of N-glycosylation at the mutated sites to be used to mark the extracellular loop regions [147].

These studies, taken together, show that AE1 traverses the bilayer approximately 14 times, with transmembrane (TM) segments, which are probably α-helical in structure.

1.6.2.1.3 The First Eight TM Segments

The topology of the first eight TM segments is clearly and consistently defined. AE1 enters the membrane at Val405. The boundaries of the EC loops 1-4 have been demonstrated by N-glycosylation insertional mutagenesis [146, 147], chemical accessibility [148, 149], proteolysis [150] and through the observation that some natural mutations (R432W, E429D and E480K) can cause the production of antibodies against human red cells, and must therefore be external.

The endogenous N-glycosylation site at Asn642 also serves as a marker placing this region (EC4) on the extracellular side of the membrane [108].

TM 8 contains the residue Glu681, which is crucial for anion exchange [151], is comprised of the residues Met664-Glu683, in which all substituted cysteines are poorly labelled by BMA. Cysteines substituted from Ile684-Ser690 are labelled by BMA and this is not blocked by LYIA, indicating that they are on the cytoplasmic side of the membrane [152], meaning that Glu681 is located very close to the cytoplasmic side of the membrane at TM8.

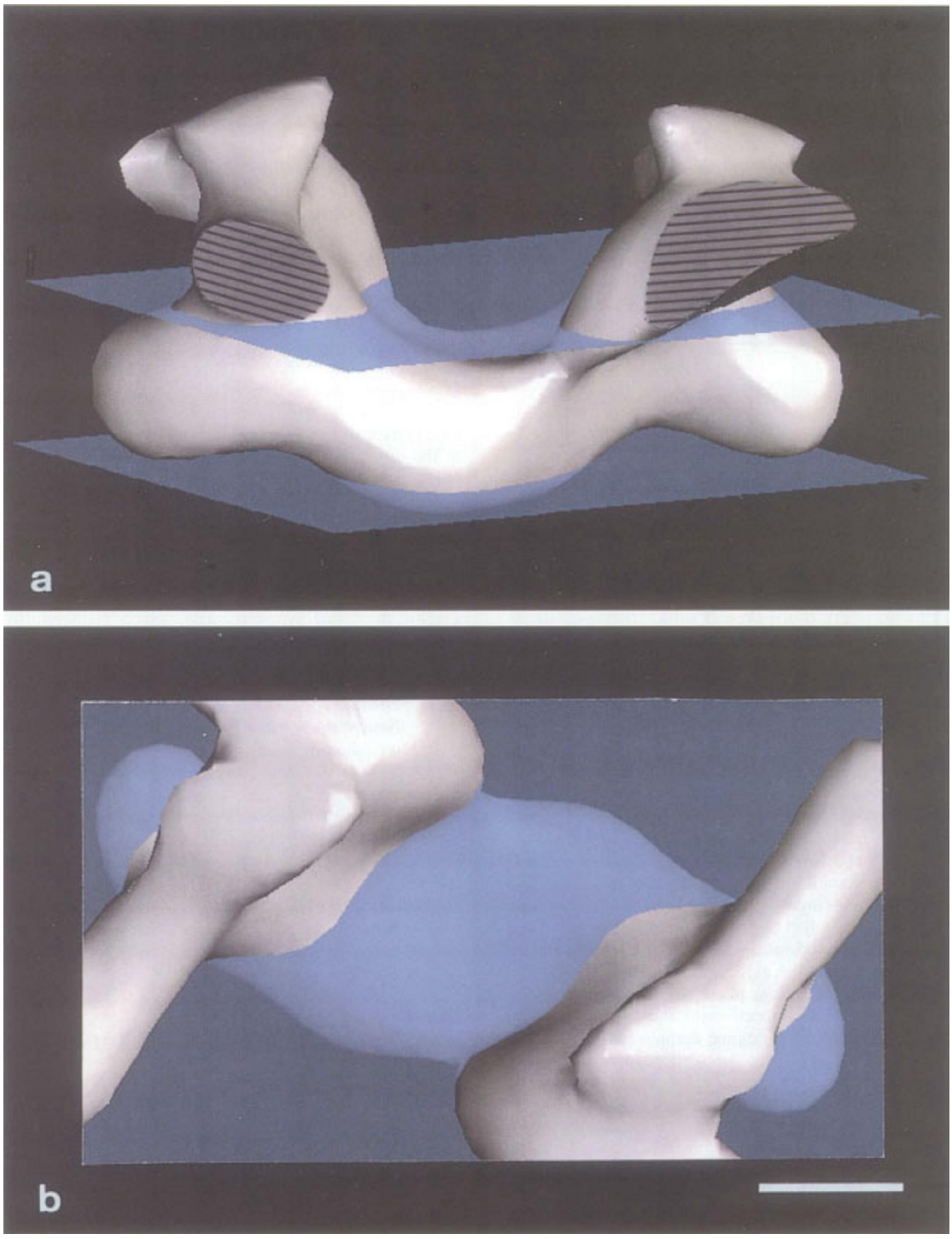

Figure 1-3 3D map of the dimeric transport domain of the Band 3 protein.

(a) Perspective view and (b) top view. The bulky basal domain is embedded in the lipid bilayer, indicated by the two blue planes. The protrusions above it are probably on the cytosolic side of the membrane. They form two sides of a canyon the floor of which is probably the entrance to a pore. The bar represents 20 angstrom. (Wang EMBO journal 1994)

1.6.2.1.4 The Remaining TM Segments

1.6.2.1.4.1 The T-Loop

The region between Ala726 and Ile761, the so-called ‘T-loop’ (trypsin sensitive loop) has been the subject of much investigation and speculation. The centre of the loop is thought to lie on the cytoplasmic side of the membrane, as it is cleaved by cytoplasmic trypsin at residue Lys743. Trypsin treatment inside sealed ghosts, or of inside out vesicles produced the cleavage products, external trypsin treatment of intact red cells did not [153].

However, cysteines substitute at positions Se731, Gly742, Ser745 and Ala751 were accessible to both BMA and LYIA, showing that these residues are accessible from the extracellular side of the membrane [152].

When a N-glycosylation sites were inserted into this loop, N-glycosylation was observed, but at levels less than seen at the endogenous site, Asn642[147]. Moreover, when expressed in HEK 293 cells, glycosylation was abolished, apart from the site at Gly754 [146].

Taken together, these data suggest that the T-loop folds back in on itself, with both the N-terminal and C-terminal ends of the loop on the extracellular side of the membrane. This agrees with two other observations, firstly that all the other large extracellular loops have antibody-producing mutations, such as EC3 and EC4, and even short loops like EC1 and EC5 have them, but none are evident in the T-loop, which would seem strange if it were totally extracellular.

Secondly, as I will discuss later, His734 apparently interacts with Glu681 during anion exchange, and a purely extracellular T-loop would place these residues too distant from each other for plausible interaction.

1.6.2.1.4.2 TM12

Beyond TM10 and TM11, the region between Asp807 and His834 (TM12) also has an unusual topology.

Here, substituted cysteines at Lys814 and Thr830 are unreactive with BMA, but Asp821 is open to BMA and extracellular LYIA [152].

A different study showed that Asp821 was labelled by an impermeant positively charged carbodiimide from the cytoplasmic side [154]. Thus, Asp821 is accessible to the negatively charged LYIA from the outside and to the positively charged carbodiimide from the inside.

Also, a glycosylation signal inserted at Asp821 is not N-glycosylated, which is evidence that it is not extracellular [146].

The Bric132 monoclonal antibody will (weakly) recognise the epitope Phe813-Tyr824 only in leaky erythrocytes, suggesting that the binding occurs from the cytoplasmic side [155].

It should also be noted that there are an unusual concentration of positively charged residues in this TM region, six positive charges compared with two negative charges. This would be an attractive environment for anions, were it to form part of a channel for them to diffuse down.

This region is therefore modelled as an extended helix with an attachment on the extracellular face of TM11 and on the intracellular face of TM13.

1.6.2.1.4.3 TM13-14

Cysteine accessibility scanning of the sequence from Trp831 to Gln884 show only two TM helices joined by an exceptionally short extracellular loop [152], A855C is accessible to BMA, and the mutant P854L is a blood group antigen, confirming the extracellular nature of this short sequence.

1.6.2.1.4.4 N-terminal cytoplasmic domain

The residues from Arg880 onward comprise the C-terminal cytoplasmic tail, which as mentioned previously, binds to carbonic anhydrase 2 to form the metabolon, and the terminal 11 amino acids comprise an important tyrosine based signalling mechanism, necessary for proper trafficking of the AE1 molecule to the basolateral cell surface in the α-intercalated cell.

1.6.3 Structure/Function

Unfortunately, it will become necessary, later on, to relate the functional transport properties of AE1 to structural changes. Therefore we are obliged to consider some of the data that relates to the structure/function of the molecule. The following discussion, which I have tried to keep as simple as possible, is however, by its very nature quite esoteric. There will be some mention of the permeability barrier, which is the theoretical point in the AE1 molecule that actually forms the functional barrier between the cytoplasmic and external compartments through which anion transport happens. The transforming conformational change (TCC) is the conformational change, which occurs in the molecule in order to transport anions across the permeability barrier.

1.6.3.1 Proton binding sites

As mentioned previously, AE1 can function as a cotransporter of protons and sulphate ions.

The anionic, carboxyl-reactive reagent, Woodward's reagent K (WRK) inhibits anion transport in intact red cells when added to the extracellular medium. When the reaction product is cleaved with borohydride (together, W-B treatment), this converts the reactive carboxyl group, $R\text{-}COO^-$ into the corresponding alcohol, $R\text{-}CH_2OH$, chloride transport is still inhibited, but sulphate transport increases dramatically at neutral pH [156], where sulphate

exchange is usually slow compared to more acidic conditions (i.e. where incident protons are more common). This shift in pH dependency is seen for both internal and external pH, suggesting that the WRK reactive COO^- group is accessible from either side of the membrane-and thus might be the site that binds protons and that translocates them across the permeability barrier (and which itself be at the permeability barrier).

These effects occur when the W-B treatment is highly specific for one carboxyl group in the AE1 molecule, namely Glu681 [151, 157]. As we have seen, there is evidence that Glu681 is located very close to the cytoplasmic side of the membrane-which implies that the impermeant reagent WRK is able to penetrate deeply into the molecule, which means that there must be an aqueous channel in the AE1 molecule that leads from the external surface of the molecule to a point almost at the cytoplasmic side of the membrane.

Normally, proton and sulphate symport in exchange for chloride is electroneutral. After W-B treatment, chloride/sulphate exchange becomes electrogenic[158], resulting in a net negative flow of one charge across the membrane with the sulphate anion. This is what would be expected if the proton remained bound to AE1 and was not co-transported across the permeability barrier. The W-B treatment converts the carboxyl group to an alcohol, which binds the proton much more avidly, so that it cannot be released along with the sulphate.

The idea that Glu681 is the site of proton transport is supported by data from experiments in which site directed mutants of Glu681 are expressed in Xenopus oocytes. Substitution of Q, T, R, K or G for Glu681 abolishes chloride exchange for either chloride or sulphate. Sulphate/sulphate exchange is also abolished, except in the case of the Q (Gln) substitution mutant, which has increased sulphate/sulphate exchange compared to wild type AE1, and even greater sulphate/chloride exchange [159]. This chloride sulphate exchange has a 1:1 stoichiometry and is electrogenic, similarly to the situation seen after W-B treatment of the wt protein, above.

This was echoed in a separate study, in which Gklu681 was substituted for Gln or Ala, and a much-decreased dependence on pH for sulphate transport was seen [160]. Substitution of glutamine for glutamate removes the negative charge from the R-COO- group, and thus prevents it from transporting a proton, as does W-B treatment.

Furthermore, the apparently conservative substitution of Asp for Glu681 inhibits chloride exchange [161], and alters the pK for it's inhibition by protons. This is a conservative substitution, because Asp differs from Glu by a single $-CH_2-$ group in the side chain, which implies that the structure around this residue is sufficiently delicate that this small change in position of its negative charge is enough to seriously compromise its function.

1.6.3.2 Eosinyl-5-malemide probing

The covalent modification of Lys430 by eosinyl-5-malemide (EMA) causes almost complete inhibition of chloride exchange [162], but does not prevent chloride binding [163], and mutation of the residue does not inhibit anion transport [164]. This suggests that the inhibition of anion transport by EMA is not a defacto part of its interaction with Lys430.

External iodide can quench the eosin triplet fluorescence of EMA bound to AE1 Lys430, and negatively charged quencher were effective from the external side, but positively charged quenchers were effective from the cytoplasmic side [165]. This suggests that the hydrophobic ring moiety of EMA may actually insert itself into the parts of AE1 that form the permeability barrier, so that it is accessible to quenchers from either side of the barrier. As Lys430 is topologically very close to the external surface of the molecule, the quenching by positively charged reagents from the cytoplasmic side indicate that there must be an aqueous channel that runs from the cytoplasmic side of AE1 to almost the external side of the bilayer.

1.6.3.3 Histidine modification

Inhibition of AE1 phosphate transport occurs with the cytoplasmic administration of the histidine sensitive reagent, diethyl pyrocarbonate (DEPC), and increases with increasing internal pH in red cell ghosts[166], indicating that the DEPC sensitive His is accessible to protons from the cytoplasmic side of the plasma membrane. Furthermore the binding of 4, 4-dinitrostilbene-2, 2-disulfonate (DNDS) from the outside greatly reduced the ability of DEPC to inhibit anion exchange by reacting at it's evidently inward facing site, and cytoplasmic DEPC binding greatly reduced labelling by extracellular 4,4'-diisothiocyanodihydrostilbene-2,2'-disulfonic acid (H_2DIDS), these data are suggestive that this DEPC reactive His residue lies at the permeability barrier.
The role of histidine residues was then explored by site directed mutagenesis, mutation of His703, His819 and His834 to Gln, greatly reduced chloride transport. However, none of these mutants reduced the DEPC reaction rate, but a mutation of His734 to Ser caused the DEPC reaction to decrease to approximately one third of that seen in the wildtype AE1, indicating that His734 is the main site for DEPC inhibition of anion exchange [167].

This H734S mutation also shifted the external pH dependence of chloride transport from a pK of 5.8 to 6.9 [161], very reminiscent of the pK change (5.8 to 6.7) seen when Glu681 was changed to Asp.

That His734 is accessible to protons only from the internal side of the membrane, but mutations at Glu681 and His734 have similar effects on the pK for external acidity on chloride transport is striking.

This can be accounted for if the external protons are reacting with the carboxyl group at Glu681, which is close to and interacts with the positive charge at His734. A substitution of Asp for Glu681 would shorten the side chain by one $–CH_2$- group, moving the negatively charged carboxyl group away from the positively charged His734, and tend to raise the pK, likewise the substitution of Ser for His734 would similarly separate the charges,

causing the Glu681 pK to increase just as if it had been substituted for Asp [161].

There is, however, a fly in the ointment, Yin et al found that with DEPC treatment of AE1 in red cell ghosts analysed by liquid chromatography with electrospray ionised mass spectrometry, that of the six His residues in the membrane spanning domain of AE1, only one (His834) had a large interaction, and was also the only one which was pH sensitive and sensitive to DNDS inhibition.

These authors did not find that His743 was modified by DEPC, but conceded that it is an important residue for anion exchange [168].

1.6.3.4 Evidence for anion access channels in AE1

1.6.3.4.1 External Access Channel

As Glu681 lies very close to the cytoplasmic side of the membrane, yet the bulky impermeant WRK can reach it from the outside means that there must be an aqueous channel in AE1 leading from the external surface almost to the cytoplasmic side of the phospholipid bilayer.

This is consistent with the observation that some agents inhibit anion exchange as if they deny chloride access to the transport site, but do not compete directly with it [169].

The observation that chloride and DIDS are able to bind with AE1 even after WRK has reacted with Glu681, indicates that they are both lie on the extracellular side of Glu681 [170].

This idea is reinforced by a study that showed that DNDS or H_2DIDS binding was able to block WRK from reacting with Glu681 [157].

More specific information suggests that TM8 forms part of the anion access channel-for example the action of p-chloromercurybenzene sulphonate (pCMBS), a hydrophilic sulfhydryl reagent, on chloride/bicarbonate exchange in HEK 293 cells expressing a variety of single cysteine mutants. Mutants with introduced cysteine residues at Ala666, Ser667, Leu669, Leu673, Leu677 and Leu680 had anion exchange inhibited by pCMBS [171]. In an α helical wheel model of TM8, these residues line up on the same side of the helix as Glu681, and thus might line the external anion access channel. pCMBS had no effect on cysteines beyond Leu680, as would be expected if Glu681 lies at the innermost part of the external access channel.

A different negatively charged sulfhydryl reagent 2-(sulphonatoethyl)-methanethiosulphonate (MTSES), inhibited anion exchange in mutants with cysteine at Ser852 and Ala858 [152], suggesting that these residues on the external side of TM13 and TM14, face an aqueous region close to a functionally important site. They lie close to Lys851, which is the site of H_2DIDS cross-linking to Lys539, and so must be within 15 angstrom of TM5.

The extracellular span bridging the last two transmembrane domains, from residues 852 to 857 as well as the adjacent ends of the transmembrane helices form the so-called ‘anion selectivity filter’. It was demonstrated that a large number of cysteine substituted residues in this region were sensitive to sulfhydryl inhibition, but only those forming the extracellular region were inhibitable by a positively charged sulfhydryl inhibitor, although deeper residues were inhibited by the uncharged ones. Also of those residues that were inhibited by the uncharged pCMBS, none of the superficial extracellular residues had inhibition competed with by Cl^-, indicating anion selectivity in this region [172]. This anion selectivity was speculated to be due to the positive charge at residue 851, as well as possibly the σ^+ helical pole charge from the last transmembrane segment.

We can infer then, that TM5, TM8, TM13 and TM14 may form parts of an aqueous channel leading from the external surface of AE1 into the molecule. The T-loop and TM12 may also be involved, as they can be labelled by LYIA

[152]. The external ends of TM13 and TM14 as well as the short segment that joins them may act as a positively charged filter for anions [172].

1.6.3.4.2 Cytoplasmic Access Channel

A positively charged membrane-permeant reagent 2-(aminoethyl)-methanethiosulphonate (MSTEA), inhibited anion exchange by reacting with cysteines substituted at Ile684 and Ile688 [171], suggesting that these residues might line an aqueous channel extending into AE1 from the cytoplasmic side. The channel is quite deep, as positively charged quenchers can quench the fluorescence of externally reacted EMA [165], which labels Lys430 [148], which is located at the external side of the phospholipid bilayer.

Thus, AE1 has an anion permeable channel that reaches from the outside to Glu681, as well as an aqueous channel that extends from the cytoplasm to Lys430. This means that the permeability barrier must lie between the external surface of the bilayer, to a point almost at the cytoplasmic side of the bilayer.

1.6.4 Conclusions

- AE1 is expressed chiefly in the erythrocyte (eAE1), and also as a truncated isoform in the kidney α-intercalated cell (kAE1), which lacks the N-terminal 65 amino acids.
- The N-terminal cytoplasmic domain binds to several cytoplasmic proteins associated with the cytoskeleton.
- The membrane-spanning domain carries out transport across the membrane; however, our knowledge of the topology of the membrane-spanning domain is inexact, as it is inferred from functional studies rather than high-definition crystallography.
- The first eight transmembrane segments are well defined, topographically, the remaining portion of the membrane spanning

domain is not, possibly as it is mobile as part of the Transporting conformational change.

- The residue Glu681 is involved in proton binding in proton sulphate symport and is crucial for anion exchange. It is at the permeability barrier.
- It is accessible via an external aqueous channel that reaches from the external surface of the molecule, to Glu681, which is located very close to the cytoplasmic side of the membrane.
- There is also an internal aqueous channel that reaches from the cytoplasmic side of the molecule, which reaches as far as the Lys430 residue, which seems to lie in or very near to the opening of the external aqueous channel.
- One of the histidine residues in the membrane spanning part of AE1 is crucial for anion exchange, and appears to interact with Glu681. This residue is probably His743, but may be His834. Both are clearly important.
- The external access channel is probably comprised of TM5, TM8, TM12, TM13 and TM14, with the external ends of TMs13 and 14 and the segment linking the two acting as a positively-charged ‘anion selectivity filter’.
- The internal aqueous channel appears to incorporate Ile684 and Ile688.

1.7 AE1 and the α-intercalated cell

As mentioned before, dRTA is a clinical syndrome arising from an inability of acid secretion by the intercalated cells of the cortical collecting duct, causing decreased net acid excretion and an inability to acidify the urine to a pH of less than 5.3, despite spontaneous acidosis or acid loading. This leads to positive acid balance and subsequent chronic metabolic acidosis. This favours the precipitation of calcium salts in the urine or renal parenchyma (as renal calculi or nephrocalcinosis respectively) due to a reduction of urinary citrate excretion and concomitant hypercalciuria. Acidosis also favours metabolic bone disease, and as discussed previously, hypokalaemia.

The hereditary forms of this disease can be caused by a defect in the apical proton extruding vH^+ATPase in the α-intercalated cell, or by a defect in the basolateral anion exchanger, AE1, which reclaims bicarbonate from the α-intercalated cell to the systemic circulation.

The defects in these two proteins arise because of mutations in the genes responsible for causing hereditary dRTA. Mutations of two genes encoding two subunits (B1 and a4) of the vH^+ATPase have been reported to cause autosomal recessive dRTA [2, 173-175].

The respective genes are *ATP6V1B1* (chromosome 2p13.1), which encodes the B1 subunit of the catalytic V_1 domain and *ATP6V0A4* (chromosome 7q33-q34), which encodes the a4 subunit in the Vo domain of the vH^+ATPase.

Mutations of in the human anion exchanger, or human solute carrier family 4, member 1 gene (*AE1 or SLC4A1,* found on chromosome 17q21-q22) may also cause dRTA, as first reported by Bruce and co-workers [1].

An AE1 mutation that leads to defective basolateral bicarbonate extrusion through the basolateral membrane will cause bicarbonate retention in the α-intercalated cell, facilitating the intracellular retention of hydrogen ions, and

thus inhibit the dissociation of carbonic acid. The resulting failure of hydrogen ion excretion from the α-intercalated cell would (by definition) cause dRTA.

Mutations in SLC4A1 can cause autosomal dominant (AD) dRTA [1, 176-178] as well as autosomal recessive dRTA [63, 179-181]. The mechanisms of these different Mendelian inheritance patterns are being revealed by work on the intracellular trafficking of these various mutants.

1.7.1 AE1 and the intercalated cell

1.7.1.1 AE1 regions important for intracellular targeting (the C-terminal tail)

There is a sequence ($Y_{904}DEV_{907}$) present on the c-terminal tail of AE1, which corresponds to a tyrosine based signalling pattern, the so-called 'YXXΦ motif'. This pattern consists of tyrosine residue (the 'Y'), two other amino acids (the 'XX's) and a hydrophobic amino acid (the 'Φ') [182], and is involved in protein localisation to both clathrin and clathrin-independent (caveolae) endocytic mechanisms, as well as sorting to the basolateral membrane in polarised cells[183-185]. Other membrane proteins are known to undergo basolateral membrane sorting via interactions with tyrosine motifs on the cytoplasmic domains via adaptor-protein complexes [186, 187].

This motif has an important role in kAE1 sorting in polarised cell models. Y904, as part of this motif, has been examined in MDCK cells and rat inner medullary collecting duct (IMCD) cells, with an 11 amino acid deletion (R901X) [188] and a substitution with alanine at position 904 [189] respectively, with the protein being erroneously sorted to the apical membrane.

The so-called 'acidic patch' ($D_{905}E_{906}$), and the last 4 amino acids ($A_{908}MPV_{911}$) at the C-terminal end of the protein may also play an important part in proper kAE1 localisation. The latter sequence has been proposed as a possible PDZ protein-binding domain (XΦXΦ). Intracellular localisation of kAE1 in transfected HEK 293 and non-polarised LLC-PK1 cells was the result of deletion of the last 5 amino acids [190].

1.7.2 Autosomal dominant dRTA

The AE1 mutations associated with autosomal dominant (AD) dRTA were the first described [1, 176-178, 191], the commonest mutation in this group being a missense mutation at position R589, usually by histidine or cysteine, and more rarely serine. The frequency of different, (and on at least two occasions, denovo) substitutions at this position has led to the suggestion that the responsible codon is a 'mutational hotspot' [177], (possibly due to methylation and deamination altering cytosine to thymine).

The first SLC4A1 mutations described causing AD dRTA were R589H, R589C and S613F, all the cases were heterozygotes and had normal red cells. Red cell anion transport was reduced with R589H and R589C, but markedly increased with S613F. The eAE1 proteins, when expressed in Xenopus oocytes, had normal chloride influx activity, with the exception of R589H, which had an approximately 40% reduction. When co-expressed with wild type (wt) eAE1, the mutant eAE1 did not affect the chloride influx, indicating that the mutant did not affect transport activity of the molecule directly.

Karet et al screened 26 kindreds with hereditary dRTA for *SLC4A1* mutations, and found none in any of the kindreds with AR dRTA, confirmed by linkage analysis[176]. However, they found SLC4A1 mutant heterozygotes in one dominant dRTA kindred, one sporadic case and one kindred with two affected brothers, the mutations being R589S, R589H and R901X (which resulted in a premature truncation of the protein, missing the last 11 amino acids from the C-terminal tail). However the provocative title of the paper, which suggested that SLC4A1 mutations could not cause AD dRTA has been proven wrong by subsequent data from SE Asia [63, 180, 181, 192, 193].

A heterozygous *SLC4A1* mutation causing a missense mutation at position 888, followed by a premature termination codon (A888L+889X) was reported in two infants with dRTA and their father, who had incomplete dRTA [194].

A different novel missense mutation was reported in a large AD dRTA family who suffered with extensive nephrocalcinosis and renal impairment, G609R [195]. Again, this had no loss in anion transport function when expressed in Xenopus oocytes.

As these reports show, although all of these *SLC4A1* mutations clearly co-segregate with AD dRTA, when expressed in Xenopus oocytes, all had normal or near normal anion transport activity, thus the loss of activity must arise from another mechanism than simple abolition of transport activity.

1.7.3 Autosomal recessive dRTA

The first *SLC4A1* mutation to be found associated with AR dRTA was reported in 2 siblings in NE Thailand, who had dRTA associated with a hemolytic anemia and dysmorphic red cells, with normal red cell eAE1 content and anion transport. They had the mutation G701D, which was also associated with the two common polymorphisms, M31T and K56E [180]. When expressed in Xenopus oocytes, G701D (as both eAE1 and kAE1) showed a lack cell surface expression. However, when coexpressed with the red cell AE1 chaperone protein, Glycophorin A (GPA), the plasma membrane expression, and thus anion transport activity was 'rescued'. Thus the normal anion transport activity in the patient's red cells, with their abundant GPA was explained, and the dRTA, due to defective anion transport in the GPA-less α-intercalated cell was understandable as well. The red cell abnormalities, and the hemolytic anemia seemed to be due in part to the siblings being affected by homozygous hemoglobin E and in part to the G701D mutation, as subsequent reports of G701D heterozygotes in five different Thai families without hemoglobin E found only slight red cell dysmorphia [193].

Compound heterozygotes for G701D and Southeast Asian Ovalocytosis (SAO) were described shortly afterwards; two cases of dRTA and SAO were reported in patients with G701D/SAO *SLC4A1* mutations from two families from southern Thailand [181]. These had a few more red cell abnormalities than normally found in SAO, and a 40% decreased red cell sulfate flux.

Two novel mutations were reported in compound heterozygotes in families from SE Asia, AR dRTA was found in a Malaysian family due to SAO/A858D, and in association with SAO/ΔV850, ΔV850/ ΔV850 and ΔV850/A858D in patients from six families from Papua New Guinea [63]. Again haemolytic anemia and abnormal red cell shapes were noted. Red cell and Xenopus oocyte studies showed that ΔV850 and A858D mutants had severely decreased anion transport when expressed as a compound heterozygote. The heterozygous A858D mutation was found to be associated with incomplete dRTA by the original reporting group, and was thus assigned as an AD dRTA causing mutation. As will be seen later, this can cause some confusion, and it must be remembered that the labels AD and AR represent clinical phenotypes, which may be very variable in the degree of expression.

Severe haemolytic anemia and dRTA in a homozygote for *SLC4A1* V488M was the next report of an AR dRTA causing *SLC4A1* mutation [179]. Another two novel mutations were described in two Thai families; one had dRTA due to a compound heterozygote G701D/S773P. The second family had two siblings with both SAO and dRTA (one complete, the other incomplete), both were compound heterozygous *SLC4A1* SAO/R602H [196].

As will be fairly obvious by now, the AD dRTA *SLC4A1* mutations co-segregate mainly with occidental populations, whereas the AR dRTA mutations are all clustered in Southeast Asia. I will return to this point later.

1.7.4 Molecular mechanisms of AD dRTA

The localization of two *SLC4A1* mutants has been studied in detail in cell models, R589H and R901X.

Quilty et al showed that a dominant negative effect could account for the AD dRTA phenotype [197, 198]. They transfected HEK 293 cells with wt eAE1, wt kAE1 or R5898H kAE1. Erythroid AE1 and kAE1 when transfected singly were expressed at the cell surface, but R589H was retained intracellularly, as

demonstrated by immunofluorescence, cell surface biotinylation and anion transport assays [198]. Coexpression of kAE1 and R589H reduced the expression of wt kAE1 due to heterodimer formation and a dominant negative effect, in which, it was postulated, the mutant protein in the heterodimer caused the whole heterodimer to be retained intracellularly. The R589H mutant was not grossly misfolded as it had unaffected binding to an inhibitor affinity resin. Other mutations at the same position (R589C and R589S) had the same effect, preventing the normal targeting of wt kAE1 to the cell surface, suggesting that the arginine at position 589 (which is evolutionarily conserved) is important for proper protein targeting.

In studies using both transiently and stably transfected MDCK cells, it has been reported that the kAE1 mutant R589H and S613F are retained in the endoplasmic reticulum (ER) of non-polarised cells and that they fail to reach the cell surface in polarised cells [188, 199]. A coexpression study in MDCK cells showed that R589H caused wtkAE1 to be retained intracellularly, again, probably via heterodimer formation [199].

The R901X kAE1 mutant has been studies in Xenopus oocytes, HEK 293 cells and non-polarised MDCK cells [197, 200]. R901X demonstrates normal anion transport when expressed in Xenopus oocytes, however when expressed in MDCK cells, it was retained intracellularly, suggesting that the C-terminal tail, truncated in the R901X mutant is important for transport to the cell membrane. It was again proposed that wt kAE1 was prevented form reaching the cell surface when coexpressed with R901X due to heterodimer formation, trapping the wt protein in the cell interior [200].
Quilty showed that mutant proteins heterodimerised with wt protein, preventing it's expression at the cell surface, by showing that R901X kAE1 colocalised with His tagged wt kAE1 form transfected cell lysates, and that coexpression of the wt and mutant kAE1 resulted in the intracellular retention of wt proteins in a pre-medial Golgi compartment of the transiently transfected HEK 293 cells [197].

Serial truncations of the AE1 C-terminus also resulted in impaired protein exit from the ER, the degree of impediment depending on the length of the truncation [190].

Wild type and R901X epitope tagged kAE1 distribution in polarised MDCK and rat IMCD cells was examined by Devonald and co-workers [189]. In both cases, wt kAE1 localised to the basolateral membrane, whilst the mutant was found at the basolateral and apical membrane as well as intracellularly. This non polarised sorting of R901X might be due to the loss of a targeting signal form the truncated C-terminal end of the protein, namely the so-called "YXXΦ motif", which is involved in targeting proteins to the basolateral surface of polarised cells. The residues YDEV at positions 904-907 correspond with this motif, and when the tyrosine at position 904 was mutated to an alanine, the distribution of the resulting protein in the polarised transfected cell was similar to that seen with R901X. YXXΦ motifs interact with the α subunits of adaptor protein (AP) complexes, on e of which is specific to polarised epithelial cells, AP-1B. To determine whether AP-1B was involved in sorting AE1 to the basolateral membrane, sorting in LLC-PK1 cells (which are derived from proximal tubular cells and lack the α1B subunit) was observed with two AE-CD8 chimera proteins, constructed from the membrane reporter protein, CD8, and the C-terminal end of AE1, the full tail in one case and the truncated to lack the last 11 amino acids, as R901X does. Sorting was no different in this experiment, with the truncated protein being seen at the apical membrane, and the fully tailed protein being transported to the basolateral membrane. The authors concluded that AP-1B wasn't involved in AE1 basolateral sorting [189].

This finding was confirmed by another study in stably transfected MDCK cells-where it was demonstrated that the 11 terminal amino acids on the C-terminus were not recognised by α1B containing AP-1B adaptor complexes [188]. Also, it appeared that the N-terminus played a role in AE1 addressing-in the absence of the N-terminus, the C-terminus was not sufficient to localize kAE1 to the basolateral membrane [188, 201].

A further mutation, G609R was reported in a European family [195] that caused AD dRTA. When kAE1 was expressed in Xenopus oocytes, had, like all the other dRTA causing mutants, normal anion transport function. In polarised MDCK cells, G609R localised sub-apically, in a manner reminiscent of R901X. Due to the proximity on the AE1 secondary structure to R589 and S613, the authors postulated that this region must be important for the trafficking or sorting of the protein. G609R was not examined for a dominant negative effect, to explain its phenotype.

1.7.5 Molecular Mechanisms of AR dRTA

The trafficking of the AR mutants G701D and S773P were studied in transfected HEK 293 cells [202], where it was found that S773P had approximately 30% of the expression of wt kAE1, and had a two fold decrease in its half life, being targeted by the proteosome for degradation. It could not be detected at the cell membrane. In contrast, it was demonstrated that when coexpressed with either wt kAE1 or G701D, it was able to form heterodimers with them, as could G701D and wt kAE1 with each other. Furthermore, these heterodimers were expressed on the cell membrane, unlike heterodimers of R589H and wt kAE1. These two mutants, then, showed a dominant positive effect, in being ‘rescued’ to the cell surface by the wt kAE1 that they were heterodimerised with.

When expressed in polarised MDCK cells, the S773P and G701D mutants displayed distinct trafficking defects. S773P, whilst retained largely in the ER in non-polarised MDCK cells, was predominantly targeted to the basolateral membrane in polarised MDCK cells [203]. However, G701D was retained in the Golgi both polarised and non-polarised MDCK cells. Coexpression with wt kAE1, showed that, as shown before, R589H caused the retention of coexpressed wt kAE1, whilst the recessive dRTA mutants did not. The coexpression of S773P and G701D showed some co-localisation of S773P and G701D in the Golgi, but still with trafficking of S773P to the basolateral membrane, no G701D was detected at the plasma membrane, demonstrating that ‘rescue’ of G701D does not occur with S773P.

1.7.6 Conclusions

- The phenotypes of hereditary AE1 associated AD and AR dRTA are determined by *SLC4A1* point mutations or deletions which affect AE1 folding and tertiary structure without significantly changing the anion transport properties of the protein.
- These structural alterations do not seem to affect the dimerization of these mutant proteins as hetero- or homodimers.
- They do, however, affect the trafficking of the mutant homodimers, from the ER and the trans-Golgi network to the cell membrane.
- The trafficking of the mutant/wildtype heterodimer determines the dominant or recessive nature of the phenotype. In AD dRTA the mutant kAE1 in the heterodimer exerts a ‘dominant negative’ effect, inducing a trafficking defect on the dimerised wt kAE1. In AR dRTA, the wt kAE1 in the heterodimer corrects the defective trafficking of the mutant kAE1, resulting in a ‘dominant positive’ effect and thus normal cell surface expression of kAE1 in the heterozygote.
- In two cases (R901X and G609R) the dominant mutants can exit the ER and a partially mis-sorted to the apical membrane. This, and the reduced basolateral expression of AE1, leads to the dRTA phenotype.

1.8 AE1 and the red cell

1.8.1 AE1 and the red cell

As stated before, AE1 is the predominant plasma membrane protein in the red cell, where its main function is the extrusion of bicarbonate reclaimed by carbonic anhydrase 2 (CA2) from the hydration of CO_2 that has diffused into the cell from the respiring peripheral tissues.

Also, as mentioned before, it has two main domains, a N-terminal cytoplasmic domain that attaches to ankyrin, protein 4.2 and the red cell cytoskeleton, all of which affect the stability of the red cell membrane, and the cell shape [139]. It also binds glycolytic enzymes, altering the rate of glycolysis [204, 205], hemoglobin, controlling hemoglobin cooperativity [206] and hemichromes (partially denatured hemoglobin), affecting cell senescence signalling.

The membrane-spanning domain crosses the membrane 12-14 times and carries out ion transport. The short cytoplasmic C-terminal tail binds CA2.

AE1 carries out a more diverse set of functions in the red cell than it appears to in the intercalated cell, mainly due to the other proteins that it associates with at the plasma membrane. Its trafficking is also a little different, in that in the red cell, AE1 is trafficked with the chaperone protein, Glycophorin A (GPA).

1.8.2 AE1 interaction with Glycophorin A

Glycophorin A (GPA) is a bitopic integral membrane sialoglycoprotein that is present in the red cell in similar abundance to AE1. There is a considerable body of evidence that GPA interacts with AE1 in the red cell membrane.

Anti-GPA antibodies decrease the rotational mobility of AE1 in the red cell membrane [207]. Anti-Wright b (Wr^b) antibodies (against the common Wright b erythrocyte antigen) require both GPA and AE1 to be present to react with red cells and co-immunoprecipitate both GPA and AE1 [208]. The GPA residues 61-70 are thought to form the Wr^b antigen, along with residue Glu658 of AE1.

GPA augments the movement of AE1 to the cell membrane in Xenopus oocytes, and coexpression of GPA and wt AE1 induces increased AE1 mediated chloride influx in the oocyte, by both enhancing the amount of AE1 at the membrane, and possibly also by increasing AE1 anion transport function [209]. This augmentative effect of GPA on AE1 transport activity is not dependent on the oligomeric state of GPA; GPA mutants that are unable to form stable dimers have the same effect on AE1 as wt GPA [210].

AE1 and GPA appear to interact at an early stage following the synthesis and processing of the two proteins [211]. The N-glycan chain of AE1 in increased in erythrocytes that lack GPA [212], but is decreased in red cells that have

more GPA than normal [213]. The sulfate transport ability of AE1 is diminished in human red cells that lack GPA, even though the amount of AE1 is unchanged [212].

GPA forms SDS-stable dimers by self-association of the transmembrane (TM) regions. Mutagenesis studies have demonstrated that seven residues in the GPA TM span are critical for dimer formation [214], although other residues may also be important for this process [215].

Work expressing GPA constructs in Xenopus oocytes also suggests that the C-terminal cytoplasmic tail enhances trafficking of AE1 to the cell surface, whereas the (extracellular) residues 68-70 increase the specific anion transport activity of AE1 [215]. This area is within the Wr^b antigen, and thus is likely to interact with Glu658 on AE1, which is probably at the extracellular end of TM8. How this might affect AE1 anion transport remains unclear.

1.8.3 Haemoglobin

Haemoglobin (Hb) binds weakly to the N-terminus of AE1, but as the concentration of Hb is so high in red cells, about 50% of AE1 molecules are bound to Hb under physiological conditions [216].

Hemichrome, a partially denatured form of Hb, binds to AE1 more avidly than normal Hb, forming AE1-hemichrome aggregates [217]. These clustered aggregates are thought to form a cell surface epitope that is identified by antibodies, which bind and signal the cell for phagocytosis [218].

This formation of a senescence antigen by AE1 copolymerisation with hemichromes could also mediate the clearance of sickle and β-thalassaemic red cells, which have unstable Hb that degrades into hemichromes.

1.8.4 Membrane skeletal proteins

Ankyrin-1 links to the major membrane protein spectrin by binding to a number of sequences in the N-terminal cytoplasmic domain of AE1 [219]. This forms the basis of the skeletal membrane attachment, which is essential for the plastic/elastic properties of the red cell [219]. Ankyrin-1 preferentially binds to AE1 tetramers, and may contribute to tetramer stabilisation [220]. It has been estimated that about 70% of red cell AE1 exists as dimers and 30% as higher order oligomers, with these latter species predominantly associating with ankyrin-1 [221].

Protein 4.1 which links the spectrin-actin skeleton to the plasma membrane via interactions with Glycophorin C (GPC), has also been shown to bind to the cytoplasmic domain of AE1 [123] although AE1 does not seem to be important in linking the spectrin-actin complex to the plasma membrane [222]. Protein 4.1 competes with ankyrin for binding to AE1 in vitro, with consequences for membrane mechanical properties [122].

Protein 4.2 also interacts with AE1's cytoplasmic domain [223]. This is thought to strengthen the ankyrin-1 mediated linkage of the membrane skeleton to AE1, as protein 4.2 deficient red cell membranes have increased AE1 rotational mobility and extractability [125].

1.8.5 The Rh Complex

AE1 interacts with the proteins of the Rhesus (Rh) complex, the polypeptides that comprise the antigens of the rhesus blood group system, and which are reduced or absent in Rh_{null} red cells. These include the Rhesus-associated glycoprotein (RhAG), the Rh polypeptides (RhD, RhCE, that carry the epitope for the Rh antigens; D, E/e and C/c), CD47, LW (both adhesion molecules; CD47 is also a marker of self) and glycophorin B.

RhAG is thought to form a gas channel, although the gases that it transports are somewhat unclear. The discovery that RhAG has homology with the MEP/AMT ammonium transporters led to the hypothesis that RhAG transports

ammonia/ammonium [224]. Cell studies, in erythrocytes, Xenopus oocytes, yeast and HeLa cells described RhAG variously as a NH_3/NH_4 exchanger, ammonium exporter, an ammonium channel etc. The possibility remains that ammonium is not the principal substrate of this molecule and that it may transport nitric oxide or CO_2 along with ammonium ions, a role for AE1 in the efflux of nitric oxide from deoxygenated erythrocytes has been reported [225, 226]. Cysteine residues in the N-terminal cytoplasmic tail mediate the transfer of nitric oxide from bound deoxyhemoglobin to the cell exterior. This metabolon increases the efficiency of the transfer and protects the nitric oxide from reacting with other substrates in the cell or the membrane.

CD47 is a candidate as a sensor for the extracellular environment of the red cell, it interacts with thrombospondin-1 and SIRPα. Is involved in cell recognition and cell adhesion in many cell types, and when complexed with integrins, can activate G protein signalling [227]. Although red cells do not have integrins, CD47 signalling could be mediated by protein 4.2. This is supported by the observation that young sickle cell erythrocytes show different CD47 mediated adhesion properties under static and flow conditions, suggesting that CD47 can sense these two differing external environments [228].

There also appears to be a role for protein 4.2 in mediating and stabilising the interaction of AE1 and the RH complex-this is suggested by studies of human red cells with total deficiency of protein 4.2, but normal AE1. The cells almost completely lacked CD47 and had altered RhAG, indicating that protein 4.2 provides a major binding site for CD47 and the Rh complex, and anchors the Rh complex to the cytoskeleton [229]. The observation that Rh proteins are associated with the red cell cytoskeleton [230] fits with this model, and suggests that the Rh complex selectively interacts with the ankyrin-associated tetrameric fraction of AE1.

AE1 may thus act as a scaffold for assembling macro-complexes of proteins in the red cell membrane, which modulate the red cell's metabolic, transport, and mechanical properties in response to the environment (Figure 1-4). This

may be particularly important in the microcirculation, where the red cell is in close contact with the endothelial wall. The red cell undergoes substantial morphological changes to pass through the small capillaries, and reduction of its rigidity during this deformation would minimise its resistance to flow. Nitric oxide is also released from red cells under these conditions, which acts to relax the tone of blood vessel walls and increase blood flow to oxygen-starved tissue [225]. Rapid movement of CO_2 into and nitric oxide out of the cell is required due to the small amount of time the red cell spends in the capillary system (0.3-1 sec). CD47 might act as a sensor for the contact with the endothelium and activate CO_2 and nitric oxide membrane transport via Rh/RhAG. CD47 may also signal the reduction in erythrocyte rigidity need for the red cell to pass through the capillary at all, by altering the erythrocyte cytoskeleton via protein 4.2.

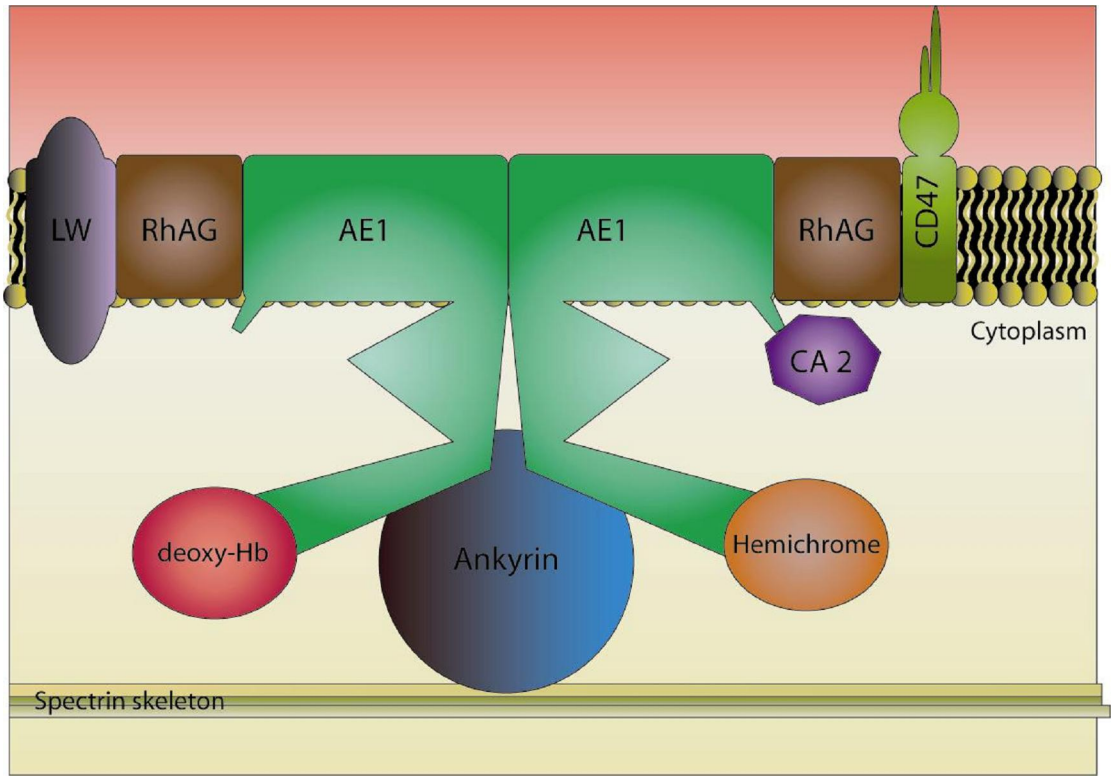

Figure 1-4 A cartoon of the Rhesus complex, showing ankyrin binding to the spectrin skeleton and supporting the AE1 dimer/oligomer.

This is associated in the lipid bilayer with RhAG, LW and CD47. The N-terminal of AE-1 associates with deoxy-hemoglobin or hemichrome material. The C-terminal end binds carbonic anhydrase 2, forming the metabolon.

1.8.6 AE1 and red cell disease

1.8.6.1 Hereditary Spherocytosis

Hereditary Spherocytosis (HS), a condition that was first described by two Belgian physicians in 1871 [231]; is a common (1 in 2000) inherited hemolytic anaemia that causes erythrocytes to become spherical and osmotically fragile, due to a progressive loss of surface area, and to be destroyed prematurely in the spleen.

HS results from mutations in protein 4.2, ankyrin or AE1. Ankyrin and protein 4.2 mutations result in a slight reduction in membrane AE1, however various mutations of SLC4A1, the AE1 gene (including missense, nonsense and frameshift mutations) have been reported to cause autosomal dominant HS, associated with a 20-40% reduction in AE1 protein levels in the red cell plasma membrane, with an associated decrease in protein 4.2 content [232-237]. These mutations account for approximately 20% of HS cases. Loss of AE1 in the cell membrane reduces the number of anchoring interactions between the cell membrane and the cell cytoskeleton [113], causing areas of AE1-free membrane to become susceptible to 'blebbing', reducing the surface area to volume ratio and thus the spheroidal shape.

Heterozygotes have a mild to moderate hemolytic anaemia, homozygotes, whom would be predicted to have no AE1 at their red cell membrane would fare much worse, with much more fragile red cells and seriously impaired CO_2 handling.

Only three cases of homozygous HS have been reported; one case with the Val488Met mutation (band 3 Coimbra) which caused severe transfusion dependent hemolytic anaemia and dRTA with Nephrocalcinosis [179]; one with band 3 Neopolis (a mutation affecting the donor splice site of exon 2), which resulted in an N-terminal 11 amino acid truncated protein, causing severe spherocytosis, but no dRTA, due to the nature of the defect [238] and one with the Ser677Phe mutation (band 3 Courcouronnes) which caused spherocytosis and incomplete dRTA [239]. The Ser667Phe mutation is

interesting as it causes a trafficking defect that can be partially rescued by GPA and more completely rescued by wt AE1, which may explain its mild phenotype in heterozygotes, who have only a small reduction in their total red cell AE1.

1.8.6.2 Hereditary Stomatocytosis

Hereditary Stomatocytosis (HSt) and it's allied disorders (cryohydrocytosis, familial pseudohyperkalemia and hereditary xerocytosis) is a group of dominantly inherited diseases in which red cells have an increased permeability to monovalent cations. Like hereditary spherocytosis, there appear to be a number of causes of this group of disorders, including mutations of AE1, and an as yet undetermined mutation that has been mapped to chromosome 16.

Like HS, the cells have a reduced surface area to volume ratio, causing a typical appearance with a slit like central concavity; which looks a little like a mouth (figure 1-5), hence its name. Stomatocytes, macrocytosis, increased red cell Na^+ and decreased red cell K^+ are classical features. The cells usually have increased cell water content, but some variants (xerocytosis) can be dehydrated, osmotic fragility is increased and a degree of hemolysis is present, and may be severe. Splenectomy reduces the rate of hemolysis [240], which is presumably the site of removal of the defective red cells, it may not be beneficial in xerocytosis [241].

Various subtypes are classified based on the temperature dependence of their leak [242]. Some fall under the rubric of 'cryohydrocytosis', which means that they have a leak, which is at its greatest at 4^oC, and these are caused by mutations in AE1 [243]. The mutant AE1 is inactive as an anion exchanger and has a cation channel-like activity (a 'cation leak') causing the red cells to leak monovalent cations. This is discussed later in this chapter.

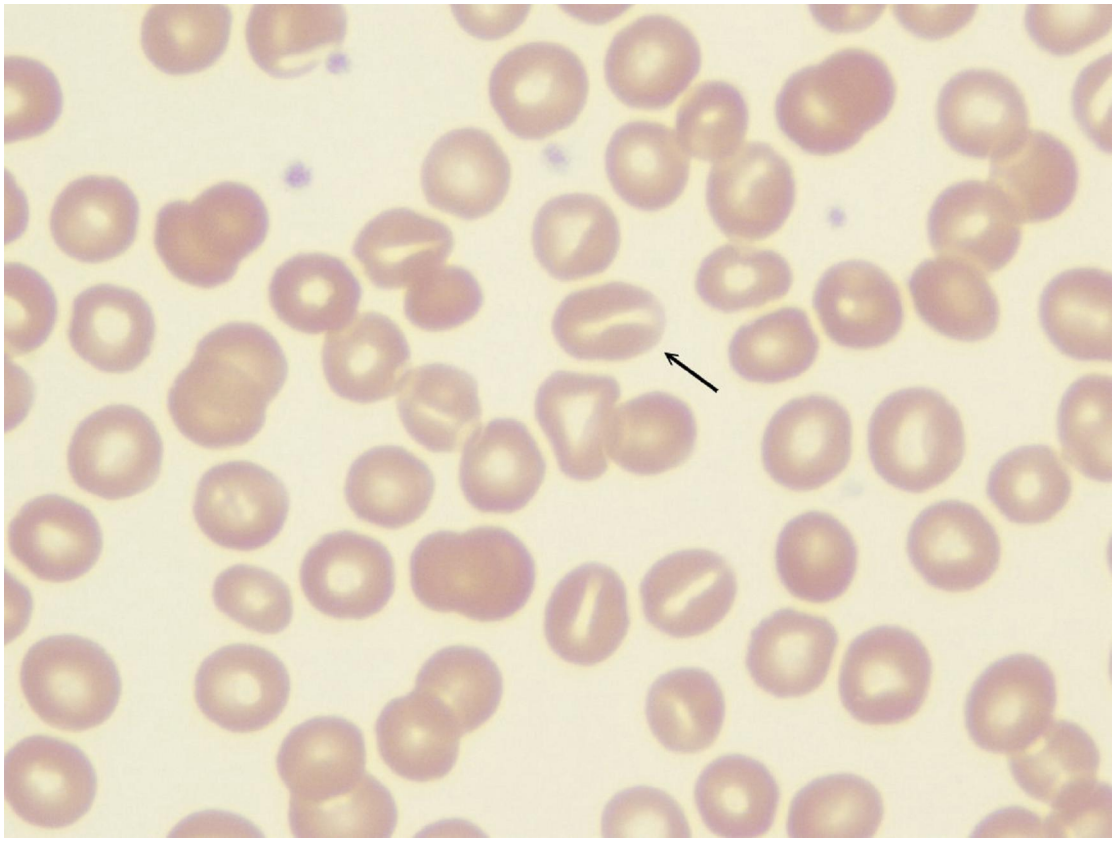

Figure 1-5 A blood film from a patient with hereditary stomatocytosis.

The arrow points at a stomatocyte, with its slot like central depression.

1.8.6.3 Southeast Asian Ovalocytosis

Southeast Asian Ovalocytosis (SAO), also known as hereditary ovalocytosis, Melanesian elliptocytosis or stomatocytic elliptocytosis, is another autosomal dominant red cell disorder, resulting from a mutation of AE1 (the deletion of amino acids 400-408), homozygosity is probably lethal in utero [244, 245].

It is found in the native populations of Melanesia (where it is very common [246, 247]) and Malaysia and in parts of Indonesia, Madagascar and the Philippines [247-250]. It is rare in Western populations but has been reported [251, 252].

The affected patient's red cells have a reduced surface area to volume ratio, causing typically 20% of the red cells to be rounded elliptocytes (see figure1-6). Stomatocytes are present in all patients including those with the AE1 mutation who lack elliptocytes (up to 25% in one series [253]). These stomatocytes have characteristic 'stoma', which are similar to cells seen in cryohydrocytosis.

Hemolysis is reduced or absent [247, 248, 250], and the red cell membrane is rigid, with a rigidity of 10-20 times that of normal [254, 255], indicating that the membrane rigidity is not a major determinant of erythrocyte survival. The cells are also unusually heat resistant [256], resistant to pharmacological induction of endocytosis [257] and strongly resist crenation [257].
The red cells are also cation leaky, with increased red cell Na^+ and K^+ permeability and increased glycolysis to compensate for increased cation pumping [250, 258], in a strikingly similar fashion to that seen in the HSt spectrum disorders. It has in fact been suggested that SAO be grouped with the HSt spectrum disorders on this basis [258].

SAO is also interesting because it is found with the highest frequency in very malarious areas of Papua New Guinea, where its gene frequency can be as high as 35% in some communities [259]. This is probably because this mutation is subject to a positive evolutionary selection pressure; it has been

shown to confer a strong protective effect against cerebral malaria by an unknown effect [245, 260].

Malaria is endemic to the lowland areas in which SAO is commonly found in the aboriginal tribes of Melanesia [246, 259, 261], with rates of SAO carriage of 5-25%. The prevalence of SAO increases with age in populations challenged by malaria [262], which implies that there is a survival advantage for SAO affected individuals. SAO shows strong clinical protection against cerebral malaria, but exacerbates malarial anaemia [253, 260]. In vitro, SAO red cells have been shown to be resistant to invasion by falciparum parasites, which was attributed to the membrane rigidity [256, 263], but may, in fact be an artefact of ATP depletion in cold stored cells due to compensatory cation pumping in the face of increased membrane cation leakiness, as this is not seen in freshly taken SAO red cells [258, 264].

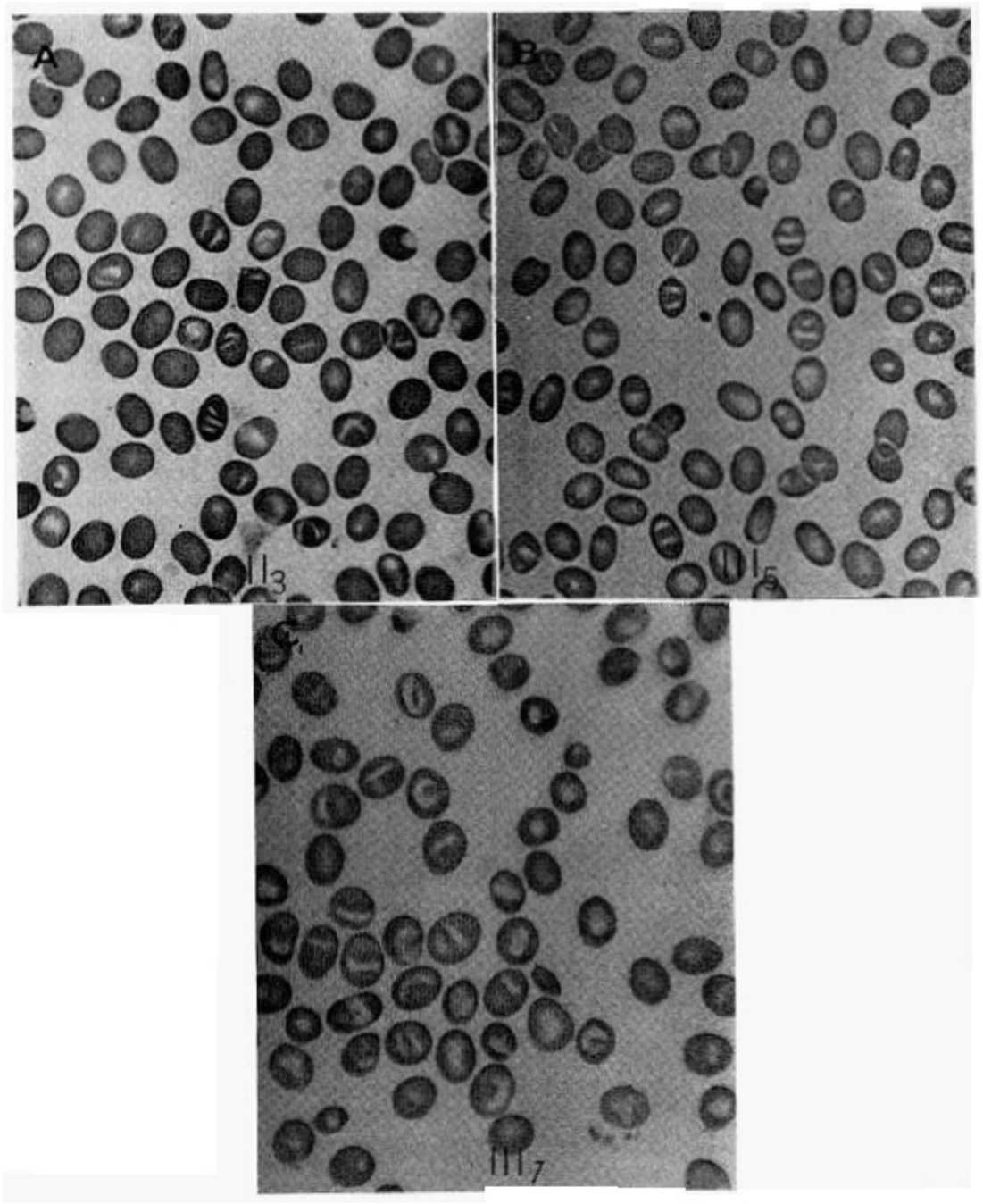

Figure 1-6 Blood films from three of the original family described with SAO by Honig et al in 1971.

The elliptocytes are clearly seen in all three films.

1.8.7 Conclusions

- GPA and AE1 interact at an early stage after synthesis, GPA increases the amount of AE1 in the cell membrane, and it may increase AE1 anion transport function too.
- Denatured haemoglobin binds to AE1 forming aggregates, which act as a senescence antigen, signalling for the removal of the red cell.
- AE1 links ankyrin to the membrane protein spectrin, forming an important link between the membrane and the membrane skeleton. It also binds protein 4.1 and 4.2 for similar structural reasons.
- AE1 associates in the cell membrane with the Rh complex, which comprises RhAG RhD, RhCE, CD47, LW and GPB.
- In this complex, RhAG may mediate the transport of ammonium and possibly CO2 and nitric oxide.
- CD47 may play a role in sensing the external environment of the red cell, possibly mediating changes in the red cell plasticity via AE1 and protein 4.2 to the cytoskeleton.
- HS results from mutations in AE1, ankyrin or protein 4.2. Resulting red cells are spherical and are much more fragile, prone to haemolytic anemia.
- HSt and its allied disorders have red cells with a reduced surface area to volume ratio and have an increased permeability to monovalent cations. This affects their hydration and causes a tendency toward haemolytic anemia.
- SAO also causes a reduced surface area to volume ratio and increased permeability to monovalent cations, but also causes increased cell membrane rigidity. It is strongly protective against cerebral malaria, but may worsen malarial anaemia.

1.9 AE1 and the cation leak

Having detailed the numerous physiological functions of AE1 already, I'm now going to describe the work delineating a more novel physiological (and sometimes pathophysiological) function of AE1; it's ability to function as an ion channel.

1.9.1 AE1 channel permeability and cell volume regulation

Most cells need to be able to adapt to changes in external osmolality by regulating their volume. After swelling in hypo-osmotic medium, cells recover their previous volume by the process of regulatory volume decrease (RVD).

RVD is achieved by the loss of osmotically active molecules from the cell interior, followed by the osmotic loss of water. These molecules may be inorganic ions, such as potassium or chloride, or small organic solutes of varying classes, such as polyols (e.g. sorbitol or myo-inositol), amino acids (e.g. taurine) and methyl amines (e.g. betaine). These organic solutes may comprise as much as half of the RVD response [265], and the loss of these solutes appears to occur via a specific pathway.

A number of authors have observed that the volume-activated transport of organic osmolytes is via a single pathway that resembles a channel and is inhibited by a range of anion transport inhibitors, in Madin Darby Canine Kidney (MDCK) cells [266], flounder erythrocytes [267] and rat C6 glioma cells [268].

This sensitivity to anion transport inhibitors led a number of authors to suggest that the anion exchanger AE1 might play a role. Goldstein et al suggested that AE1 was the swelling activated transport system itself, based on the close relationship between the dose response curves for the effect of DIDS on anion exchange and the volume activated transport of organic solutes [269]. Motais and co-workers proposed that AE1 acted as a regulatory protein, as

hypotonic swelling activated not only taurine and potassium efflux, but also a broad range of other solutes, such as sodium, choline and tetramethylammonium to diffuse out of the cell [265, 270, 271]. Moreover, these effluxes are all inhibited by DIDS (and other AE1 inhibitors), and the dose-response curves are identical.

Its pharmacological profile led to the suggestion that this pathway was a swelling activated anion channel [266, 267], a suggestion that was bolstered by data from single channel patch clamp experiments, demonstrating that some amino acids, that were involved in the RVD in MDCK cells, could permeate a swelling activated anion channel in MDCK cells [272], work that was replicated in C6 glioma, and other, cells.

This swelling activated channel has certain characteristics:

1) It is an outwardly rectifying conductance (the current-voltage relationship is not linear, the slope of the curve becoming steeper as the inside of the cell becomes more positive).
2) It exhibits a high permeability for anions over cations, but has a broad anion specificity.
3) The conductance is inhibited by a variety of anion exchange inhibitors, including stilbene derivatives (e.g. DIDS), 5-nitro-2-(3-phenylpropylamino)benzoic acid (NPPB), tamoxifen, dideoforskalin, lanthanum and ketoconazole. Although the drug sensitivity varies between cell types.

The observation was made that fish erythrocytes respond to osmotic swelling by undergoing the RVD, which involves the efflux of KCl and amino acids (mainly taurine) [265], whilst non-nucleated mammalian erythrocytes have no swelling activated taurine transport, with volume regulation being achieved via activation of K^+/Cl^- cotransport. However, both fish and mammals have AE1 in their red cell membranes. On this basis, the transport properties of cloned trout AE1 (tAE1) were compared to cloned mouse AE1 (mAE1) when expressed in Xenopus Laevis oocytes [273].

Both isoforms showed anion exchange activity, but tAE1 expression induced a large increase in oocyte Cl^- conductance. This conductance had a near linear current-voltage relationship, was not inactivated by depolarisation and was correlated to the amount of expressed proteins in a sigmoidal fashion. It also induced a large increase in Na^+ independent taurine permeability, which was correlated linearly with Cl^- conductance. Oocytes expressing mAE1 induced neither Cl^- nor taurine transport.

These data provided strong evidence that when expressed in the Xenopus oocyte, tAE1 was capable of spontaneously acting as an anion/organic osmolyte channel, note, however that in the trout erythrocyte, this channel activity is only activated by cell swelling. tAE1 is DIDS sensitive in trout erythrocytes, is insensitive to it when expressed in Xenopus oocytes, which is when it also spontaneously demonstrates channel activity. This implies that tAE1 adopted a different conformation when expressed in oocytes. tAE1 differs structurally from mAE1 in that the extracellular loop connecting the transmembrane domains TM5 and TM6 is large in tAE1 (the so-called 'Z-loop'), compared to mAE1. Oocyte expression of a chimera construct tAE1, with the Z-loop shortened, was sensitive to DIDS and demonstrated no spontaneous channel activity.

Guizouarn et al showed that in trout erythrocytes, the RVD had two different pathways, depending on how the cell swelling was activated, a broadly specific channel (q.v.) and a K^+/Cl^- cotransporter. The channel was activated by a decrease in intracellular ionic strength, the K^+/Cl^- cotransporter by cell enlargement, the K^+/Cl^- cotransporter was also down regulated by decreasing intracellular ionic strength. Therefore cells swollen by salt accumulation responded by activating the K^+/Cl^- cotransporter, whilst those cells swollen by electrolyte dilution, activated both pathways, with a resulting reduced loss of electrolytes and an increased loss of taurine [274].

The same author demonstrated that tAE1 when expressed in Xenopus oocytes also mediated a cation leak permeability of Na^+ and K^+, which, like the anion channel activity and anion exchange, was blocked by H_2DIDS. Site

directed mutagenesis of Lys-522 to Arg abolished the inhibitory effect of H_2DIDS on these transport properties. Also, the initiation of a non-tAE1 related anion conductance (via the expression of CFTR) did not induce a cation permeability in the oocyte, suggesting that the cation permeability was mediated by tAE1 rather than an endogenous oocyte transporter activated by the anion transport of tAE1 [275].

Martial and co-workers collected further data on tAE1, providing more evidence that tAE1 acts as a channel, whilst identifying specific regions in the protein important for the channel activity. They performed site directed mutagenesis at a targeted region around TM7 and identified several amino acid residues which when mutated, altered the anion conductance without altering the anion exchange ability of the protein. In contrast, point mutagenesis at the C-terminal domain of the protein increased the anion conductance and reduced the anion selectivity, increasing the Cl- influx nearly threefold [276, 277].

1.9.2 AE1 channel activity in humans

A definite link between AE1 channel activity and disease in humans began with the characterisation of the molecular defect in hereditary stomatocytosis and it's allied disorders, which comprise HSt, cryohydrocytosis, familial pseudohyperkalemia and hereditary xerocytosis. As mentioned previously, these are rare syndromes characterised by stomatocytic red cell morphology (red cells with a mouth shaped area of central pallor-see figure 1-5), varying degrees of haemolytic anaemia, very large monovalent cation leaks and relative Na^+/K^+ pump failure.

Cation permeabilities as great as 15 to 40 times greater than normal have been observed [240, 278, 279], these permeabilities may affect the hydration of the cell, which may become over-hydrated or dehydrated.

The cation leak is temperature dependent, and a classification system has been described that stratifies this group of disorders on the basis of the temperature dependence of the associated cation leak. In pseudohyperkalaemia, for example, the cation leak that is greatest at $0^{o}C$ can cause artefactually high serum K^{+} measurements in venesected blood samples that have been allowed to cool.

Monovalent cation transporters, such as the Na^{+}/K^{+} pump or the K^{+}/Cl^{-} co-transporter [280] are stimulated by the influx of Na^{+}, but become overwhelmed. Pump kinetics are normal [281], and the number of pumps is increased several-fold [240, 282]. The stomatocytes expend extremely large amounts of ATP [283] to try and correct the cationic milieu by pumping, to avoid osmotic rupture.

Bruce et al identified 11 human families with either stomatocytic or spherocytic autosomal dominant haemolytic anaemias, with an increased red cell membrane permeability to monovalent cations. These were found to be associated with a number of single amino acid substitutions in AE1 (S731P, H734R, L687P, H705Y and R760Q). Red cells from these individuals had much reduced anion transport, and the cation leak in these red cells was inhibited by AE1 inhibitors (SITS, dipyridamole and NS1652). When the mutant proteins were expressed in Xenopus oocytes, they induced Na+ and K+ fluxes in the oocytes, and the induced Cl- flux was much lower than that seen in oocytes expressing wt AE1. The cation leak was temperature sensitive and varied between the different pedigrees [243].

Guizouarn et al further characterised the transport characteristics of 4 of these AE1 mutations (L687P, D705Y, S731P and H734R) by expressing the AE1 proteins in Xenopus oocytes, demonstrating that they convert the protein from an anion exchanger into a cation conductance [284].

1.9.3 Conclusions

- Cells that undergo osmotic swelling need to reduce their volume by, means of a regulatory cell volume decrease (RVD) by ejecting osmotically active molecules from the cell interior.
- AE1 was suspected as a stretch activated osmolyte transporter on the basis of its transport characteristics and pharmacokinetics.
- Trout AE1, when expressed in Xenopus oocytes, showed a large anion permeability, including taurine, and also a significant cation permeability. This was not seen in oocytes expressing mouse AE1. The properties of trout AE1 when expressed in oocytes were different to those seen in trout erythrocytes. Modification of the z-loop abolished the spontaneous permeability seen previously.
- Several HSt and HS AE1 mutants were shown to have a cation permeability that was temperature dependent when expressed in Xenopus oocytes, although they had much reduced anion exchange activity.

1.10 Hypothesis

I hope that I've managed to outline that both sodium and potassium losses occur in dRTA, for reasons that are not clearly understood, but may be directly related to the failure of the α-intercalated cells to acidify the urine. I have also summarised the molecular mechanisms of AE1 related dRTA, and the cation channel property that AE1 can display, in known human mutants and in other vertebrates, as a part of the RVD. It is in this context that I formulated my hypotheses.

1) The increased delivery of sodium to the CCD, with its subsequent uptake into principal cells is a potent and robust stimulus of urinary acidification and can form the basis of a test to distinguish between

those with incomplete dRTA and those with normal urinary acidification.

2) The AE1 mutations that cause mistrafficking in α-intercalated cells and thus dRTA also cause AE1 to act as a cation channel and thus contribute to urinary potassium losses.

2. General Methods

2.1 Introduction

Many of the methods and materials employed in these studies were unique to that given set of experiments, but the last two chapters have a great deal in common in terms of their experimental techniques, which I will detail here and outline any differences in the text of the appropriate chapter.

2.2 DNA synthesis

The pSP65erythroid human AE1 (hAE1) plasmid was used to construct the kidney AE1 (kAE1), deleting the 65 N-terminal amino acids. The erythroid construct was amplified by polymerase chain reaction (PCR) between the Val65 and the Tyr390 with a forward primer introducing a SacII restriction site in 5' and a reverse primer overlapping the EcoRV site in hAE1 sequence. The pSP65erythroid hAE1 had the N-terminal part deleted by SacII-EcoRV digestion with the SacII-EcoRV PCR product introduced in replacement. The obtained pSP65kAE1 plasmid was checked by sequencing and used to make point mutations using the QuickChange Site-Directed Mutagenesis kit (Stratagene, USA).

For point mutations, primers where used with appropriate codon substitutions. Primers were purchased from Eurogentec (Seraing, Belgium); polymerase chain reactions (PCRs) were performed using a Biometra "UNO Thermoblock" thermocycler (Göttingen, Germany). Sequences generated by PCR were sequenced in their entirety to ensure that no polymerase errors were introduced (Gexbyweb, Meylan, France).

HindIII linearised pSP65kAE1 wildtype and mutant plasmids were transcribed using SP6 polymerase (Ambion transcription kit). HindIII linearised BSXG-GPA plasmid was transcribed using T7 RNA polymerase (Ambion transcription kit). RNA concentrations were determined on a formamide/formaldehyde agarose gel in MOPS (3-[N-Morpholino]propanesulphonic acid) buffer.

2.3 Agarose gel electrophoresis

This was used for the routine separation of nucleic acids. Electrophoresis was performed in a Horizon 58 horizontal format tank (Life Technologies, Paisley UK). Power was from a Consort E831 supply (Turnhout, Belgium). All other materials were from Sigma unless otherwise stated.

A 1% agarose gel was prepared by dissolving 1g of molecular biology agarose in 100 ml of Tris-HCl pH 8.3, 100 mM borate, 2 mM ethylene diamine tetra-acetic (EDTA) (Tris-borate-EDTA buffer, TBE) by heating in a microwave oven. The agarose solution was allowed to cool to 50^{o}C and cast in a gel deck. Samples were loaded in 0.04% bromophenol blue, 0,04% xylene cyanol, 5% glycerol. Gels were run at 75 V in TBE until the bromophenol blue and xylene cyanol had migrated an appropriate distance through the gel. 0.5 µg/ml ethidium bromide was added to the gel solutions and running buffer to enable visualisation of the nucleic acid bands. Ethidium bromide-stained gels were photographed through a number 15 orange filter using a Polaroid GelCam (Wheathampstead, UK)

2.4 Buffer solutions

2.5 Xenopus oocyte harvesting

Xenopus laevis frogs were placed in MS222 (0.2%) until completely anaesthetised, according to the protocol approved by our animal ethics committee. The surgery consisted of the removal of 5 oocyte-containing ovarian lobes. After surgery, animals were put back in cold water between 0 and 4^{o}C to recover from the anaesthesia, monitored for 4 hours and then replaced in the aquarium.

2.6 Oocyte injection

Collected oocytes were washed in Modified Barth's Solution (MBS) composition:

NaCl	85 mM
KCl	1 mM
$NaHCO_3$	2.4 mM
$MgSO_4$	0.82 mM
$Ca(NO_3)_2$	0.33 mM
$CaCl_2$	0.41 mM
HEPES	10 mM
NaOH	4.5 mM
pH	7.4
Penicillin	10 U/ml
Streptomycin	10 μg/ml

After washing in MBS, defolliculation was carried out by 16h incubation in 18°C MBS containing 1.3 mg/ml collagenase (SERVA, Heidelberg, Germany), followed by 30 minutes incubation in Ca^{2+} free MBS. Stage V-VI oocytes were then injected with a mixture of 10 ng of kAE1 and 2.5 ng GPA cRNA, and were maintained in 18°C MBS for three days before starting the experiments.

2.7 Western blot of oocyte membrane proteins

Oocyte membranes were prepared by homogenization of 20 oocytes (control or injected) in cooled Tris-HCl buffer, 20 mM, pH 7.4, 250 mM sucrose, and 0.5 mM of a protease inhibitor Pefabloc (Roche, Paris, France).
The mixture was centrifuged (3 X 10 min) at 4°C; 350g, then 1,400g and finally 3,000g in an Eppendorf tube; after each centrifugation, the pellet was discarded. The third supernatant was ultracentrifugated at 255,000g, 2 h, 48C and membrane pellet solubilised in the homogenisation buffer. Protein concentration was measured with the BioRad (Hercules, CA) kit and 50 mg of proteins were then loaded/lane of SDS–PAGE electrophoresis gel. Western blot transfer was done with a semi-dry transfer system from Biometra on nylon membrane (Hybond-C extra, Amersham, Orsay, France).

The presence of kAE1 was detected by antibody Bric 170 directed against the C-terminus of kAE1. The secondary antibody was anti-mouse IgG-peroxidase, which was detected by chemiluminescence using a Fujifilm Las-3000 Luminescence image analyser.

2.8 Intracellular Cation Measurements

Injected oocytes were incubated in MBS containing ouabain (0.5 mM) and bumetanide (5 µM) at 19^{o}C for 3 days. Five oocytes were quickly washed in 7.5 ml of milliQ water (Millipore) and dried on aluminium foil for 7 hours at 80^{o}C after removing excess extracellular fluid. Dried oocytes were measured to determine dry cell solids. Intracellular ions were extracted by suspending dried oocytes in 4 ml of milliQ water overnight at 4^{o}C. Perchloric acid (80µl of 70% v/v) was then added to the suspension. After centrifugation at 30 000g for 10 minutes the clear supernatant was saved for analysis of cations. Measurements of sodium and potassium were done with a flame spectrophotometer (Eppendorf). Results were expressed as micromoles per gram dry cell solids (µmol/g d. wt.).

2.9 Intracellular pH measurements

Oocyte intracellular pH was measured using selective microelectrodes made as follows. Glass micropipettes were pulled from clean borosilicate capillaries (GC 150F-10) (Harvard Apparatus), placed in an oven, and dried at 120^{o}C for one hour. The microelectrodes were vapour-silanised with N,N-Dimethyltrimethylsilylamine (Fluka 41716) and then baked for 2 hours at 150oC. A small drop (0.3 µl) of a proton ion exchanger (hydrogen ionophore I-Cocktail A: ref Fluka 95291) was introduced into the electrode shank. The selective microelectrodes were kept in the dark overnight, tips downwards, to allow the exchanger to reach the tip and then were back filled with phosphate buffer (pH 7.0) and calibrated in solutions of pH 6.8 and 8.0. A standard microelectrode filled with 3M KCl was used for measurement of membrane potential. The electrodes were connected to a high-impedance probe of a two

channel FD 223 electrometer (World Precision Instruments). The bath was grounded via a 3M KCl agar bridge connected to an Ag-AgCl wire. The slope of the pH microelectrodes was between 54 and 58 mV per pH unit.
The ability of the expressed AE1 proteins to regulate intracellular pH was assessed by measuring intracellular pH of oocytes kept in MBS without HCO_3^- then incubated in the following medium:

NaCl	63.4 mM
KCl	1 mM
Na HCO_3^-	24 mM
$MgSO_4$	0.82 mM
$Ca(NO_3)_2$	0.33 mM
$CaCl_2$	0.41 mM
HEPES/NaOH	5 mM
pH	7.35
CO_2	5%
O_2	95%

The oocytes were then bathed in MBS without Cl^-, composed as follows:

Na-gluconate	63.4 mM
K-gluconate	1 mM
$NaHCO_3^-$	24 mM
$MgSO_4$	0.82 mM
$Ca(NO_3)_2$	0.74 mM
HEPES/NaOH	5 mM
pH	7.35
CO_2	5%
O_2	95%

Results were given in ΔpHi per min ± standard error. ΔpHi was measured when acidified oocytes were exposed to the Cl^- free mediumThis corresponds to the initial slope of the alkalinisation phase of the curve (Figure 2-1). . Expression of proteins was assumed to have an equal effect on intracellular buffer capacity, which was not measured.

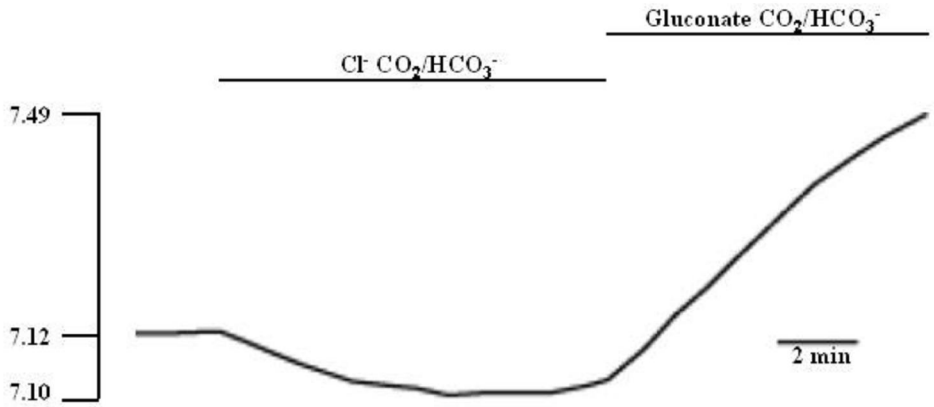

Figure 2-1 An example intracellular pH trace for an oocyte expressing wt AE1.

There is an initial decrease in intracellular pH during CO_2 irrigation when the extracellular medium contains chloride. When this is removed, the intracellular pH rises again due to bicarbonate transport from the oocyte ceasing, demonstrating that it is chloride dependent.

3. Novel Clinical Assessment of Urinary Acidification

3.1 Introduction

As outlined previously, the clinical features of dRTA can vary, ranging from an asymptomatic urinary acidification defect without systemic acidosis (so-called 'incomplete' dRTA), with or without the incidental finding of renal tract calcification, to major effects in childhood with acidosis, growth retardation, rickets and extensive medullary nephrocalcinosis, sometimes progressing to renal failure. Detection and diagnosis are worthwhile, even in those with asymptomatic or incomplete dRTA, so as to minimize future skeletal and renal complications [285], and in familial cases to assist genetic counselling.

In those patients with a metabolic acidosis and near normal GFR, a diagnosis of dRTA can be made when urine pH is consistently >5.3 [286]; but if there is no systemic acidosis and plasma bicarbonate concentration is within the normal range, a test of urinary acidification is required.

The history of the different assays tried for these have been described in the introductory chapter. Briefly, they comprise 3 approaches.

Firstly, acidification can be tested by inducing a systemic acidosis, this was the approach taken by Wrong and Davies with the short ammonium chloride test [41]. This remains the 'gold standard' test for incomplete dRTA, but due to gastric irritation is unpleasant, takes 8 hours to complete, and may induce vomiting which can render the test invalid.

Secondly, examination of the difference between blood and urine CO_2 tensions (U-B pCO_2) was suggested by Halperin and colleagues [52]. This has been criticised as a low U-B pCO_2 has been observed in pRTA and advanced renal failure[53, 54], the test therefore has low specificity.

Finally, assays based on an indirect and elegant approach of simply increasing the load of sodium ions reaching the distal nephron have been described. Sodium is absorbed rapidly in the CCD by principal cells via apical ENaC channels, whilst chloride diffuses slowly from the lumen via the paracellular route; this disparity in diffusion potentials generates a net

negative electrochemical gradient in the lumen, which drives proton secretion into the lumen via the apical proton pump in the intercalated cell (see Figure 3-1). This method is the basis of the intravenous sodium sulfate test [48], and also the oral furosemide test [55] (in which furosemide inhibits NaCl uptake in the loop of Henle, thus increasing distal delivery). Experience has found these methods are unsatisfactory due to inconvenience and unreliability, even when urine pH changes in response to an increased distal delivery of sodium have been reported to be greater in normal subjects when they are sodium depleted [56] or following prior administration of a mineralocorticoid [57].

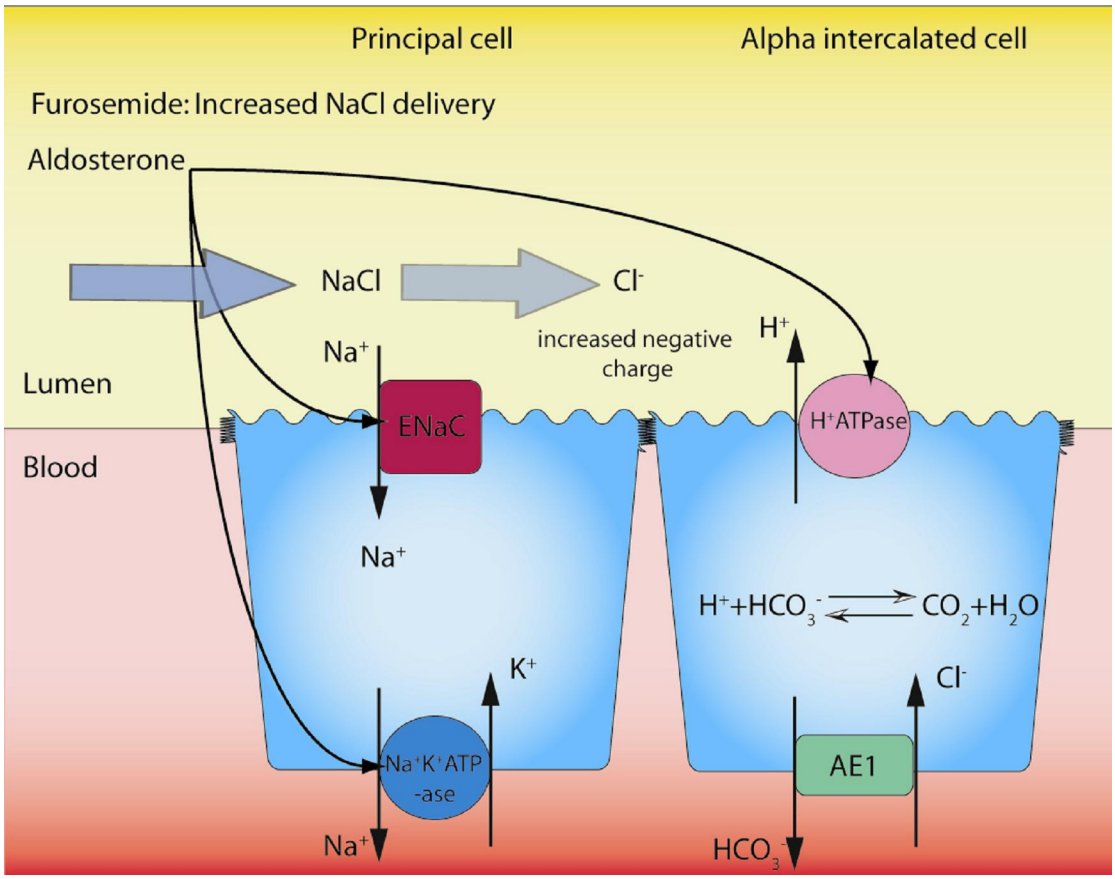

Figure 3-1 A cartoon of the mechanism of action of the furosemide and fludrocortisone test.

Furosemide increases delivery of NaCl to the CCD, which is represented by the arrows running from left to right in the figure. Aldosterone increases the uptake of Na^+ from the lumen by increasing the amount of ENaC at the principal cell apical surface and the amount and activity of basolateral Na^+K^+ATPase. The slow paracellular absorption of Cl^- ions results in a net negative luminal charge, which favours alpha intercalated cell proton extrusion by the apical proton pump, which is also increased by aldosterone.

Although our own initial observations suggested that the addition of fludrocortisone led to a more consistent effect than furosemide alone [287], the timing of the mineralocorticoid seemed to be important. This is because the relevant action of a mineralocorticoid like aldosterone is in part 'non-genomic' and can occur more rapidly than was originally supposed. Aldosterone increases epithelial sodium channel (ENaC) density on the apical surface of principal cells within 30 minutes of administration via mobilization of endocytic stores of pre-formed EnaC [288]. Basolateral Na^+,K^+-ATPase activity is also increased acutely following mineralocorticoid administration [289], as is α-intercalated cell vH^+-ATPase activity; the latter has been shown to occur within 15 minutes of exposure [290-292].

With these observations in mind, we hypothesised that simultaneous dosing of furosemide (to increase distal tubular sodium delivery) and fludrocortisone (to enhance principal cell sodium reabsorption and α-intercalated cell H^+ secretion) should provide a sufficient and consistent stimulus to unmask an acidification defect in dRTA, without the need for NH_4Cl. (see Figure 3-1) To test this, we examined urinary acidification in response to the standard short NH_4Cl test and compared it with the response to the furosemide/fludrocortisone test in healthy subjects and in a group of patients with known dRTA.

3.2 Aims

1) To compare the sensitivity and specificity of the novel simultaneous furosemide and fludrocortisone test against the short ammonium chloride test in a group of healthy control subjects and a group of patients with dRTA.
2) To ascertain the urinary physiological parameters of individuals undergoing each test, namely urinary ammonium, titratable acidity, potassium and sodium concentrations as well as flow rates.
3) To compare both tests for adverse effects and convenience.

3.3 Methods and Materials

3.3.1 Subject selection

Ten patients with previously diagnosed dRTA were recruited (see Table 3-1), along with 11 healthy volunteers. Of those who completed the study, mean creatinine clearance (adjusted for weight) was 69 ± 8 ml/min (± SE) in the dRTA patients and 100 ± 11 ml/min in the controls.

Those from the dRTA group had their diagnoses confirmed by either a previous ammonium chloride test or failure to acidify their urine in the presence of systemic acidaemia. Two had autoimmune-associated dRTA, 4 had familial dRTA and 4 had idiopathic dRTA. The group comprised 2 males and 8 females, age range 26 to 56 years. All patients in this group had hypokalemic or normokalaemic dRTA; patients with hyperkalaemic dRTA were not selected (even if the diagnosis of a complicating type 1 dRTA seemed likely) to exclude any confounding effect of a potentially coincident type 4 RTA. The control group (8 males, 2 females, aged from 21 to 51 years) comprised healthy volunteers recruited from the medical school and junior medical staff.

All subjects underwent a short NH_4Cl test and a furosemide/fludrocortisone test on separate days, and in random order, without fasting, with at least one week between tests.

3.3.2 The NH_4Cl protocol

The NH_4Cl test involved taking a baseline urine sample, followed by oral NH_4Cl at a dose of 100 mg/kg body weight given as 500 mg gelatine capsules. This dose was taken over 1 hour (hours 0-1 in each figure) with water to minimise gastric irritation. Urine was then collected every hour, starting 2 hours after dosing began, until 8 hours after the baseline sample.

3.3.3 The furosemide/fludrocortisone protocol

The furosemide/fludrocortisone test involved taking a baseline urine sample, followed by oral administration of furosemide (40 mg) and fludrocortisone (1

mg). Fluid intake was *ad libitum.* Urine was collected hourly for 6 hours after the hour following drug dosing.

3.3.4 Urine collection and measurement

Subjects were instructed to note the time at which they had passed urine before the baseline urine sample, to allow baseline values to be determined. Urine pH was measured immediately with an electrode pH meter (Hannah piccolo ^{tm}), as was urine titratable acidity (against 0.1M NaOH, titrated to a pH of 7.4). Each sample was also analysed for urine sodium, potassium and ammonium concentrations. Sodium and potassium were measured by flame photometry and ammonium by a variation of the indophenol detection method using a spectrophotometer (Tecan Sunrise 96-well plate reader)[293].

3.3.5 Ethical approval

Protocols were approved by the University College London Hospital Ethics Committee and informed consent was obtained from all subjects.

3.3.6 Statistical analysis

Statistical analysis was by Student's t-test for unpaired data, or by ANOVA followed by Student's t test for paired data, as appropriate. Values are given as means ± SE; $P<0.05$ significant and NS non-significant differences.

Table 3-1 Biochemical parameters for patients with dRTA who completed the study

Patient number	Diagnosis	Plasma Na (mmol/L)	Plasma K (mmol/L)	Plasma HCO_3 (mmol/L)
1	Sjögren's syndrome	136	3.8	14
2	Idiopathic	137	3.9	21
3	Familial	140	4.7	19
4	Idiopathic	136	3.2	25
5	Idiopathic	139	3.7	22
6	Idiopathic	139	3.9	23
7	Familial	140	3.1	16
8	Familial	141	3.3	19

3.4 Results

Three subjects (2 from the dRTA group and 1 from the control group) had to withdraw from the study because of vomiting after taking NH_4Cl. Eight subjects remained in the dRTA group and 10 in the control group. Six subjects (3 in each group) reported nausea following NH_4Cl, while one subject in the dRTA group had difficulty swallowing the required number of NH_4Cl-containing capsules. No subjects reported any difficulties with the furosemide/fludrocortisone test.

3.4.1 Urinary acidification

All subjects in the control group acidified their urine to a pH of less than 5.3 when given the NH_4Cl test and also when given the furosemide/fludrocortisone test (Figures 3-2 and 3-3). The minimum pH values were 4.87 ± 0.07 after NH_4Cl and 4.92 ± 0.10 after furosemide/fludrocortisone (NS).

Urinary acidification appeared to be more rapid after the furosemide/fludrocortisone test than after NH_4Cl, although it should be noted that the complete dose of NH_4Cl took an hour to ingest, unlike the dosing of furosemide plus fludrocortisone. All control subjects acidified their urine to a pH <5.3 by 3-4 hours after furosemide/fludrocortisone, whereas this was achieved 5-6 hours after NH_4Cl (Figure 3-4), that is, 4-5 hours following the end of NH_4Cl ingestion. In the dRTA group all patients failed to acidify their urine to pH <5.3 with either test. Minimum pH values were 6.83 ± 0.10 after NH_4Cl and 6.59 ± 0.13 after furosemide/fludrocortisone (NS).

3.4.2 Ammonium excretion

In the control group ammonium excretion increased during both tests. For the NH_4Cl test ammonium excretion increased from a baseline of 26 ± 9 µmol/min to a maximum of 64 ± 17 µmol/min (at 6 hours). For the furosemide/fludrocortisone test baseline ammonium excretion was 33 ± 8 µmol/min, rising to a transient peak of 85 ± 23 µmol/min at 2 hours (Figure 3-6 A).

In the dRTA group changes in ammonium excretion were less striking. After NH_4Cl, ammonium excretion was variable, but increased significantly at 4 and 7 hours; no significant increase in ammonium excretion was seen with the furosemide/fludrocortisone test. (Figure 3-6 B).

3.4.3 Titratable acidity

In the control group titratable acidity (TA) increased during both tests (Figure 3-6). With NH_4Cl TA rose from a baseline of 11 ± 3 µmol/min to a peak of 48 ± 9 µmol/min (at 6 hours). With furosemide/fludrocortisone TA rose from a baseline of 10 ± 3 µmol/min to a peak of 42 ± 5 µmol/min (at 3 hours).

In the dRTA group there were much smaller, but significant, rises in TA during both tests.

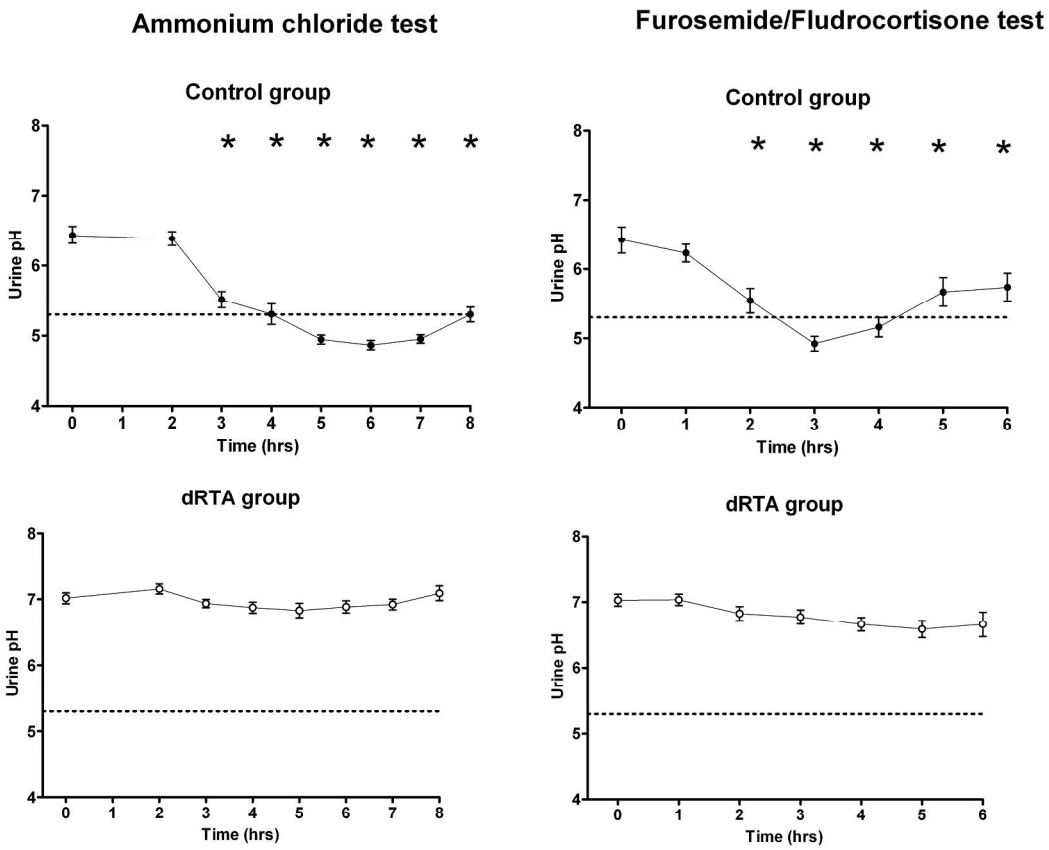

Figure 3-2 Time-course of changes in urine pH after the NH_4Cl and furosemide/fludrocortisone tests

Values are means ± SE. The dotted line indicates the threshold pH of 5.3. Asterisks indicate significantly ($p<0.05$, ANOVA) lower pH than baseline (time 0 hrs).

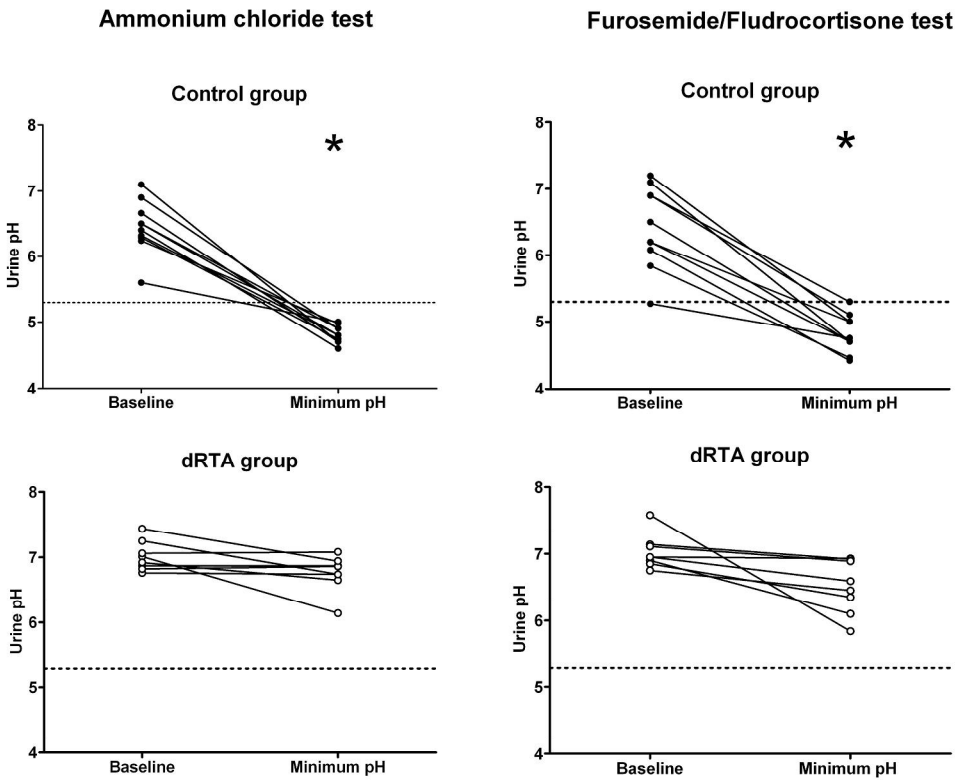

Figure 3-3 Baseline to minimum urinary pH achieved in individual subjects undergoing the NH_4Cl and furosemide/fludrocortisone tests.

The dotted line indicates the threshold pH of 5.3. Asterisks indicate significantly ($p<0.05$, paired t-test) lower pHs than in the corresponding dRTA group.

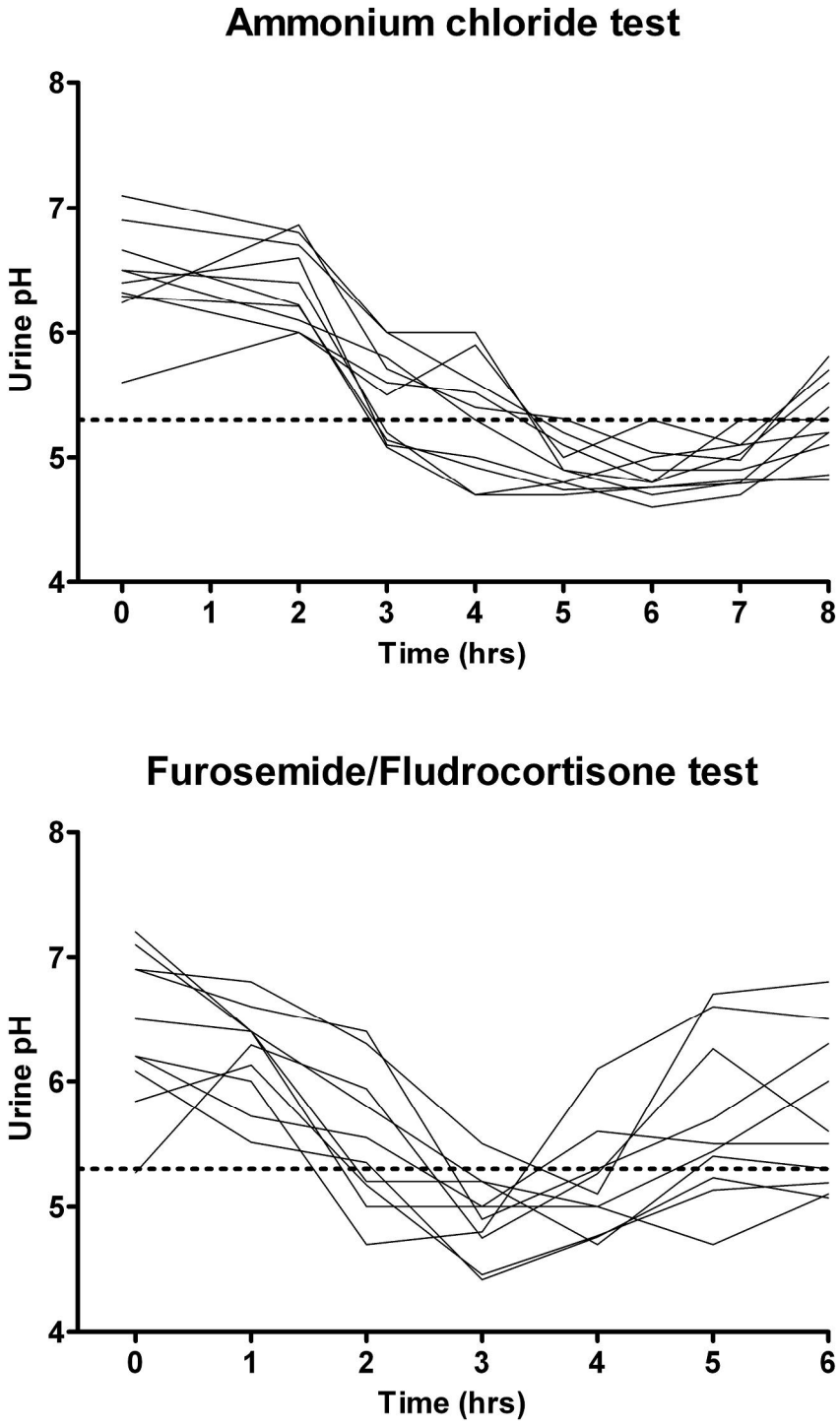

Figure 3-4 Individual sequential urine pH measurements in control subjects.

Each line connects individual values in a single subject. The dotted line indicates the threshold pH of 5.3.

Urine flow rate and electrolyte excretion

Baseline urine flow rates were higher in dRTA patients than in control subjects. Urine flow rates were generally raised following NH_4Cl, reflecting the usually higher fluid intake at the time of NH_4Cl ingestion. As expected, a diuresis, natriuresis and kaliuresis followed furosemide/fludrocortisone administration in control subjects and dRTA patients, reaching a peak at 2 hours (Fig 3.4.4 C). The natriuretic response was similar in the dRTA group to that previously described[55] and somewhat greater in the control group, possibly reflecting the furosemide naïvety of our controls.

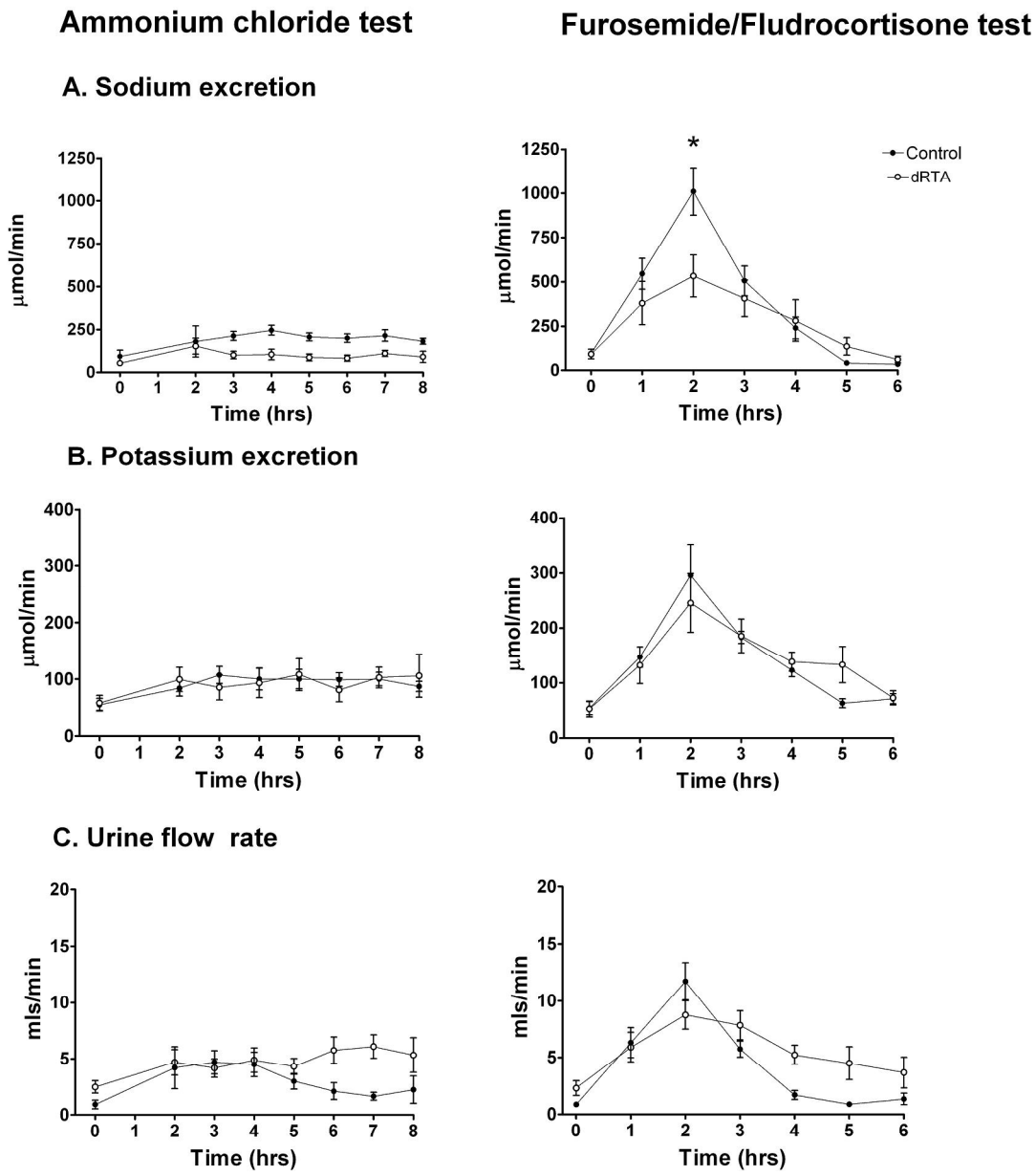

Figure 3-5 Electrolyte excretion and urine flow rate

A: sodium excretion; B: potassium excretion; C: urine flow rate during the NH_4Cl and furosemide/fludrocortisone tests. Closed circles: control subjects; open circles: dRTA patients. The asterisk indicates a result significantly ($p<0.05$) greater in the control group than the dRTA group.

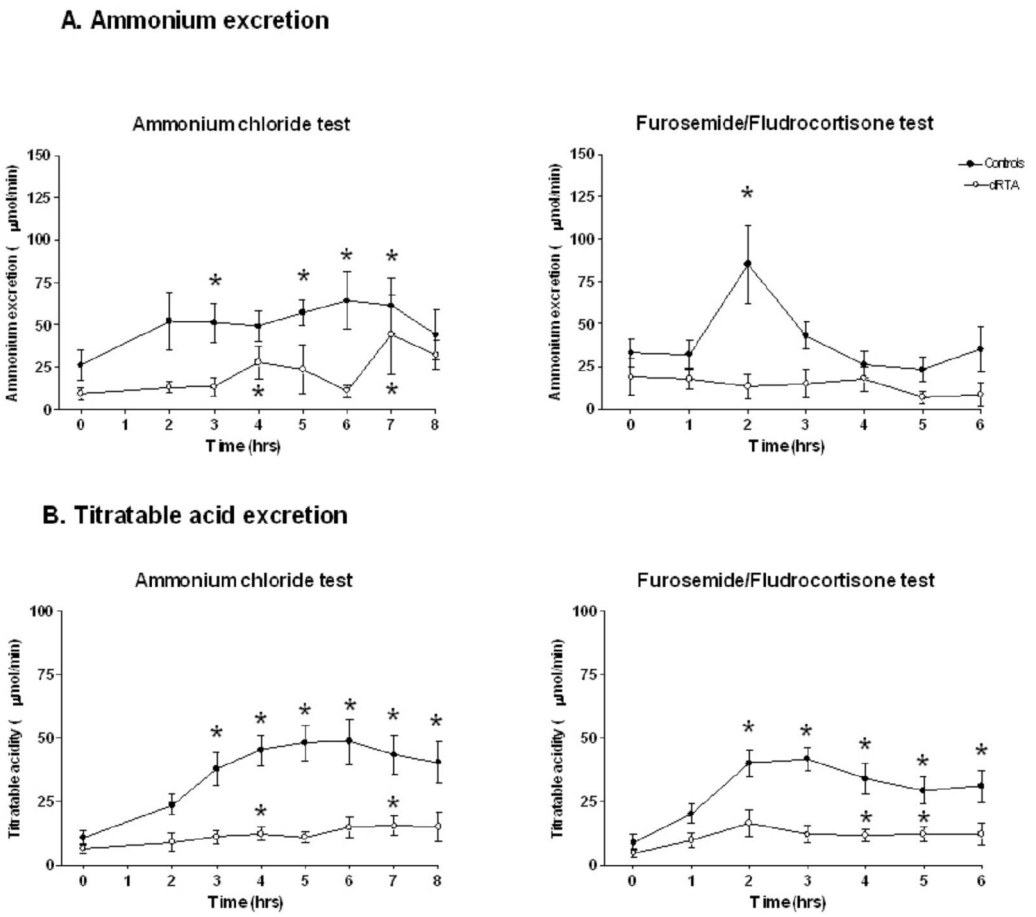

Figure 3-6 Ammonium and titratable acid excretion.

A: ammonium excretion; B: titratable acid excretion during the NH_4Cl and furosemide/fludrocortisone tests. Closed circles: control subjects; open circles: dRTA patients. An asterisk indicates a value significantly higher (*P*<0.05 or less) than the baseline measurement.

3.5 Conclusion

3.5.1 Efficacy

The purpose of this study was to assess the efficacy and reliability of the furosemide/fludrocortisone test compared with the well-established short NH_4Cl test, and whether or not it had any practical advantage. In terms of efficacy, the furosemide/fludrocortisone test performed as well as the short NH_4Cl test. The control subjects all acidified their urine to a pH below 5.3, whereas all the dRTA patients failed to acidify to pH <5.3 with either test (see Figures 3-2 and 3-3).

As Wrong and Davies defined the syndrome of 'incomplete dRTA' using the short ammonium chloride test, defining it as an inability to reduce the urine pH to less than 5.3 following the administration of ammonium chloride[41], the test itself by definition has a sensitivity and specificity of 100%, with the caveat that the test must be successfully completed, in other words all of the ammonium chloride must be ingested (and not vomited).

Therefore, the simultaneous furosemide and fludrocortisone test, in this assessment has a sensitivity and specificity of 100% (albeit in a study of 8 cases and 10 controls) -which would be remarkable apart from the fact that the condition of incomplete dRTA is *defined* by the urinary pH response to the acidifying stimulus of ammonium chloride. It appears form our data that simultaneous furosemide and fludrocortisone is as potent a stimulus for urinary acidification as systemic acidosis, at least in the limited groups that we have tested.

3.5.2 Physiological parameters

As anticipated, in control subjects the NH_4Cl test caused significant and sustained increases in titratable acid and ammonium excretion, as they excreted the acid load.

Following furosemide/fludrocortisone, control subjects showed smaller increases in titratable acid and ammonium excretion compared with NH_4Cl, although there was a striking peak in ammonium excretion at 2 hours, and in titratable acidity at 2-3 hours (Figure 3-6). This peak coincided with the maximum urine flow rate and excretion rates of sodium and potassium (figure 3-5), occurring at the time of maximal delivery of sodium and chloride to the CCD. The minimum urine pH occurred 1 hour later, which is compatible with a dilutional effect from the pronounced diuresis in the second hour reducing the urinary pH. This is a similar pattern to that observed by Batlle [55]. Titratable acidity remained elevated until the end of the test, presumably relating to the continuing effect of mineralocorticoid.

In the dRTA patients, the pattern of urinary acidification was similar for each test. Both tests evoked smaller increases in titratable acid and ammonium excretion compared with those seen in control subjects, there was no observed rise at all in ammonium excretion in the peak second hour seen in the dRTA patients with the simultaneous furosemide and fludrocortisone test, and minor non-significant rise in titratable acidity.

Although a natriuresis and kaliuresis occurred following furosemide/fludrocortisone in the dRTA group (Figure 3-5), the magnitude of the natriuresis was less than in the control group. The difference between the sodium excretion rates was quite large, but in our analysis did not reach statistical significance. The reason for this difference is not clear, it is possible that our dRTA patients were more sodium deplete that our controls and thus had a higher basal uptake of sodium in the CCD, although one would expect this to be a small effect compared to the increased sodium uptake stimulated by the mineralocorticoid. Batlle, using furosemide alone, found similar rates of sodium excretion in controls and dRTA patients[55], so perhaps there is a differential response to mineralocorticoid in those with dRTA; possibly due to low level chronic salt wasting.

3.5.3 Adverse effects

The furosemide/fludrocortisone test was advantageous in that its side-effect profile was much better than that of the NH_4Cl test: no subject in either group had any side effects from furosemide/fludrocortisone, whereas 3 subjects (2 dRTA and 1 control) had to abandon the NH_4Cl test due to vomiting, and 6 subjects (3 dRTA, 3 controls) experienced nausea. One dRTA subject had difficulty swallowing the NH_4Cl capsules, which are large and numerous (the protocol dose was 14 large 500mg capsules for a 70kg subject).

3.5.4 Convenience

The furosemide/fludrocortisone test is a quicker test to complete than the NH_4Cl test: 9 out of 10 control subjects had achieved a urine pH <5.3 by 3 hours after furosemide/fludrocortisone administration, and all had achieved it by 4 hours; and the majority then quickly returned to a normal (baseline) urine pH (Figure 3-4). In contrast, with the NH_4Cl test, only half the subjects had acidified their urine to pH <5.3 by 4 hours after NH_4Cl administration began, although most had achieved this by 5 hours (*i.e.* within 4 hours of completing NH_4Cl ingestion); with this test, urine pH continued to fall or remained low for up to 8 hours.

With simultaneous dosing of furosemide and fludrocortisone, one can also be sure that the mineralocorticoid is taken, rather than with the dosing of mineralocorticoid the evening before as had been tried before [287].

3.5.5 Physiologic basis

As already mentioned, it should also be borne in mind that the NH_4Cl and furosemide/fludrocortisone tests assess urinary acidification in different ways:

one by providing an acid load for the distal nephron to excrete and the other by producing direct and indirect stimulation of distal nephron H^+ secretion.

This assumes that increasing the distal delivery of NaCl is equivalent to inducing a systemic acidosis, as far as the secretion of protons by the α-intercalated cell is concerned. Our knowledge of the molecular mechanisms of acid secretion by the α-intercalated cell would tend to support such an assumption, but a number of older theories concerning dRTA, (albeit in unusual circumstances, such as amphotericin, toluene or vanadium toxicity) posited mechanisms such as increased apical permeability of the intercalated cell permitting 'back leak' of protons from the urine [294] or inhibition of H^+K^+ATPase[70]. One can fairly easily construct thought experiments in which increasing luminal electrochemical negativity would have different effects to a systemic acidosis on urinary acidification in these circumstances. Thus, comparison of the two tests in clinical subgroups of patients with dRTA will need to be made to see if they can provide any further insights into underlying mechanisms of abnormal urine acidification.

3.5.6 Conclusion

In conclusion, the simultaneous furosemide/fludrocortisone test differentiated between patients with distal acidification defects and normal subjects as reliably as the short NH_4Cl test. It did so without causing side effects, a major drawback of the NH_4Cl test. Moreover, the simultaneous furosemide/fludrocortisone test took less time to complete, with differences between normal and impaired urinary acidification apparent by 3-4 hours from the start of the test, as the acidification effect is relatively transitory; whereas with NH_4Cl, urine pH can remain low for up to 8 hours or more.

Therefore the furosemide/fludrocortisone test should last a maximum of 4 hours, with hourly urine pH measurements being made starting immediately before dosing. The test can be terminated at 4 hours (after the maximal acidification effect has passed), or after the urine pH falls below 5.3, signifying normal urinary acidification.

No other measurements would need to be made, unless hypokalemia was known to be present beforehand, in which case, oral potassium supplementation prior to the test in case the furosemide and fludrocortisone cause a transient depression in serum potassium might be prudent.

This would be possible to do in a half day, for instance, during the course of an outpatient clinic, if trained nursing staff were available (necessary for accurate calibrated pH measurements), which would enable new patients to have incomplete dRTA excluded at clinic and be discharged without follow up, a considerable advantage compared to current practice.

4. The Cation Leak Activity of dRTA Associated AE1 Mutants

4.1 Introduction

As previously detailed, in the red cell, AE1 has an N-terminal cytoplasmic domain that acts as an anchorage site for the cell membrane cytoskeleton, and a membrane-associated domain (predicted to span the membrane 12-14 times) that carries out anion exchange [152, 295]. A kidney isoform of AE1 (kAE1) is present in the α-intercalated cell (α-IC) of the distal nephron. It differs from the erythroid form (eAE1) in lacking the 65 N-terminal amino acids and is located in the basolateral membrane of the α-IC, where it plays a key role in normal urinary acidification linked to apical membrane electrogenic proton (H^+) secretion [296]. Mutations in AE1 protein can cause two distinct phenotypes: erythroid and renal.

Of the erythroid phenotypes, one group encodes polymorphisms of blood group antigens; another group is associated with autosomal dominant (AD) spherocytosis (in which red cells are characterised by increased osmotic fragility and reduced membrane surface area); and a third group consists of the hereditary stomatocytoses and their allied disorders (HSt), and Southeast Asian ovalocytosis (SAO). Both are AD red cell defects characterised by cold-induced cation leaks [242, 258, 283] in which the mutant protein is expressed normally at the cell surface, but has reduced or absent anion exchange activity [63, 243]. Several AE1 mutations (L687P, D705Y, S731P, H734R) associated with HSt or spherocytosis appear to abolish the anion transport property of the protein, which is converted to a non-selective Na^+ and K^+ conductance [297].

The renal phenotype associated with AE1 mutations is distal renal tubular acidosis (dRTA), a disorder characterised by impaired urinary acidification and increased urinary losses of potassium and sodium [296]. These mutations are distinct from the mutations causing HSt and SAO, in that anion exchange activity is preserved or only moderately reduced when expressed in Xenopus oocytes.

Studies in polarised cells show that the defect associated with these mutations is due to cytosolic retention or mistargeting of the AE1 protein. In the α-IC, kAE1 is synthesised in the endoplasmic reticulum (ER) before being trafficked to the basolateral membrane in oligomeric form [201]. Known AD dRTA-associated mutations cause disease in heterozygotes by the mutant kAE1 'capturing' the wildtype kAE1 as a heterodimer, which is retained in the ER [199] or is mis-sorted to the apical membrane [188].

Autosomal recessive (AR) dRTA-associated mutations (G701D, S773P, ΔV850 and A858D) have been found only in Southeast Asia [63, 188, 202] and seem to exhibit different trafficking behaviour. Polarised mammalian cells co-expressing wildtype AE1 with G701D or other AR mutant show 'rescue' of the mutant and expression at the cell surface [199, 203].

4.1.1 The hypokalaemia hypothesis.

Hypokalaemia due to potassium wasting is a feature of dRTA. We hypothesised that a dRTA-associated AE1 mutant might also have a cation leak property, and be involved in a pathological transport of potassium from the α-intercalated cell to the urine, either directly mediating the transport via mis-sorting to the apical membrane, as has been observed in some dRTA associated mutants in polarised cell models[188], or alternatively by activating another apical transporter system.

Therefore, we decided to characterise the anion and cation transport properties of four dRTA-associated kAE1 mutations, selected on the basis of their proximity to the red cell disease mutations on the primary structure of the AE1 molecule - R589H, G609R, S613F and G701D - using the Xenopus oocyte expression system.

4.2 Aims

1) To express the selected kAE1 mutants (R589H, G609R, S613F and G701D) in Xenopus oocytes.

2) To characterise the anion transport characteristics of the selected kAE1 mutants by observation of $^{36}Cl^-$ uptake into oocytes and by measurement of intra-oocyte pH during CO_2 acidification with and without chloride containing extracellular medium.

3) To examine the expressed mutants for a possible cation channel activity by observation of $^{86}Rb^+$ uptake into oocytes at 0^oC and room temperature, and measurement of intracellular cation contents of oocytes after prolonged incubation in standard incubation medium.

4) Electrophysiological characterisation by twin electrode voltage clamping of any cation conductances that we found.

4.3 Methods and materials

4.3.1 Xenopus oocyte harvesting

Xenopus laevis oocytes were harvested as detailed in the general methods chapter.

4.3.2 Oocyte injection

Collected oocytes were washed and defolliculated as detailed in the general methods chapter.

Stage V-VI oocytes were then injected with a mixture of 10 ng of kAE1 and 2.5 ng GPA cRNA, when co-injected with GPA cRNA, and were maintained in 18^oC MBS for two or three days before starting the experiments.

4.3.3 Plasmid and DNA construction

The pSP65erythroid human AE1 (hAE1) plasmid was used to construct the kidney AE1 (kAE1), deleting the 65 N-terminal amino acids, as described in the General Methods chapter. For point mutations, primers were used with the following codon substitutions: G609R: GGG/CGG, R589H: CGC/CAC, S613F: TCC/TTC, G701D: GGC/GAC. Primers were purchased from Eurogentec (Seraing, Belgium); polymerase chain reactions (PCRs) were performed using a Biometra "UNO Thermoblock" thermocycler (Göttingen, Germany). Sequences generated by PCR were sequenced in their entirety to ensure that no polymerase errors were introduced (Gexbyweb, Meylan, France).

HindIII linearised pSP65kAE1 wildtype and mutant plasmids were transcribed using SP6 polymerase (Ambion transcription kit). HindIII linearised BSXG-GPA plasmid was transcribed using T7 RNA polymerase (Ambion transcription kit). RNA concentrations were determined on a formamide/formaldehyde agarose gel in MOPS (3-[N-Morpholino]propanesulphonic acid) buffer.

4.3.4 Western blot

Oocyte membranes were prepared by homogenization of 20 oocytes (control or injected) in cooled Tris-HCl buffer, 20 mM, pH 7.4, 250 mM sucrose and 5 mM protease inhibitor, Pefablock (Roche, Paris, France), as described in the general methods chapter. The presence of kAE1 was detected by antibody Bric 170 directed against the C-terminus of kAE1. The secondary antibody was anti-mouse IgG-peroxidase, which was detected by chemiluminescence using a Fujifilm Las-3000 Luminescence image analyser.

4.3.5 Chloride influx experiments

For chloride influx experiments, eight oocytes were incubated at 18^{o}C in 80 µl MBS containing $^{36}Cl^{-}$ (Amersham) with a specific activity of 360 d.p.m. (nmol chloride)$^{-1}$. After a 15 minute incubation, the oocytes were washed twice in ice-cold MBS and transferred individually into counting vials. The washing procedure took less than 30s. The volume of extracellular fluid dropped with each oocyte being variable, it was quickly removed and 20 µl of SDS was

added before vortexing. Radioactive chloride uptake by each oocyte was determined after scintillation counting with an external procedure to account for quenching. The incubation medium was counted in duplicate in 5 µl aliquots, using the same protocol to determine the specific activity in each experiment. Chloride uptake was calculated as the mean of eight values and expressed as pmol per minute per oocyte.

4.3.6 Intracellular pH measurements

Oocyte intracellular pH was measured using selective microelectrodes, as described in the general methods chapter. The ability of wt and mutant kAE1 to regulate intracellular pH was assessed by measuring intracellular pH of oocytes adapted in MBS without HCO_3^-, then incubated in media as described in the general methods chapter. Results are given as ΔpHi per min ± s.e. ΔpHi was measured when acidified oocytes were exposed to Cl^- free medium and corresponds to the initial slope of the alkalinization.

4.3.7 Rubidium influx experiments

For the Rb^+ influx measurements, eight oocytes were incubated for 2 hours at 22°C or 0°C in 80 µl of MBS with ouabain (0.5 mM) and bumetanide (5 µM), containing ^{86}Rb with a specific activity of 32000 dpm/nmol. After this 2-hour incubation, the oocytes were washed twice in ice-cold MBS and transferred individually into counting vials. The washing procedure took less than 30s. The volume of extracellular fluid dropped with each oocyte being variable, it was quickly removed and 20 µl of SDS was added before vortexing. Radioactive rubidium uptake by each oocyte was determined after scintillation counting with an external procedure to account for quenching. The incubation medium was counted in duplicate in 5 µl aliquots, using the same protocol to determine the specific activity in each experiment. Rubidium uptake was calculated as the mean of eight values and expressed as pmol per hour per oocyte.

4.3.8 Intracellular cation measurements

Injected oocytes were incubated in MBS containing ouabain (0.5 mM) and bumetanide (5 µM) at 19^{o}C for 3 days. Na^+ and K^+ content of oocytes was measured by flame spectrophotometry, as previously described in the general methods section. In some experiments, the Na^+ in the MBS was substituted with NMDG (N-methyl-D glucamine).

The final NMDG MBS medium was:

NMDGCl: 85 mM

KCl: 1 mM

$KHCO_3$: 2.4 mM

$MgSO_4$: 0.82 mM

$Ca(NO_3)_2$: 0.33 mM

$CaCl_2$: 0.41 mM

HEPES: 10 mM

KOH: 4.5 mM

pH: 7.4

Cation contents were expressed as µmol per gram of dry weight (µmol/g d. wt.).

4.3.9 Electrophysiology experiments

Electrophysiological parameters were measured at room temperature using the 2-electrode voltage clamp technique with a TEV 200 amplifier (Dagan, Minneapolis, MN) monitored by computer through Digidata 1200 A/D converter/PC clamp software (Axon Instruments, Foster City, CA).9 Current and potential electrodes filled with 3 M KCl had a resistance of 1.8 to 2.3 MOhm. A KCl agar-agar bridge (3 M) was used in order to minimize

junction potentials. The offset potential between bath and electrodes was zeroed before measuring oocyte resting potential.

Resting potential was measured by reading the voltage value on the amplifier display after impaling the oocytes by the 2 electrodes. Following resting potential (Em) determination, oocytes were clamped at holding potentials of -30 mV and clamping potentials from -100 to +80 mV;

20-mV increments were applied for 800 ms and the current values recorded. Im was plotted versus Vm and the mean slope of the I/V curve between -100 mV and -20 mV was taken as an index of the membrane conductance and expressed as microsiemens (µS).

In some experiments, the Na^+ in MBS was substituted by NMDG (N-methyl-D-glucamine) or K.

For NMDG MBS, the final medium was:

NMDGCl	85 mM
KCl	1 mM
$KHCO_3$	2.4 mM
$MgSO_4$	0.82 mM
$Ca(NO_3)_2$	0.33 mM
$CaCl_2$	0.41 mM
HEPES	10 mM
KOH	4.5 mM
pH	7.4

For KCl MBS, the final medium was:

KCl	86 mM
$KHCO_3$	2.4 mM
$MgSO_4$	0.82 mM
$Ca(NO_3)_2$	0.33 mM
$CaCl_2$	0.41 mM
HEPES	10 mM
KOH	4.5 mM
pH	7.4

For experiments where Cl^- was substituted by gluconate the gluconate containing MBS was:

Na Gluconate	88 mM
K Gluconate	1 mM
$MgSO_4$	0.82 mM
$Ca(NO_3)_2$	0.33 mM
$CaCl_2$	0.41 mM
HEPES	10 mM
KOH	4.5 mM
pH	7.4

When using inhibitors (La^{3+}, Zn^{2+}, 1 mM), the MBS was devoid of HCO_3^- and SO_4^{2+}:

NaCl	87.5 mM
KCl	1 mM
$MgCl_2$	1 mM
$CaCl_2$	1.8 mM
HEPES/NaOH	10 mM
pH	7.4

4.3.10 Chemicals

Unless otherwise stated, all chemicals were purchased from Sigma (St Louis, MO). Agarose was purchased from GIBCO BRL (Life technologies, Gaithersburg, MD). Minipreps of DNA were done with a Quiagen kit (Hilden, Germany). Anti-AE1 antibodies BRIC170 and BSXG-GPA plasmid were a kind gift of Dr. Ashley Toye (University of Bristol, UK). Plasmid pSP65erythroid AE1 was a kind gift of Dr. H. Appelhans.

4.4 Results

4.4.1 Western blot results

Mutant kAE1 constructs were co-expressed in oocytes with the AE1 chaperonin glycophorin A (GPA), because without GPA there is no plasma membrane expression of G701D- kAE1 in oocytes [180]. For the other mutants that were studied, functional expression could be observed without GPA, as previously observed [1, 191, 195]. In order to compare similar experimental conditions we chose to co-express all the dRTA-mutants with GPA. Oocyte membrane expression of wildtype and mutant kAE1 was confirmed by detecting bands of the appropriate molecular mass on western blotting (Figure 4-1). No signal was detected on lanes charged with membrane of oocytes expressing mutant G701D kAE1 alone without GPA (not shown). The western blots were done at the same time as the functional studies.

4.4.2 Chloride influx experiments

To detect functional expression of the dRTA-associated mutants, $^{36}Cl^-$ influx experiments were carried out in oocytes co-expressing GPA and wildtype or mutant kAE1. Cl^- influx in wildtype kAE1 expressing oocytes was more than 18 times that measured in non-injected controls; Cl^- influx was well preserved in the dRTA mutants (see Figure 4-2 A), as previously reported [1, 180, 195].

4.4.3 Intracellular pH measurements

To confirm that Cl^- transport was dependent on Cl^-/HCO_3^- exchange activity in oocytes expressing wildtype or mutant AE1, we measured the change in intracellular pH (pH_i) following acute exposure to a solution containing CO_2/HCO_3^- (in the presence of extracellular Cl^-), which caused an initial and rapid fall in pH_i that stabilised as CO_2 reached equilibrium across the cell membrane. On replacing extracellular Cl^- with gluconate, pH_i promptly

recovered in the presence of functional anion exchange activity, due to HCO_3^- uptake in exchange for intracellular Cl^-. Oocytes expressing wildtype kAE1 showed a fall in intracellular pH_i in Cl^--containing medium that rose again on replacing extracellular Cl^- with the impermeant anion gluconate, as shown in Figure 4.4.2 B. This pattern was seen with all 4 mutants, indicating functional plasma membrane expression of Cl^-/HCO_3^- exchange. To compare the Cl^-/HCO_3^- exchange activity of wildtype with mutant kAE1, the initial rate of pH_i recovery after acid loading was estimated as ΔpH_i/minute (Figure 4.4.2 C). Mutant recovery rates were not significantly different from wildtype kAE1. It was assumend that all expressed AE1 proteins would have a similar effect on the oocyte buffering capacity, which was not measured.

4.4.4 Rubidium uptake experiments

$^{86}Rb^+$ was used as a measure of K^+ flux, to demonstrate K^+ permeability of the oocyte membrane. Rb^+ uptake experiments were performed initially at 0^oC, as previous work had demonstrated an AE1-mediated cation leak that was maximum at 0^oC in HSt-associated AE1 mutants [243]. The extracellular medium contained ouabain and bumetanide to inhibit any Rb movement through the Na^+/K^+-ATPase and the Na^+-K^+-$2Cl^-$ co-transporter, respectively. Rb^+ uptake (Figure 4.4.4 A) was low in both non-injected and wildtype kAE1-expressing oocytes. In contrast, there was significant Rb^+ uptake in all the dRTA-associated kAE1-expressing oocytes. A large Rb^+ uptake was recorded with one mutant, G701D. Compared with measurements done at 0°C, Rb^+ uptake measured at room temperature (22^oC) showed similar values for mutant kAE1-expressing oocytes; however, basal uptake (NI oocytes or expressing wt kAE1) is significantly raised by the increased temperature (Figure 4.4.4 B), obscuring any increase in Rb^+ uptake induced by expression of the R589H, G609R and S613F mutants.

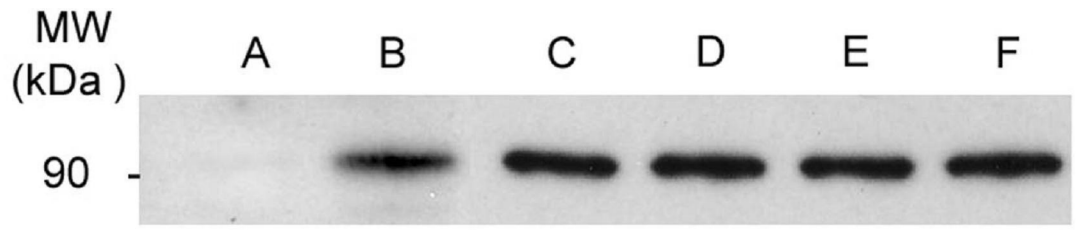

Figure 4-1 A representative western-blot of an oocyte plasma membrane probed with anti-AE1 antibodies (BRIC170).

From left to right: a) non-injected; b) wildtype kAE1+GPA; c) R589H+GPA; d) G609D+GPA; e) S613F+GPA; and f) G701D+GPA expressing oocytes. Representative of 3 experiments.

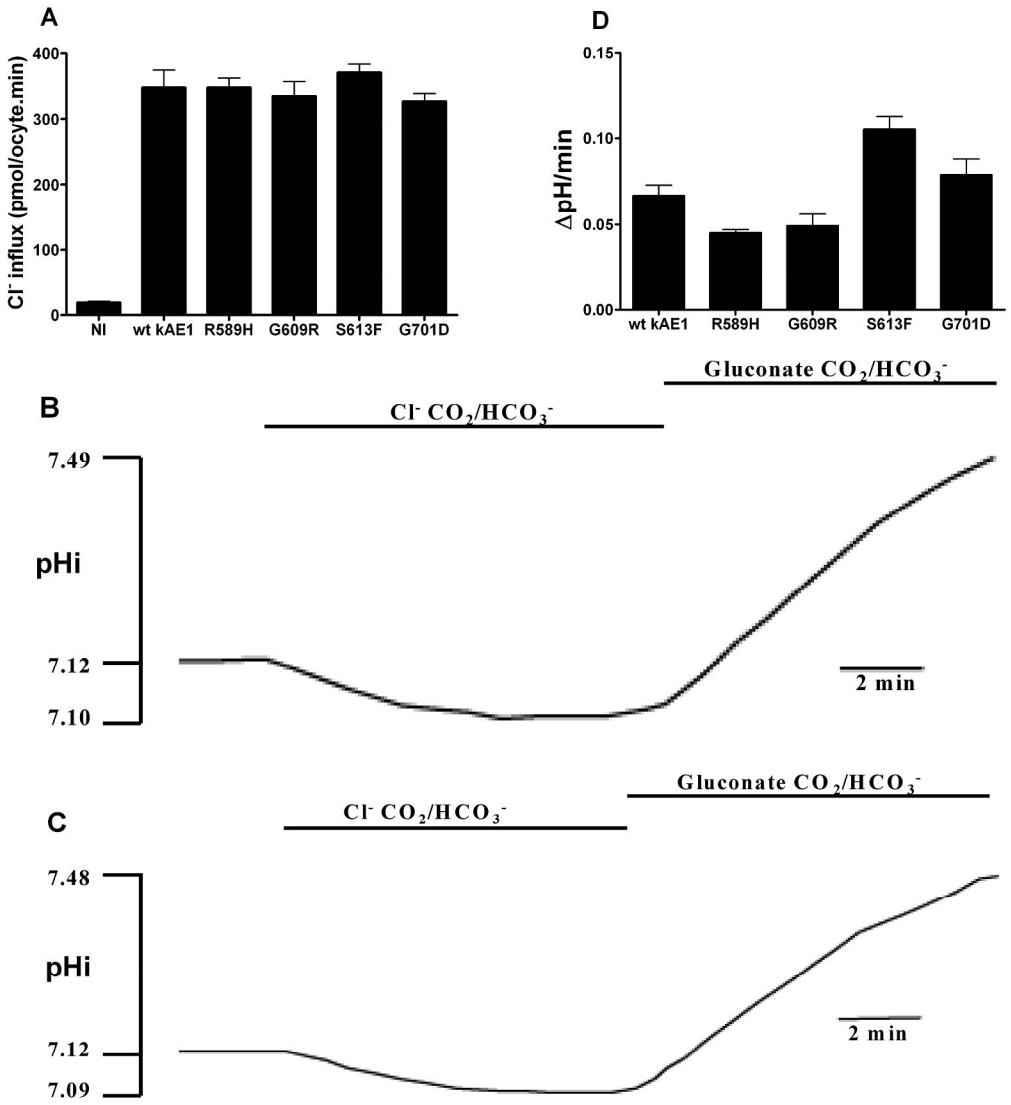

Figure 4-2 Composite figure of anion transport experiments

(A) shows $^{36}Cl^-$ uptake at 22^oC, into non-injected, wildtype kAE1- and mutant kAE1-expressing oocytes at day 3 post-injection. All injected oocytes are co-expressing GPA. Data are means+/-s.e.m of 8 experiments. (B) and (C) show representative plots of intracellular pH vs. time of an oocyte acidified with CO_2 in the presence and then absence of extracellular Cl^-. The oocytes are expressing wildtype kAE1 and the G609R mutation, respectively with GPA. (D) illustrates the pH_i recovery rate after an acid load of control oocytes (NI) or oocytes co-expressing GPA with wildtype or the different kAE1 point mutations. Data are means of 9 oocytes +/- s.e.m.

4.4.5 Pharmacological blockade

The kAE1 mutants tested are known to have stilbene-sensitive anion transport a finding supported by our observation of SITS (4-acetamido-4'isothiocyanato-stilbene-2,2'disulfonic acid)-sensitive Cl^- influx in all mutants (data not shown). The Rb^+ uptake of oocytes expressing mutant kAE1 was sensitive to 0.1 mM SITS (Figure 4-3 C: a reduction in Rb^+ uptake of 85% for R589H and S613F, 99% for G609R, and 74% for G701D). Figure 4-3 D is a dose-response curve of SITS inhibition of Rb^+ uptake in oocytes expressing the G701D mutation with GPA. It should be noted that the inhibition seen in the inhibition curve data at equivalent SITS concentration (0.1mM) is less than that seen in the preceding experiment (performed with a different batch of oocytes), stilbene inhibition of the G701D mutant is quite variable, possibly reflecting conformational differences with the wt protein.

4.4.6 Intracellular cations

Na^+ and K^+ content of oocytes expressing wildtype or mutant kAE1 was measured after 3 days of incubation in control medium (MBS), or in medium in which Na^+ had been substituted with the impermeant cation N-Methyl-D-Glucamine (NMDG). Both media contained ouabain and bumetanide. Intracellular cation measurements (Figure 4-4) showed reversal of the normal ratio of intracellular Na^+ to K^+ content in mutant-expressing oocytes compared with controls. All dRTA-associated mutants showed reversal of this ratio, with the largest change occurring in G701D-expressing oocytes, the amount of reversal seen correlating with the Rb^+ influx results. There was no fall in intracellular K^+ when extracellular Na^+ was replaced with NMDG (Table 4-1). The cation flux was large enough to produce a reversal of intracellular cation contents even after 3 days incubation in MBS without ouabain and bumetanide (oocytes co-expressing GPA and; wt kAE1: Na=43.4 ± 3, K=80.4 ± 5; R589H: Na=68.3 ± 5.7 K=52.9 ± 1.1; G701D: Na=104.9 ± 2.6 K=2.6 ± 1.9 µmol/g.d.w.).

Table 4-1 Intracellular cation content after incubation in NMDG

	Mean Na^+ ± s.e.m. (µmol/g dry wt.)		Mean K^+ ± s.e.m. (µmol/g dry wt.)	
	with ext. Na^+	with NMDG	with ext. Na^+	with NMDG
N.I.	71.0±11.8	63.0±3.8	77.3±7.1	97.2±2.3
wt kAE1	74.8±4.8	65.2±0.6	75.0±1.1	95.5±0.9
R589H	151.7±4.9 #	67.6±4.4	9.6±7.6 #	84.2±4.3
S613F	127.1±8.7 #	63.2±5.3	38.6±2.3 #	90.1±3.4
G701D	175.7±1.9 #	74.2±10.2	U	94.0±13.9

The intracellular cation measurements for non-injected, wildtype (wt) and mutant kAE1-expressing oocytes after 3 days incubation in MBS with either Na^+ or NMDG. Both media contained 0.5 mM ouabain and 5 µM bumetanide. Note the lack of K^+ loss seen in intracellular cation content of oocytes incubated in NMDG medium compared with oocytes incubated in Na^+ containing MBS. (U = undetectable). Data are means ± s.e.m. of 15 experiments. In each column cation content measurements were compared # indicates a significant statistical difference ($p<0.05$) between the relevant cation measurements compared to non-injected oocytes.

4.4.7 Oocyte electrophysiology

The cation leak induced by the erythroid AE1 mutations has been characterised definitively as a non-selective cation conductance [284]. Therefore, we investigated the conductive properties of the dRTA-associated kAE1 mutant G701D, as it exhibited the highest cation permeability. As shown in Figure 4-5 A, co-expression of G701D with GPA increased oocyte membrane conductance compared with non-injected oocytes, or those expressing wildtype kAE1 with GPA. The resting membrane potential was depolarised by 7 mV in oocytes expressing G701D compared with wildtype kAE1 (Table 4-2). The conductance in oocytes expressing G701D and GPA was sensitive to SITS (Figure 4-5 B).

Next, extracellular NaCl was replaced with KCl, Na^+ with the impermeant cation NMDG, and extracellular Cl^- with the impermeant anion gluconate (Table 4-2). These manipulations showed that the resting membrane potential of non-injected oocytes, or oocytes expressing wildtype kAE1, is largely sensitive to changes in extracellular K^+ concentration (high extracellular K^+ caused a 42 mV depolarisation) and to a lesser extent extracellular Cl^- (Cl^- removal caused a 4 mV depolarisation); but in G701D-expressing oocytes it is sensitive to both Na^+ and K^+ concentrations. In these oocytes, resting membrane potential was hyperpolarised (by 7 mV) in the absence of extracellular Na^+, but it was depolarised (by 24mV) in the presence of high extracellular K^+.

Table 4-2 Measurements of resting membrane potential as a function of the ionic composition of the extracellular medium

E_m (mV) / Medium	NI	kAE1 wildtype	G701D
NaCl/KCl	-50.6±3.3	-54.6±2.5	-47.6±2.5 *
NMDGCl	-53.8±2.9	-52.9±0.9	-54.3±3.6 #
KCl	-7.9±0.9 #	-13.1±0.5 #	-23.3±1.7 #&
Gluconate	-40.8±3.0 #	-49.7±0.8 #	-44.4±2.0&

Resting membrane potentials (E_m in mV) of oocytes expressing either wildtype kAE1 or G701D with GPA incubated in different media. Regular MBS with 85mM NaCl and 1 mM KCl (NaCl/KCl), no extracellular NaCl substituted with NMDGCl and 1 mM KCl (NMDGCl), no extracellular NaCl and 85 mM KCl (KCl) and MBS, where NaCl and KCl were substituted with Na gluconate and K gluconate.

Data are means±sem of 5 oocytes. In each column, E_m mean values were compared; #indicates a significant statistical difference ($p<0.05$) between E_m of indicated oocytes, compared to equivalent oocytes in NaCl/KCl medium; *indicates a significant statistical difference ($p<0.05$) between E_m of oocytes expressing wildtype kAE1 and G701D mutation in regular MBS; &indicates a significant statistical difference ($p<0.05$) between E_m in KCl or in gluconate for G701D compared to wtkAE1 expressing oocytes.

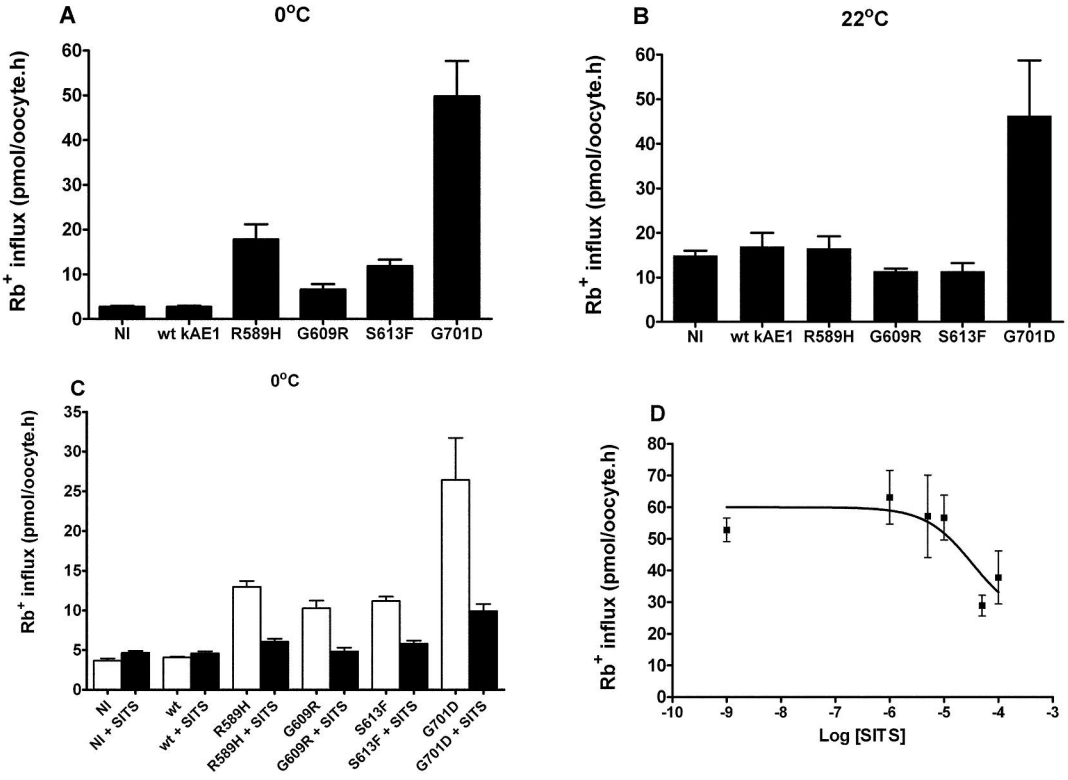

Figure 4-3 Composite figure of $^{86}Rb^{+}$ uptake experiments.

Representative experiment of ouabain- and bumetanide-resistant $^{86}Rb^{+}$ uptake is given at 0°C (A) and at 22°C (B) into non-injected, wildtype kAE1- and mutant kAE1-expressing oocytes 3 days after injection. All injected oocytes are co-expressing GPA. Data are means +/- s.e.m. of 8 oocytes. (C) Shows a representative experiment of ouabain- and bumetanide-resistant Rb^{+} uptake at 0°C into non-injected, wildtype kAE1- and mutant kAE1-expressing oocytes without (white bars) and with 10^{-4}M SITS (black bars). All injected oocytes are co-expressing GPA and measurements were done 3 days after injection. Data are means +/- s.e.m. of 8 oocytes. (D) Dose-response curve of SITS-inhibition of ouabain and bumetanide resistant Rb^{+} uptake induced by G701D and GPA expression. The Rb^{+} uptake measured in control oocytes (NI) was subtracted and data are means +/- s.e.m. of 8 oocytes.

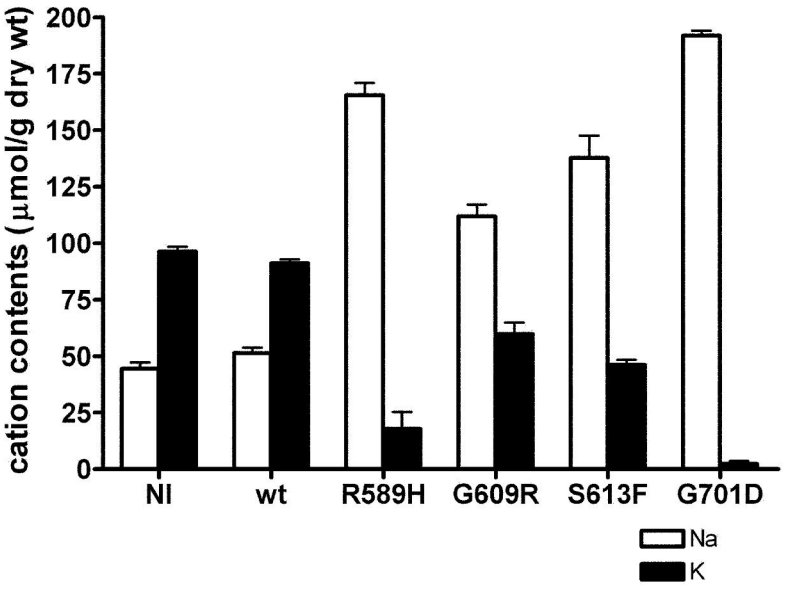

Figure 4-4 Intracellular cation contents.

Na^+ (white bars) and K^+ (black bars) content was measured in oocytes that were either non-injected or expressing wildtype or mutant kAE1, and GPA, 3 days after incubation in MBS at 19^{o}C, with 0.5 mM ouabain and 5 µM bumetanide. Data expressed in µmol per g of dry weight (dry wt.) are means +/- s.e.m. of 15 oocytes.

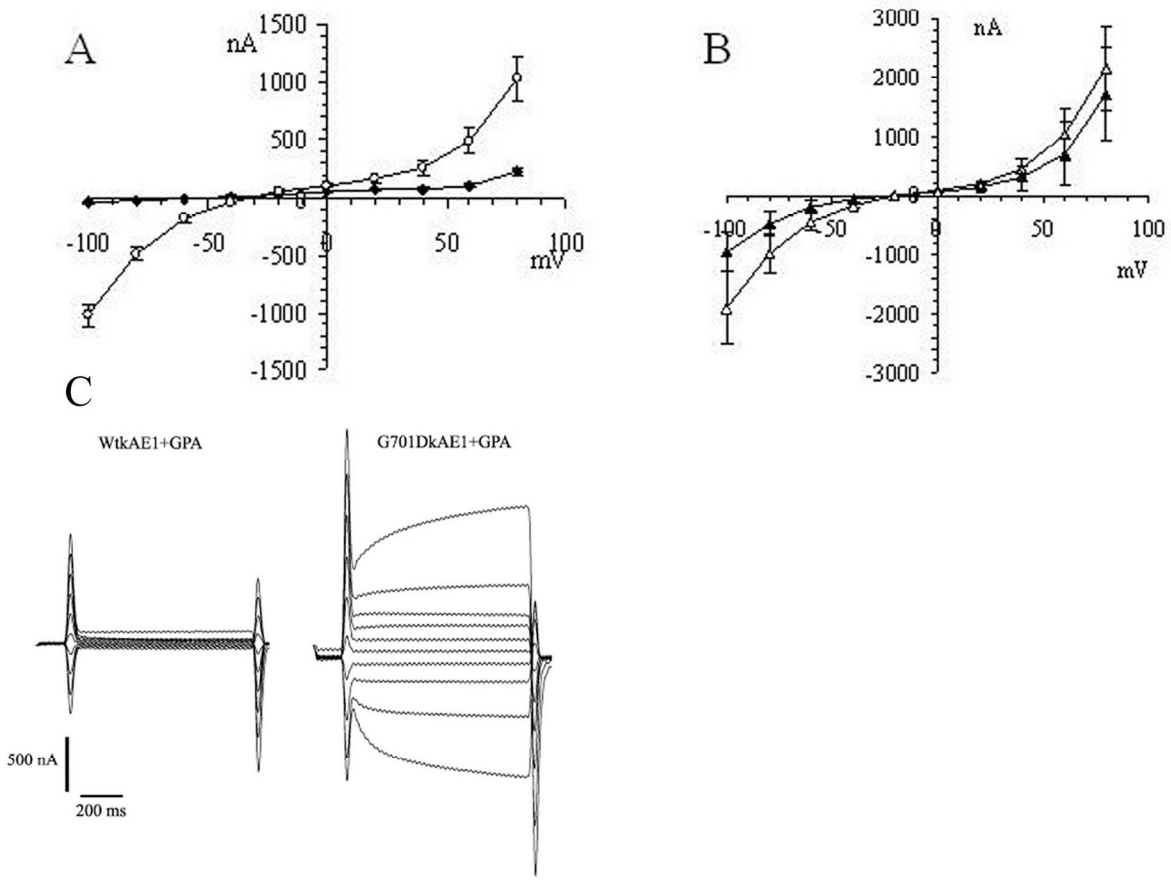

Figure 4-5 Composite figure of electrophysiology experiments.

A) Current-voltage (I/V) curves of oocytes non-injected (black circles) or co-expressing GPA and wildtype kAE1 (black diamonds) or G701D mutation (white circles). The basal currents in non-injected oocytes are superimposed on the currents recorded in oocytes co-expressing GPA and wildtype kAE1. Currents were recorded at 500 ms of clamped potential in regular MBS. Data are means +/- s.e.m. of 28 oocytes (G701D mutant) or 15 oocytes (wildtype kAE1) or 8 oocytes (NI). B) Current-voltage curves of oocytes co-expressing GPA and G701D mutation in the absence (white triangles) or in the presence of 10^{-4} M SITS (black triangles). Data are means +/- s.e.m. of 5 paired oocytes and differences (below -40 mV and above 40 mV) were statistically significant with p=0.05 (t-test). C) Inset: current recordings of wildtype kAE1+GPA and G701D+GPA expressing oocytes (left and right, respectively).

4.4.8 Oocytes co-expressing AE1 and wildtype AE1

To investigate the effect of AE1 heterodimer formation on the cation leak property of the G701D mutant, Rb^+ uptake experiments were done in oocytes co-expressing G701D with wildtype kAE1, but without GPA. Rb^+ uptake was 57% of that observed with the same amount of G701D co-expressed with GPA (Figure 4-6). This is consistent with a 'rescue' effect of wildtype kAE1 on G701D (by forming heterodimers with G701D kAE1) and successful trafficking to the plasma membrane. Rb^+ uptake (though reduced) indicates that surface membrane-expressed heterodimers of G701D (homodimers are not surface expressed in the absence of GPA) and wildtype kAE1 still possess a cation transport property.

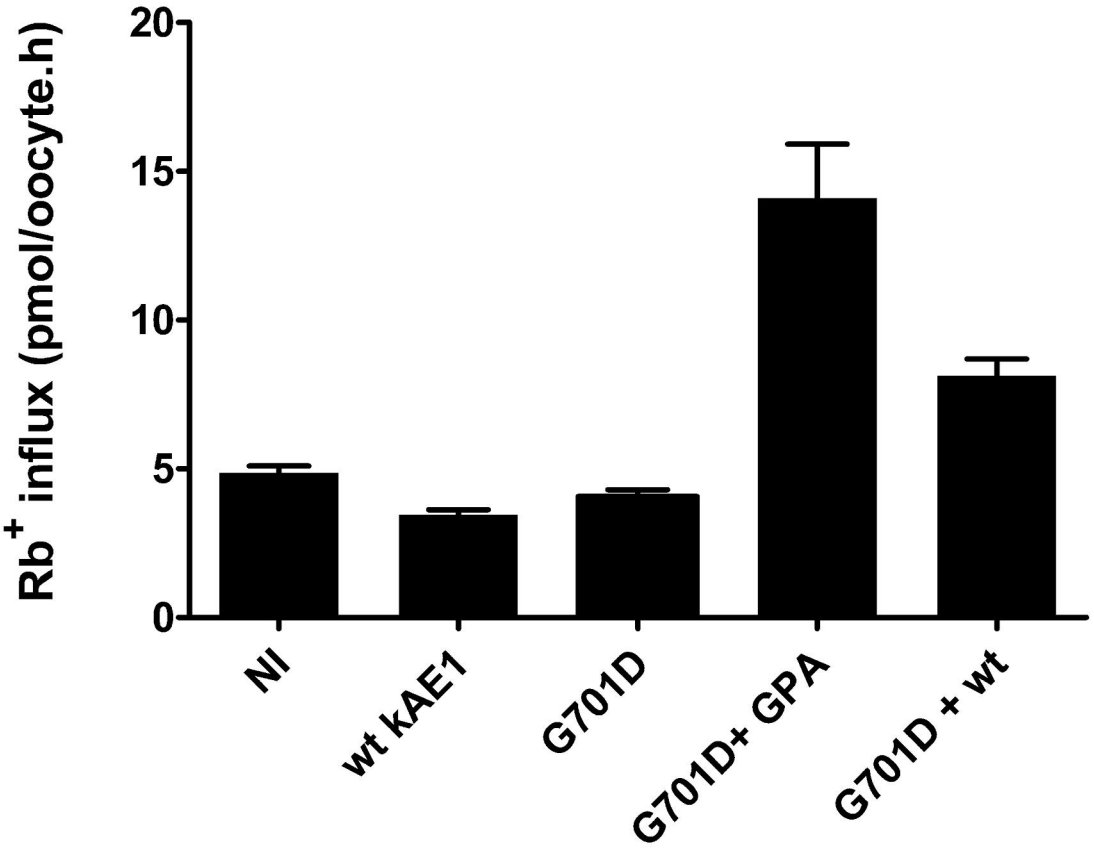

Figure 4-6 Further $^{86}Rb^{+}$ uptake in G701D expressing oocytes with and without GPA.

$^{86}Rb^{+}$ uptake was measured in non-injected (NI) oocytes and oocytes expressing wildtype kAE1, G701D kAE1 alone, or co-expressing GPA and G701D or wildtype and G701D kAE1. A similar amount of wildtype or mutant kAE1 cRNA was injected (6 ng). For co-injection, 6 ng of G701D was injected with either 2.5 ng of GPA or 6 ng of wildtype kAE1. Data are means of 8 oocytes +/- s.e.m.

4.5 Conclusions

We have found that the four dRTA-associated kAE1 mutants we investigated are capable of inducing a monovalent cation leak when expressed in Xenopus oocytes, which is not present in oocytes expressing wildtype kAE1. The leak of Na^+ and K^+ in mutant-expressing oocytes depends on the electrochemical gradients for Na^+ and K^+, with Na^+ influx counterbalancing K^+ efflux.

Electrophysiological experiments in G701D-expressing oocytes demonstrated an electrogenic leak sensitive to variations in extracellular Na^+ and K^+ concentrations, indicating the presence of a non-selective cation conductance property. Previously, it has been shown that four point mutations in erythroid AE1 converted the anion exchanger to a non-selective cation conductance (the alternative explanation of a coincidentally activated endogenous oocyte transporter having been discounted [297]).

We have now shown that four other point mutations associated with a renal phenotype also have a cation leak property; although in contrast to the four erythroid AE1 mutants studied previously, the renal AE1 mutants retain normal or near normal, anion exchange activity. This is the first time that these transport properties have been shown to co-exist in human AE1.

4.5.1 Structure function implications

The four dRTA-associated mutations all occur on highly conserved sequences in the primary structure of kAE1: in the putative transmembrane (TM) helices 6 (R589H), 7 (G609R and S613F) and 9, or the region adjacent to it (G701D) [152]. These point mutations are not essential for anion exchange function, which is preserved. This is in accordance with previous observations showing that the TM segments 6 and 7 seem to be unnecessary for anion transport, since non-complementary fragments of AE1 lacking this segment could still induce anion transport when co-expressed in Xenopus oocytes [298].

However, G701D lies in a region critical for anion exchange. This region is also the least well defined topologically; it is thought to be involved in a transport-related conformational change (TCC) and to be structurally

labile[295]. Certain residues appear to be important for anion transport in this region. E681 is thought to act as the proton binding site in H^+ and SO_4^{2-} symport [158] - even conservative site-directed mutagenesis at this site (E681D) abolishes anion exchange [161]. Another crucial amino acid site for anion exchange appears to be H734 [167]. It appears to interact with the negative charge of the E681 residue [161], apparently because of their close physical proximity [295]. The erythroid mutants L687P, S731P, and H734R are closely associated with these sites and they have been shown to abolish anion exchange [243, 297]. Indeed, these mutations should be expected to disrupt the spatial position or charge of the 734 and 681 residues.

G701D and the erythroid D705Y are also close to E681 in the primary sequence and both mutations mediate large cation leaks. The intact anion exchange activity of the G701D mutant suggests that this residue is not essential for anion exchange function, perhaps because it is situated further from the E681 residue in three-dimensional space.

If TM 9 constitutes an α-helix, as is commonly supposed, and we further suppose that it extends in an N-terminal direction as far as the proline residue at position 692. If we construct a helical wheel model of the cytoplasmic end of this proposed structure, from P692 to L708 (which is predicted to lie in the lipid bilayer [152]) we can see that D705 and G701, along with K698 and R694 are closely associated on one narrow, hydrophilic face which has a net positive charge (see figure 4-7), which would tend to align toward the cytoplasm. The G701D mutation adds a negative charge, negating the net charge of this face, implying that the net charge on this face is important for the anion selectivity of the exchange mechanism. The D705Y mutation removes a negative charge from this face, rendering the net charge more positive, but also adds a hydrophobic residue, and which could alter the rotational alignment of the helix. If the TCC of AE1 is similar to Tanford's helix rotational model [299], as has been suggested [295], then such a mal-rotation of a helix closely related to crucial binding sites (such as E681) could abolish anion transport function by altering how they are revealed in the TCC. Site directed mutagenesis experiments to insert charged or hydrophobic residues

at these positions or K698 or R694 would be required to provide evidence for this model.

There is growing evidence for the existence of ion channel activity in what until recently were considered to be exclusive symporters or antiporters [300], and that these transporters and ion channels can have structural similarities [301]. Indeed, trout AE1 may act as an ion channel [275, 276], which illustrates how closely related the AE1 exchanger is to a channel. Therefore, point mutations that directly alter the conformation of the region involved in AE1's TCC can elicit cation transport and (with at least one exception - G701D) abolish anion transport; whereas mutations distant from this region (R589H, G609R and S613F) induce a small cation leak without affecting anion transport. These mutants are thought to be misfolded [201] and it is likely that such conformational changes are sufficient to provoke a cation leak, as AE1's structure is already so closely related to that of an ion channel (cf. trout AE1).

Conformational change in the region of the TCC provides an explanation for the partial inhibition of the cation permeability observed in the G701D mutant by SITS, which also occurs in the erythroid mutants (L687P, D705Y, S731P and H734R) [297]. SITS binding and inhibition of AE1 depends on its conformation, indeed, SITS affinity chromatography is used to detect mis-folding of AE1 mutants [302].

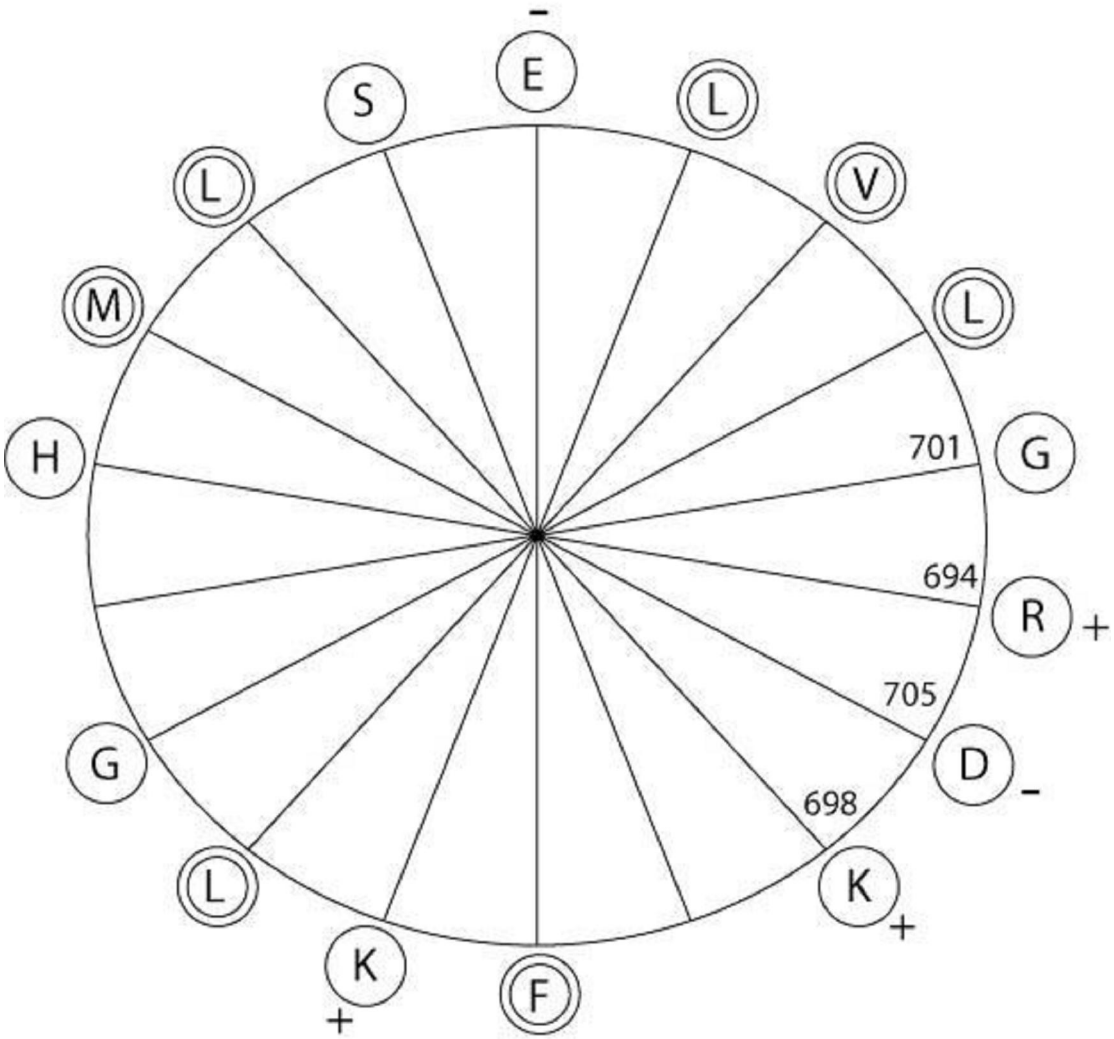

Figure 4-7 Helical wheel model of the hypothetical α-helix extending from the bottom of TM9 to residue 692.

The helical wheel model represents the helix imagined from above, with amino acid residues represented by circles showing their position on the face of the helix. Plus and minus signs denote charged amino acid residues, concentric circles denote hydrophobic residues. The numbers indicate the position number of the residue in the secondary structure.

4.5.2 Cation leak behaviour and the erythrocyte in AE1-associated dRTA

Prior to this work, cation leaky AE1 has been associated solely with red cell pathology; the cation leak described by Bruce *et al* in the mutants L687P, D705Y, S731P, H734R and R760Q [243] was postulated to be responsible for the dysmorphic red cells seen in patients with these mutations. Here we have described four other point mutations of AE1 (R589H, S613F, G609R and G701D) inducing a cation leak, which are associated with dRTA. There have been no reports of erythrocyte abnormalities or evidence of haemolytic anemia for these dRTA-associated AE1 mutations except, for G701D homozygotes [63, 180]. It may be that the cation leak is compensated in heterozygote erythrocytes and, therefore, causes no red cell dysmorphism; whereas compensation is overcome in homozygotes due to a larger cation leak mediated by the two mutant alleles. Moreover, there is a recent report of haemolytic anemia and erythrocyte abnormalities in patients with G701D (and other SE Asian AE1 mutations) and dRTA, which appears to be related to the degree of acidaemia [303]; the red cell abnormalities resolve with alkali treatment, and the lack of acidaemia in G701D heterozygotes could explain their normal red cell phenotype.

4.5.3 Cation leaky AE1 in the α-intercalated cell in dRTA

In contrast to red cells in which GPA acts as a chaperonin to address dRTA-associated AE1 mutations to the plasma membrane, the α-intercalated cell (α-IC) does not express GPA, and kAE1 is believed to be transported to the cell surface as an oligomer [188]. We simulated this in the non-polarised oocyte by co-expressing G701D kAE1 with wildtype kAE1 (without GPA) by using equal amounts of mRNA. This resulted in a smaller cation leak, approximately half the magnitude seen in the paired experiment using G701D and GPA (Figure 4-6), which is consistent with cation leaky heterodimerised G701D and wildtype kAE1 at the cell membrane - non-leaky homodimerised

wildtype kAE1 at the cell surface and homodimerised G701D retained intracellularly. However, the cation transport property of G701D is still present when heterodimerised, suggesting that functional cation leaky kAE1 may be present in the α-IC membrane of G701D heterozygotes.

4.5.4 Hypokalaemia

Is it possible that the mutations described have any pathophysiological significance for the α-IC cell, perhaps mediating potassium efflux into the urine? The AD mutants do show a cation leak when intracellular cation contents are measured at 19°C. Although largely retained intracellularly, R589H, S613F and G609R have all been observed (in varying amounts) at the apical membrane in polarised cell models [188, 195, 199], but we acknowledge the likely differences between over-expressing cell models and native α-IC cells. Moreover, the small amount of AE1 expressed at the apical membrane in these cells models (especially R589H and S613F), and the relatively small cation leak seen with S613F and G609R (and the modest leak seen with R589H) make a significant pathophysiological role for these mutants in potassium wasting in dRTA less likely. Hypokalaemia is also a more variable clinical in patients with European AE1-associated dRTA.

The G701D mutation is perhaps more likely to have some pathophysiological significance, since its cation leak is much higher than that the AD mutants. If G701D were mistargetted to the apical membrane of α-IC, a potassium leak into urine could occur; if it were expressed on the basolateral membrane only, it may cause enough membrane depolarization to activate apical maxi-K channels [304] and facilitate flow-dependent potassium secretion [305].

4.5.5 Disease distribution

In Southeast Asian AE1-associated dRTA, including G701D, severe hypokalaemia is more severe than European AE1-associated dRTA [63]. G701D has a gene frequency of 0.7% in Northeastern Thailand [192], where dRTA is endemic [306], and hypokalaemia with hypokalaemic paralysis and

sudden unexplained nocturnal death (SUND) are common [307-309]. Moreover, relatives and survivors of SUND episodes in N.E.Thailand have been shown to have high red cell Na and abnormal red cell Na,K-ATPase activity [310], a finding consistent with cation leaky red cells [258].

However, whether the red cell abnormalities seen in the Southeast Asian AE1 mutations are associated with cation leak activity or if hypokalaemic disease in Northeastern Thailand is linked to G701D heterozygosity are questions that need addressing in future studies.

5. The Cation Leak Activity of Other Southeast dRTA Associated AE1 mutants

5.1 Introduction

There are 2 phenotypes of AE1-associated dRTA; the rare European autosomal dominant (AD) dRTA, where one mutant allele will generate a mutant protein that is able to 'capture' a wild type protein in the cytosol when heterodimerised with it, when expressed in a polarised cell model [199]. The other is the commoner Southeast Asian autosomal recessive (AR) dRTA, in which one wild type allele is capable of 'rescuing' a mutant protein when heterodimerised with it, resulting in cell membrane expression of the heterodimer [199, 203].

In the previous chapter, I have shown that when expressed in *Xenopus laevis* oocytes, dRTA associated AE1 mutants are 'cation leaky'. This effect is demonstrable in the 3 European AD mutants that we characterised (R589H, G609R and S613F), but much greater in G701D, the only SE Asian AR mutant that I examined [311].

The magnitude of the cation leak property was so much larger in the AR G701D mutant than the AD European mutants, and the G701D mutation is so much more common in southeast Asia (it has a gene frequency of 0.7% in Northeast Thailand [192]) than the AD mutants are in Europe (sporadic kindreds only). On the basis of these observations, I hypothesised that the G701D mutation had undergone positive selection pressure on the basis of its large cation leak property.

There are other AE1 mutations, which also cause AR dRTA in Southeast Asia, and these too, appear to be quite common. Amongst these are the mutations S773P, ΔV850 and A858D, which are found in Northeast Thailand and Papua New Guinea [63, 180, 202], both malarious regions. I decided to

characterise these three other described SE Asian mutants, alongside the G701D mutant, using the *Xenopus laevis* expression system.

My results show that these 3 other AE1 mutations also induce a large cation leak (of the same order of magnitude as G701D) in these still functional anion exchangers. The effect of these mutations on the anion exchange structure of the protein is then discussed as the consequences of this cation leak in cells expressing AE1.

5.2 Aims

1) To express the selected kAE1 mutants (G701D, S773P, ΔV850 and A858D) in Xenopus oocytes.

2) To characterise the anion transport characteristics of the selected kAE1 mutants by observation of $^{36}Cl^-$ uptake into oocytes and by measurement of intra-oocyte pH during CO2 acidification with and without chloride containing extracellular medium.

3) To demonstrate and quantify any cation leak activity by lithium influx and intracellular cation measurements in these mutants and compare these directly to the leak activity in G701D.

5.3 Methods and materials

5.3.1 Xenopus oocyte harvesting

Xenopus laevis oocytes were harvested as detailed in the general methods chapter.

5.3.2 Oocyte injection

Collected oocytes were washed and defolliculated as detailed in the general methods chapter. Stage V-VI oocytes were then injected with a mixture of 10 ng of kAE1 and 2.5 ng GPA cRNA, and were maintained in 18^{o}C MBS for three days before starting the experiments.

5.3.3 Plasmid and DNA construction

The pSP65erythroid human AE1 (hAE1) plasmid was used to construct the kidney AE1 (kAE1), deleting the 65 N-terminal amino acids, as described in the General Methods chapter. For point mutations, primers were used with the following codon substitutions:

S773P: TCC/CCC, ΔV850: GTG was deleted, A858D: GCC/GAC.

Primers were purchased from Eurogentec (Seraing, Belgium); polymerase chain reactions (PCRs) were performed using a Biometra “UNO Thermoblock” thermocycler (Göttingen, Germany). Sequences generated by PCR were sequenced in their entirety to ensure that no polymerase errors were introduced (Gexbyweb, Meylan, France).

HindIII linearised pSP65kAE1 wildtype and mutant plasmids were transcribed using SP6 polymerase (Ambion transcription kit). HindIII linearised BSXG-GPA plasmid was transcribed using T7 RNA polymerase (Ambion transcription kit). RNA concentrations were determined on a formamide/formaldehyde agarose gel in MOPS (3-[N-Morpholino]propanesulphonic acid) buffer.

5.3.4 Western blot

Oocyte membranes were prepared by homogenization of 20 oocytes (control or injected) in cooled Tris-HCl buffer, 20 mM, pH 7.4, 250 mM sucrose and 5 mM protease inhibitor, Pefablock (Roche, Paris, France), as described in the general methods chapter. The presence of kAE1 was detected by antibody Bric 170 directed against the C-terminus of kAE1. The secondary antibody was anti-mouse IgG-peroxidase, which was detected by chemiluminescence using a Fujifilm Las-3000 Luminescence image analyser.

5.3.5 Lithium influx

Lithium influx measurements were performed by atomic absorption spectrometry: eight oocytes were incubated at 19^{o}C in Li-MBS (NaCl and KCl replaced by $LiNO_3$ and KNO_3 respectively, and HEPES-NaOH replaced by Tris-HNO3 15mM, pH 7.4). It was decided to use NO_3^- instead of Cl^- to avoid any cation movements coupled with Cl^-. However, experiments done in LiCl containing medium gave similar results to those in $LiNO_3$ containing medium. After 2 h incubation (uptake is linear up to 6 h), the oocytes were rapidly washed 3 times in ice-cold milliQ water (plus ouabain, 5.10^{-4} M) and transferred individually into microcentrifuge tubes. Extracellular water was quickly removed and oocytes were dried at 95^{o}C for 3 minutes in a block heater, then oocytes were incubated for 10 minutes at 95^{o}C in 50 µl of 0.1M NaOH and finally 250 µl of milliQ water was added to each oocyte. Intracellular lithium concentration was determined by graphite furnace atomic absorption spectrometry (Perkin Elmer AAS 3110).

5.3.6 Intracellular cation measurements

Injected oocytes were incubated in MBS containing ouabain (0.5 mM) and bumetanide (5 µM) at 19^{o}C for 3 days. Na^+ and K^+ content of oocytes was measured by flame spectrophotometry, as previously described in the general methods section.

In some experiments, the Na^+ in the MBS was substituted with NMDG (N-methyl-D glucamine). The final NMDG MBS medium was (in mM): NMDGCl: 85; KCl: 1; $KHCO_3$: 2.4; $MgSO_4$: 0.82; Ca $(NO_3)_2$: 0.33; $CaCl_2$: 0.41; HEPES: 10; KOH: 4.5; pH: 7.4. Cation contents were expressed as µmol per gram of dry weight (µmol/g d. wt.).

5.3.7 Intracellular pH measurements

Oocyte intracellular pH was measured using selective microelectrodes, as described in the general methods chapter. The ability of wt and mutant kAE1 to regulate intracellular pH was assessed by measuring intracellular pH of oocytes adapted in MBS without HCO_3^-, then incubated in the following medium: NaCl 63.4 mM; KCl 1 mM; $NaHCO_3^-$ 24 mM; $MgSO_4$ 0.82 mM; $Ca(NO_3)_2$ 0.33 mM; $CaCl_2$ 0.41 mM; HEPES/NaOH 5 mM pH 7.35; CO_2 5%, O_2 95% and then bathed in MBS without Cl^- (Na-gluconate 63.4 mM; K-gluconate 1 mM; $NaHCO_3$ 24 mM; $MgSO_4$ 0.82 mM; $Ca(NO_3)_2$ 0.74 mM HEPES/NaOH 5 mM pH 7.35, CO_2 5%, O2 95%). Results are given as ΔpHi per min ± s.e. ΔpHi was measured when acidified oocytes were exposed to Cl^- free medium and corresponds to the initial slope of the alkalinisation.

5.3.8 Chemicals

Unless otherwise stated, all chemicals were purchased from Sigma (St Louis, MO). Agarose was purchased from GIBCO BRL (Life technologies, Gaithersburg, MD). Minipreps of DNA were done with a Macherey Nagel, (Düren, Germany). Anti-AE1 antibodies BRIC170 and BSXG-GPA plasmid were a kind gift of Dr. Ashley Toye (University of Bristol, UK).

5.4 Results

5.4.1 Western Blot

Mutant kAE1 constructs were co-expressed in oocytes with the AE1 chaperonin glycophorin A (GPA), because without GPA there is absent membrane expression of G701D- kAE1 in oocytes[180]. Oocyte plasma membrane expression of wildtype and mutant kAE1 was confirmed by detecting bands of the appropriate molecular mass on western blotting (Figure 5-1). The western blots were done at the same time as the functional studies.

5.4.2 Anion Transport;

5.4.2.1 Intracellular pH recordings

To confirm that Cl^-/HCO_3^- exchange activity occurred in oocytes expressing wildtype or mutant AE1, we measured the change in intracellular pH (pH_i) following acute exposure to a solution containing CO_2/HCO_3^- (in the presence of extracellular Cl^-), which caused an initial and rapid fall in pH_i that stabilised as CO_2 reached equilibrium across the cell membrane. On replacing extracellular Cl^- with gluconate, pH_i promptly rose in the presence of functional anion exchange activity, due to HCO_3^- extrusion being dependent on exchange for intracellular Cl^-. Oocytes expressing wildtype kAE1 showed a fall in intracellular pH_i in Cl^--containing medium that recovered on replacing extracellular Cl^- with the impermeant anion gluconate (Figure 5-2 A). This pattern was seen with all 4 mutants, indicating functional plasma membrane expression of Cl^-/HCO_3^- exchange. To compare the Cl^-/HCO_3^- exchange activity of wildtype with mutant kAE1, the initial rate of pH_i recovery after acid loading was estimated as ΔpH_i/minute (Figure 5-2 B). There was no significant difference between wtkAE1 and the mutants. It was assumend that all expressed AE1 proteins would have a similar effect on the oocyte buffering capacity, which was not measured.

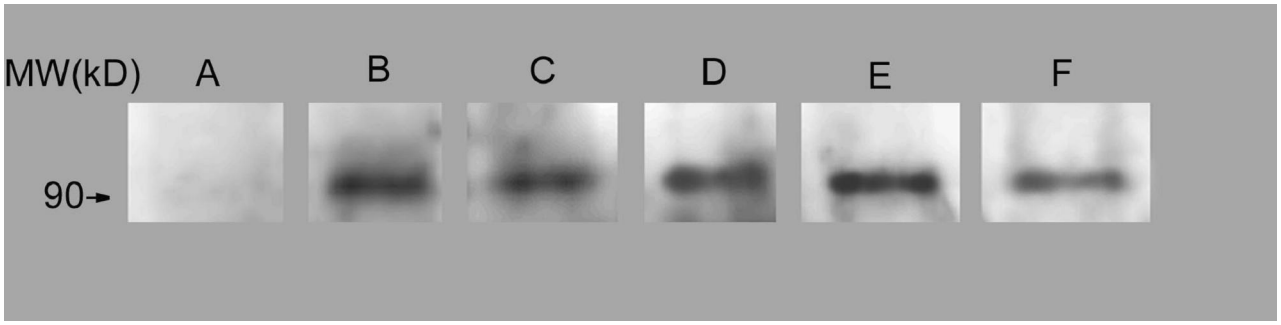

Figure 5-1 A representative western blot of an oocyte membrane probed with anti-AE1 antibodies (BRIC170).

From left to right: a) non-injected; b) wild-type kAE1+GPA; c) G701D+GPA; d) S773P+GPA; e) Δ850+GPA; and f) A858D+GPA expressing oocytes. Representative of 3 experiments.

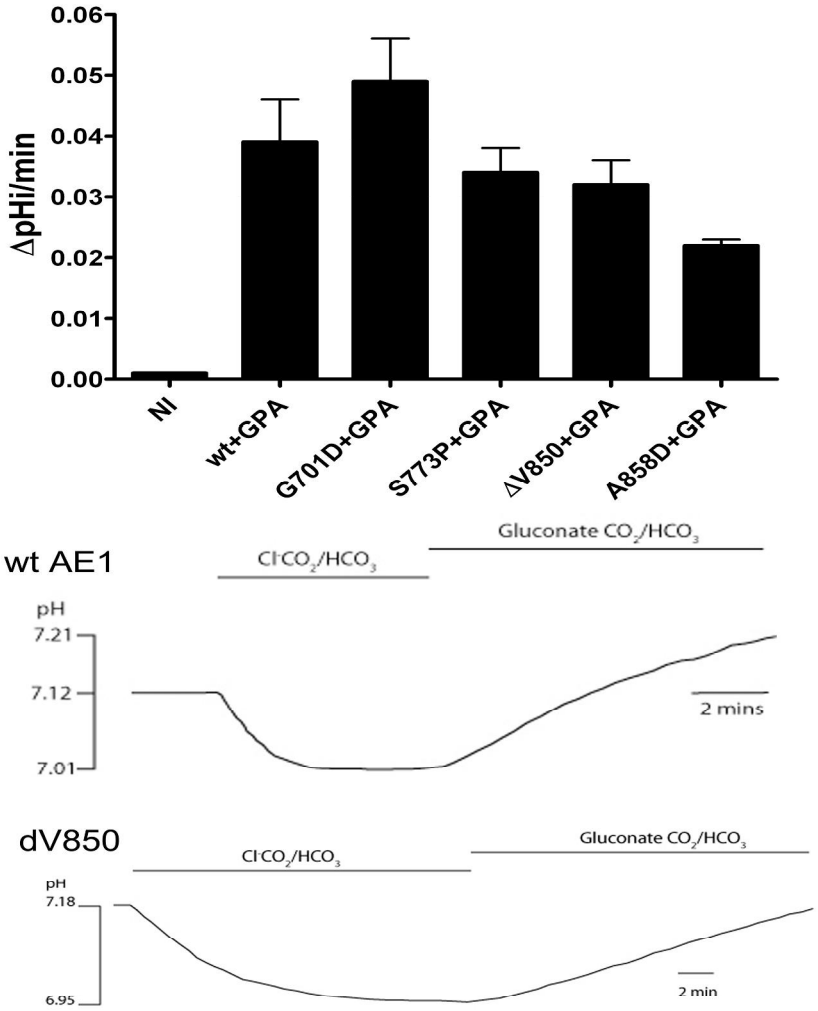

Figure 5-2 Composite figure of intracellular pH data.

A) pH_i recovery rate after an acid load of control oocytes (NI) or oocytes co-expressing GPA with wild-type or the different kAE1 point mutations. Data are means of 4 oocytes +/- s.e.m.

B) plots of intracellular pH vs. time of an oocyte acidified with CO_2 in the presence and then absence of extracellular Cl^-. The oocytes are expressing wt kAE1 and the Δ850 mutation respectively with GPA.

5.4.3 Cation Transport;

5.4.3.1 Lithium influx

We measured lithium influx into the oocytes, using Li as a surrogate monovalent cation for sodium. The extracellular medium contained ouabain and bumetanide to inhibit any cation movement through the Na^+/K^+-ATPase and the Na^+-K^+-$2Cl^-$ co-transporter, respectively.

Li influx (Figure 5-3) was low in both non-injected and wildtype kAE1-expressing oocytes, in contrast to the influx seen in all 4 of the tested mutants, who had similar Li influx to G701D.

5.4.3.2 Intracellular cation contents

Na^+ and K^+ content of oocytes expressing wildtype or mutant kAE1 was measured after 3 days of incubation in control medium (MBS), or in medium in which Na^+ had been substituted with the impermeant cation N-Methyl-D-Glucamine (NMDG). Both media contained ouabain and bumetanide. Intracellular cation measurements (Figure 5-4 A) showed reversal of the normal ratio of intracellular Na^+ to K^+ content in mutant-expressing oocytes compared with controls. All dRTA-associated mutants showed reversal of this ratio, with the changes being similar in all of the mutants tested. Moreover the Na^+ uptake is balanced by the K^+ loss with a 1/1 stoichiometry. There was no fall in intracellular K^+ when extracellular Na^+ was replaced with NMDG (Figure 5-4 B) indicating that outward flux of K^+ required a countering inward flux of Na^+ to maintain electrical neutrality.

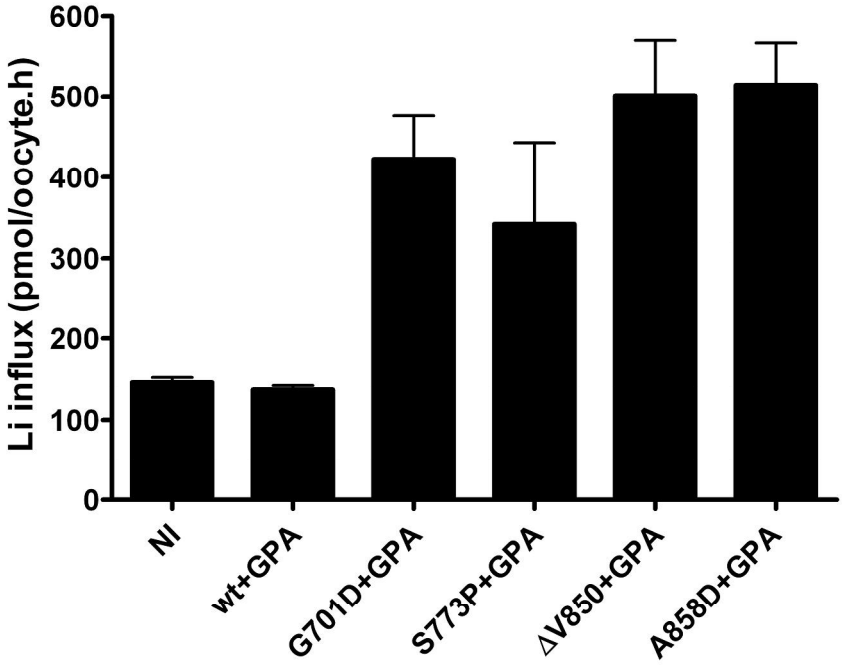

Figure 5-3 Representative experiment of ouabain- and bumetanide-resistant Li influx.

Performed at 22°C into non-injected, wild-type kAE1- and mutant kAE1-expressing oocytes three days after injection. All injected oocytes are co-expressing GPA. Data are means +/- s.e.m. of 8 oocytes.

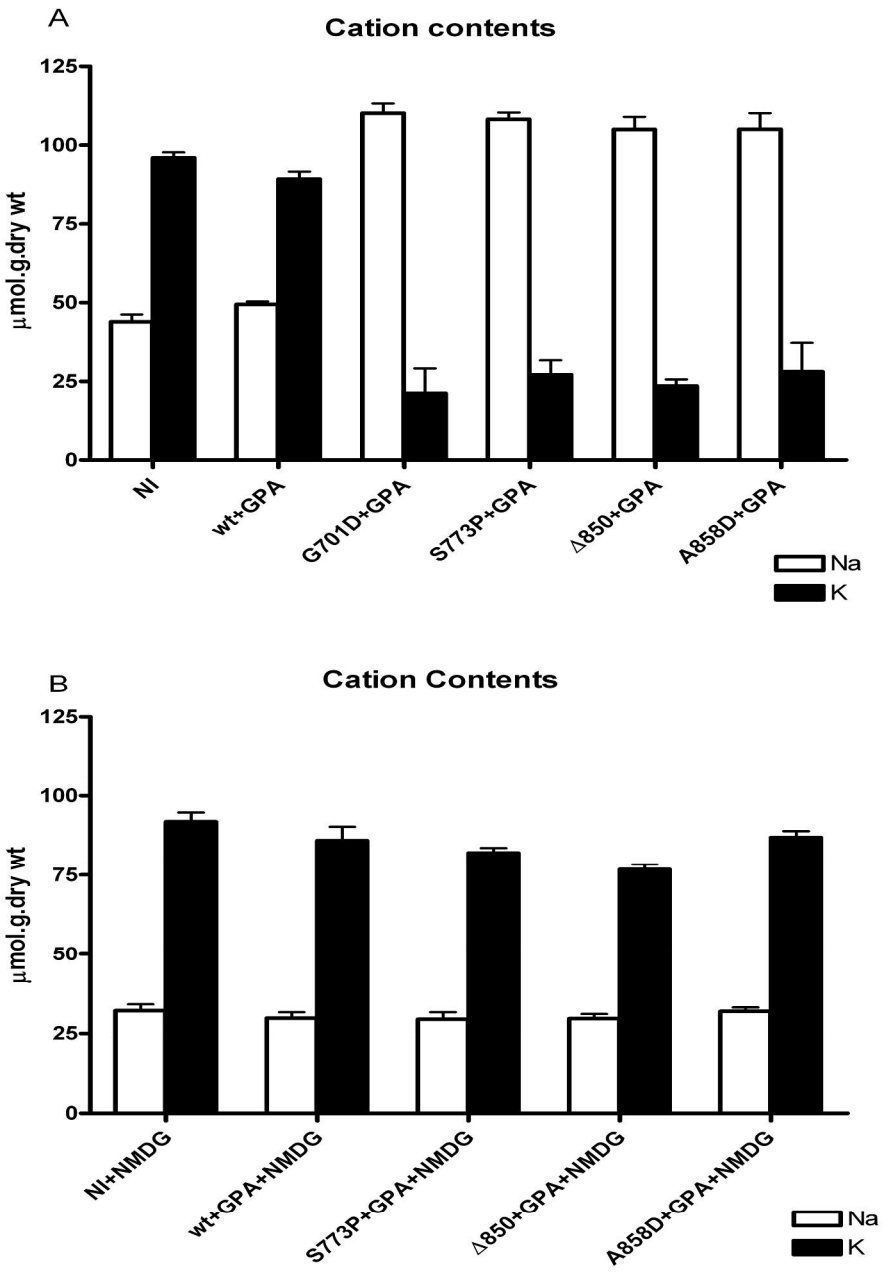

Figure 5-4 Composite figure of intracellular cation content measurements.

Na^+ (white bars) and K^+ (black bars) content was measured in oocytes that were either non-injected or expressing wild-type or mutant kAE1, and GPA, three days after incubation in Na^+ (A) or NMDG (B) containing MBS at 19^{o}C, with 0.5 mM ouabain and 5 µM bumetanide. Data expressed in µmol per g of dry weight (dry wt.) are means +/- s.e.m. of 15 oocytes.

5.5 Conclusions

I have demonstrated that in addition to G701D the 3 other AR dRTA AE1 associated mutants (S773P, ΔV85O and A858D) are all functional anion exchangers and all have a 'cation leak' that is of similar magnitude. I chose these mutants on the basis that they have autosomal recessive phenotypes and were all found in Southeast Asia, just like the G701D mutation in which I demonstrated a large cation leak [311]. S773P was found in Northeast Thailand [202], the same region that G701D is prevalent in [180]. Δ850 was found in several families from the malarious Northern coast of Papua New Guinea (PNG), and A858D was found in families from both Northern PNG and peninsula Malaysia [63] (see Figure 5-5).

5.5.1 Structure function implications

All of the mutants that I have used are on highly evolutionary conserved sequences of the primary structure of AE1, and are in a region that is important for anion exchange, namely the transmembrane portion of the molecule on the C-terminal side of transmembrane domain 8 [312]. Two of the mutants, Δ850 and A858D, are adjacent to the residue K851, which appears to be a crucial residue for anion exchange. Pyridoxal phosphate, a known inhibitor of AE1 anion exchange, binds to K851 [313] and the AE1 inhibitor H_2DIDS, which binds to AE1 in a one-one manner, covalently binds both K539 and K851, abolishing anion exchange [150]. Furthermore, the extracellular span from residues 852 to 857 bridging the last two putative transmembrane domains (TM12 and 13 according to the topology from Zhu et al [312]), as well as the adjacent ends of the transmembrane helices form the so-called anion selectivity filter-a region that constitutes part of the opening of the putative ion translocation pore and which is involved in repelling cations [172]. It was demonstrated that a large number of cysteine substituted residues in this region were sensitive to sulfhydryl inhibition, but only those forming the extracellular region were inhibitable by a positively charged sulfhydryl inhibitor, although deeper residues were inhibited by the uncharged ones.

Also, of those residues that were inhibited by the uncharged pCMBS, none of the superficial extracellular residues had inhibition competed by Cl^-, indicating anion selectivity in this region [172]. This anion selectivity was speculated to be due to the positive charge at residue 851, as well as possibly the σ^+ helical pole charge from the last transmembrane segment. This is of interest, because the deletion mutation ΔV850, in effect replaces the positively charged lysine at position 851 with a non-charged serine, which results in a cation leaky but functional AE1. It implies that the precise conformation of the extracellular domain, 852 to 857, which is likely to have been altered by the deletion mutation, is probably not important for anion exchange, which is preserved in this mutant.

Figure 5-5 Distribution of AE1 mutations in SE Asia.

The area shown covers 5200 miles from west to east and 3400 miles from north to south. Coloured arrows represent individual families with dRTA and an AE1 mutation. The PNG family shown with the A858D mutation also had members with the Δ850 mutation.

The A858D mutation replaces a small non-charged alanine residue with a negatively charged aspartate-this would disrupt the σ^+ helical pole charge and probably interfere with the positive charge at 851. But as for the ΔV850 mutation, this does not prevent the Cl^-/HCO_3^- exchange activity.

The substitution mutation S773P lies at the C terminal end of TM 10, which is predominantly hydrophobic, with a 4 charged residues at the N-terminal end, and has been speculated to form part of the lining of the anion translocation pore [314], introducing a proline residue may induce a conformational change in this region.

5.5.2 Large cation leak a class effect of SE Asian dRTA-associated AE1

I have now described a number of point mutations in AE1 associated with dRTA, which cause a cation leak in oocytes expressing these proteins, all of which have anion exchange function. Some of these are found in European families, have an autosomal dominant phenotype, and when expressed with GPA in Xenopus oocytes have a small to moderate cation leak (R589H, G609R, S613P) [311]. The others are found in Southeast Asian populations, have an autosomal recessive phenotype, and when expressed with GPA in Xenopus oocytes demonstrate a large cation leak (G701D, S773P, ΔV850, A858D). It is tempting to speculate that the European mutations, located in TM segments 6-7, cause conformational changes that are more deleterious to intracellular trafficking than to normal ion transport, whilst the SE Asian mutations, located on the less well defined, and probably more mobile, C-terminal region of the molecule cause structural changes that affect trafficking to a lesser degree, but induce a larger cation leak.

That these mutations (S773P, ΔV850, A858D) cause large cation leaks, in the same order of magnitude as the G701D mutation, is intriguing. All are found

in malarious areas of Southeast Asia (NE Thailand and PNG). Previous authors have speculated on a protective effect of these dRTA-causing mutations against malaria [63, 315].

Could such an effect be attributed to the cation leak property that I have demonstrated? AE1 is present in the intercalated cell and the erythrocyte, the isoforms differing only in that the renal isoform lacks the first 65 N-terminal amino acids. Thus, the red cell would have cation leaky band 3 at its cell membrane, even in heterozygotes. This is reminiscent of Southeast Asian Ovalocytosis, a hereditary red cell disorder caused by a 9 amino-acid deletion in AE1, in which red cells exhibit an abnormal cold-induced cation leak [258]. SAO is known to be protective against cerebral malaria [245, 260], but does not appear to protect erythrocytes against invasion by malaria parasites[258, 264].

6. Discussion

6.1 Testing Urinary Acidification

6.1.1 How good is it?

In Chapter 3 I described my data on urinary acidification following the simultaneous administration of furosemide and fludrocortisone. As I implied in that chapter, there are some other published data on urinary acidification induced by the sequential administration of fludrocortisone then furosemide.

6.1.1.1 Walter

Walter et al described the use of fludrocortisone and furosemide to induce urinary acidification [287]. In a small study using only 8 healthy subjects, with normal measured creatinine clearances were studied on 4 different occasions, where they were given a) control, b) ammonium chloride, c) furosemide alone (40mg), or d) furosemide with fludrocortisone (1mg) administered the preceding evening. Each subject drank at least 500 ml of water between 9 and 11 am, after that, water intake was *ad libitum*. Urine volume and pH were measured at hourly intervals. They found that in their subjects furosemide with fludrocortisone given the evening before achieved a minimum urine pH as low as that found after ammonium chloride administration, and all below a pH of 5.5. This was considerably better than the minimum urinary pHs achieved with furosemide alone. (See Figure 6-1)

6.1.1.2 Viljoen

In 2007, Viljoen and colleagues in a letter [316] outlined their data looking at 10 healthy controls and 10 patients with recurrent nephrolithiasis or nephrocalcinosis, 3 of whom had a family history of nephrolithiasis. All subjects underwent both the short ammonium chloride test and the same sequential fludrocortisone and furosemide test that Walter et al used (i.e. fludrocortisone given the evening before the test).

They found that all 10 controls were able to acidify their urine to a pH of less than 5.3 with both tests, but whilst all 10 patients could acidify their urine to a pH below 5.3 with ammonium chloride, only 3 could do so with sequential

fludrocortisone and furosemide. (See figure 6-2) They thus concluded that the test had a negative predictive value of 100%, but that its positive predictive value was much less.

6.1.1.3 Audit

In Appendix one, I detail the data from the Royal Free renal unit's subsequent experience with the simultaneous furosemide and fludrocortisone test, which has been very consistent with 47 patients tested and ammonium chloride tests confirming the veracity of the furosemide and fludrocortisone test when they are done in the same patient.

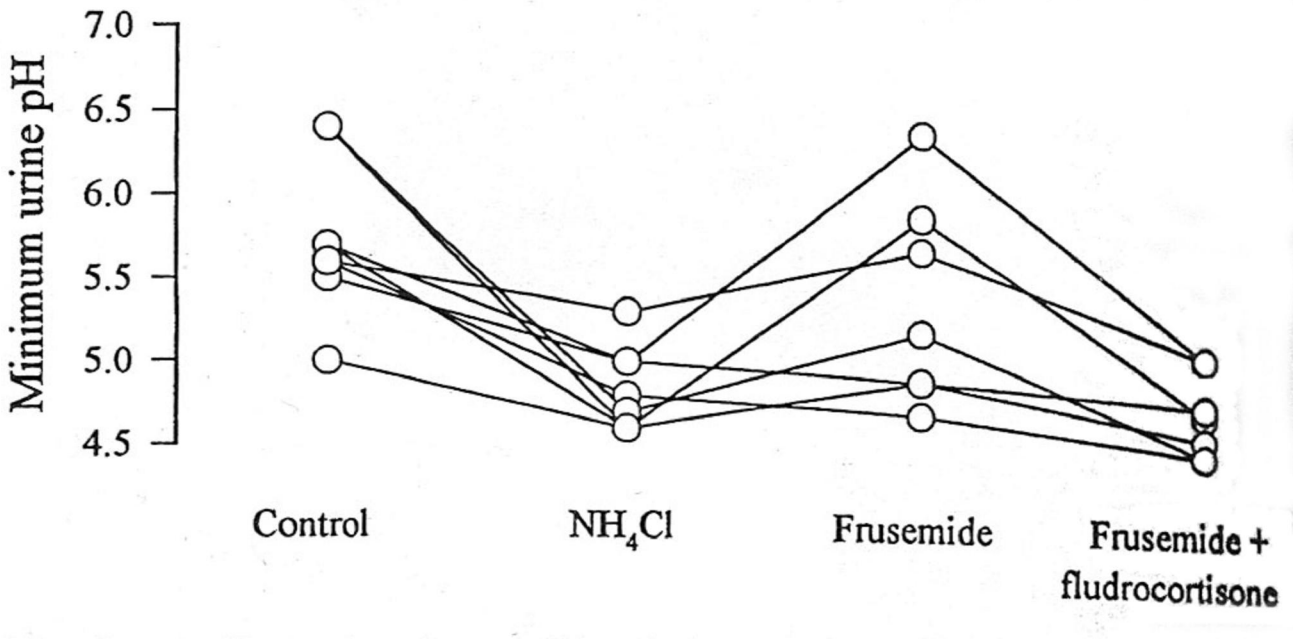

Figure 6-1 Schematic showing minimum pHs of individuals undergoing urinary acidification with control/sham, ammonium chloride, furosemide alone and furosemide and fludrocortisone.

Results from the same individual are connected by a line.

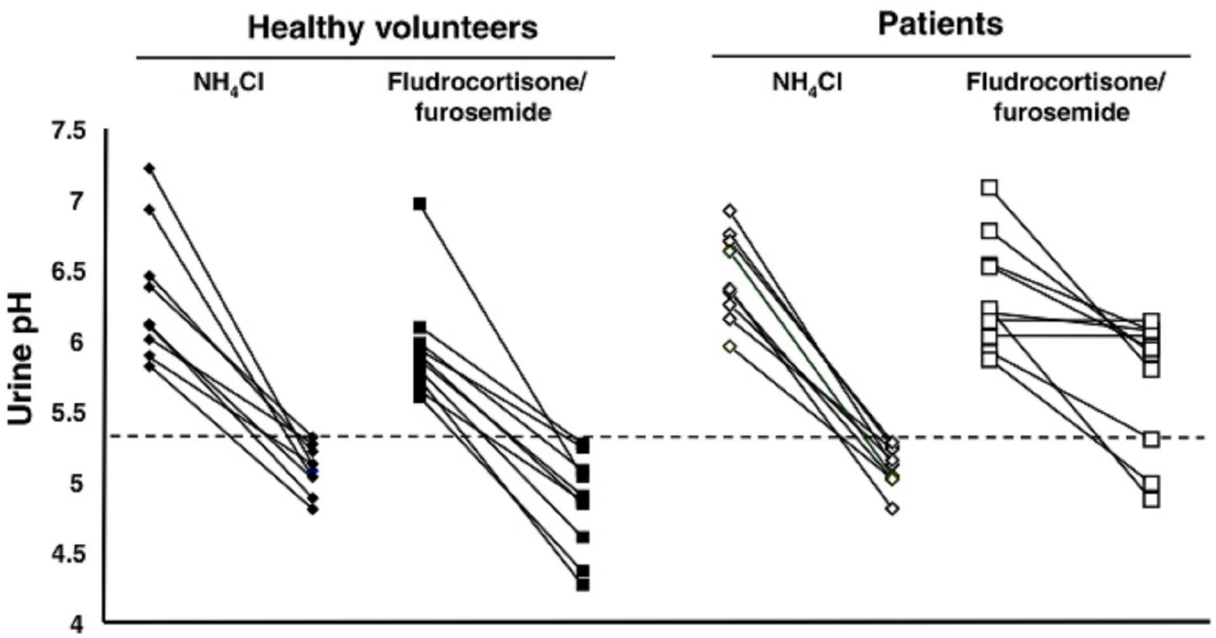

Figure 6-2 Paired pre-test and nadir urine pH values.

Shown for normal controls (closed symbols) and patients with nephrolithiasis and/or nephrocalcinosis (open symbols) subjected to NH_4Cl (diamonds) and fludrocortisone/furosemide (squares) tests.

6.1.1.4 Potassium excretion in AE1-associated dRTA

Unfortunately, the second of the initial questions that I asked at the beginning of this thesis; “Can the urinary potassium wasting observed in inherited dRTA be attributed, in part, to a property of the mutated transport protein that causes it?” is still unanswered. In Chapters 4 and 5, I have demonstrated that dRTA-associated AE1 mutations can act as a cation conductance, but that finding led to a different route of enquiry, and the role of cation leaky AE1 in the hypokalaemia of dRTA remains elusive. In Appendix 2, I have analysed subgroups of patients that I examined for the experiments detailed in Chapter 3, and the results are consistent with the patients with AE1 associated dRTA having increased urinary potassium wasting, but the numbers are so low that no firm conclusion can be drawn.

This question could be answered by stable transfection of polarised cell models, or better, animal work with a knock-in mouse, or measurements in more patients with the appropriate AE1 mutation, too rare in Western Europe to be easily achievable. These experiments are unfortunately beyond the scope of this thesis.

6.2 Molecular structure/function implications

6.2.1 Phylogeny

The SLC4 (Solute Carrier 4) family of transporters, also known as the bicarbonate transporter superfamily-includes the products of 10 human genes. These encode membrane proteins with very similar hydropathy plots, consistent with the presence of 10-14 transmembrane helices. At least 8 SLC4 proteins transport HCO_3^- (or CO_2) across the plasma membrane. These proteins fall into two functional groups: three Cl-HCO_3 exchangers (AE1-3) and five Na coupled HCO_3^- transporters (NBCe1, NBCe2, NBCn1, NDCBE and NCBE). The two remaining SLC4 members (AE4 and BTR1) do not yet have a properly established function, and homologically they fall between the other groups.

The SLC4 superfamily are ubiquitous amongst vertebrates; however, it is possible to trace SLC4-related genes to invertebrates [317, 318], yeast [319] and plants [320, 321]. These seem to perform a diverse set of functions, for example one plant SLC4 homologue, BOR1, mediates the transport of boron [321].

Guizouarn et al constructed a phylogenetic tree (Figure 6-3) of genes from the SLC4 family based on publicly available gene sequences from a number of different characterised species to investigate the observation that trout AE1, when expressed in Xenopus oocytes, acted spontaneously as an anion (and osmolyte) channel [322]. Their data supported the contention that the genes coding for the anion exchange proteins and the NBC co-transporters form two lineages (or morphophyletic clusters) that probably descended from a common ancestral gene.

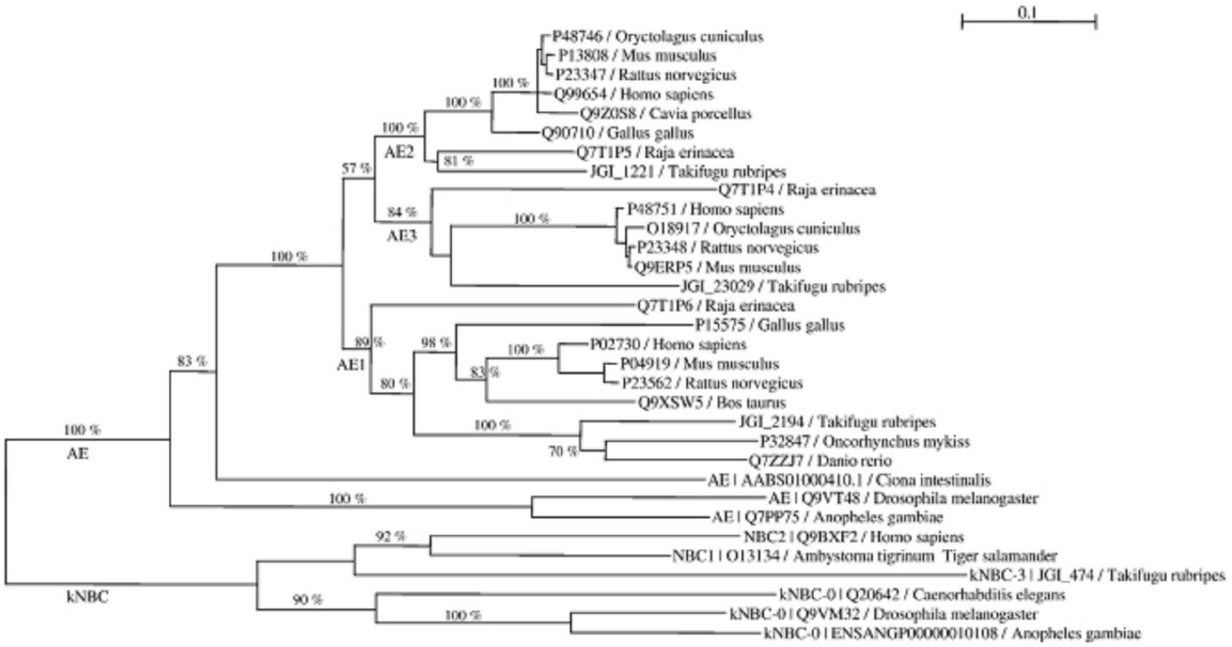

Figure 6-3 Unrooted phylogenetic tree of Cl/HCO_3^- exchangers

Inclusion of sequences for electrogenic Na^+ bicarbonate cotransporter allows a proposal of a scenario for the duplication events within the AE families.

The topology of the tree that they constructed suggested that two rounds of gene duplication formed the three AE1 genes, the first giving rise to AE1 and the putative ancestor gene A", which then itself was duplicated to form the AE2 and AE3 ancestral genes.

The distances between gene sequences was lowest in the AE2 sub family, which suggests that AE2 is under a stronger selection pressure and that it is more likely to have retained the ancestral function of the protein. AE2 is widely distributed throughout different tissues and is thought to play an important role in intracellular pH regulation. The AE1 sub family in contrast had a higher variability between species, and those from fish species appeared to have an accelerated rate of mutation.
Of the represented fish species (trout, skate and zebrafish), only trout AE1 had the spontaneous anion and osmolyte channel property when expressed in Xenopus oocytes, although both trout and skate erythrocytes developed swelling activated osmolyte loss [323]. This led the authors to speculate that the expression of trout AE1 in Xenopus oocytes caused a conformational change, which caused it to act as an anion channel that was irreversibly 'activated', in contrast to its state in trout erythrocytes, which was activation dependent. This was supported by a number of observations: that trout AE1 expressed in Xenopus oocytes is nearly DIDS insensitive, whilst in trout erythrocytes, AE1 is DIDS sensitive [324] suggesting that there is a conformational difference between the two differently expressed proteins, also that in trout erythrocytes the anion and osmolyte conductive properties are only activated by a decrease in intracellular ionic strength [271, 274].

6.2.2 Evidence for wt AE1 acting as a cation transporter

Is it possible that wtAE1 in humans might also act as an ion (anion or monovalent cation) and/or osmolyte conductance? There is evidence to suggest that this might be the case.
In the human red cell, in a number of disease states, organic osmolyte permeabilities or Na^+ and K^+ leaks have been observed and inhibited by AE1

inhibitors, in malaria [325], Southeast Asian Ovalocytosis [258] and sickle cell anemia [326]. Human red cells also exhibit Na^+ and K^+ fluxes when incubated in low ionic strength media, and these fluxes are also inhibited by AE1 inhibitors and are thought to be mediated by AE1 [327]. Similar observations have been made about red cells undergoing deformational stress [328]. Thus, one could envisage a scenario where AE1 acted as a regulator of red cell volume, in addition to its other roles in the erythrocyte, by acting as a permeability to two critical determinants of red cell volume, organic osmolytes, and monovalent cations, which determine the hydration state of the red cell. This permeability would be activated by a conformational change caused by plasma membrane deformation (that could occur with red cell swelling in times of osmotic stress, or red cell deformation when passing through capillaries, for example) and possibly by other mechanisms caused by decreasing intracellular osmolality.

6.3 Malaria resistance hypothesis

One of the most important causes of child mortality worldwide is malaria due to *Plasmodium falciparum,* which kills over 1 million children a year in Africa alone. This death toll is only one aspect of the global burden of malaria. *P. falciparum* is estimated to cause about half a billion episodes of disease each year[329] and there are hundreds of millions of cases due to other parasite species—*Plasmodium vivax, malariae,* and *ovale.* When this enormous burden of mortality and morbidity is considered, it is unsurprising that malaria acts as a strong evolutionary selection pressure, as first proposed by JBS Haldane [330].

Several human hereditary diseases have undergone a positive selection by Plasmodium species (chiefly *P. falciparum*), because they confer a survival advantage in those infected with malaria; these include mutations in the gene for β-globin, *HBB,* which cause sickle cell disease (HbS) [331, 332], and the other HBB gene variants, HbC [333, 334] and HbE [335, 336], alpha [337, 338]and beta thalassaemia, G-6-PD deficiency [339-343] and variations in the chemokine receptor *FY*, which cause the Duffy negative blood group [344-346]. Southeast Asian Ovalocytosis (SAO), caused by a deletion mutation in the red cell anion exchanger AE1, is another example; it has been shown to reduce the incidence and severity of cerebral malaria [260].

6.3.1 Epidemiology

6.3.1.1 Malaria in Thailand

Thailand has, like the other countries of Southeast Asia, endemic malaria, with 152,240 reported cases in 1992 (which is probably a significant underestimate of the true number, as no prescription is necessary to buy antimalarial drugs in Thailand).

The Thai government has designated “malaria control zones” where efforts are concentrated to control transmission, where the disease burden is heaviest. These control zones are on the western Thai-Myanmar border and the northeastern Thai-Laos and Thai-Cambodian borders. Approximately 12.7 million Thai people live in these control zones [347]. The majority of Thai malarial cases are Plasmodium falciparum (approximately 60%), the remainder almost exclusively Plasmodium vivax.

6.3.1.2 Lao-thai ethnic distribution

The Northeast Thailand, also known as Isan, is located on the Khorat plateau, which is bordered by Laos (which is separated from Isan by the Mekong river) to the north and east, by Cambodia to the southeast. It is separated from Northern and Central Thailand by the Phetchabun mountain range. It covers approximately 160, 000km^2, making it about half the size of Germany (figure 6-4).

The Lao-speaking people of this region, who comprise a large fraction of the population are known as Lao-Thai or Khon Isan. The traditional language spoken by these people is known as Isan, which may be considered a dialect of Laotian, but which is written in the Thai alphabet.

The region was dominated by the Lao Lan Xang kingdom after the Khmer empire began to decline in the 13th century. After that it was increasingly settled by Lao and Thai migrants, and when Thailand (or Siam as it was then) became dominant, it carried out forced population transfers from Laos to Isan in the 18th and 19th centuries.

In the 20th century, successive Thai governments have enforced a policy of ‘Thaification’ to promote the incorporation of Isan as an integral part of Thailand and to de-emphasise the Lao origins of the population. The forcible introduction of the Thai alphabet for writing the Isan language is one example of these policies.

Figure 6-4 Map of Thailand, showing Isan (northeast Thailand) in red.

It is bordered by Cambodia to the south and Laos to the north and east.

6.3.1.3 HbE and Thalassemia in Thailand

Haemoglobin E (HbE) disease is the second most common haemoglobinopathy in humans and is often found in high frequencies in malaria endemic regions. HbE occurs in up to 50% of Khmer people living in the region of NE Thailand at which the borders of Thailand, Cambodia and Laos meet-an area which has been dubbed the “HbE triangle”[348]. It is asymptomatic in heterozygotes and homozygotes, but homozygotes have a microcytic anaemia of the same degree of severity as that seen in β thalassemia trait. There is linkage dysequilibrium evidence to suggest that it arose from a single mutation some 1,200 to 4,400 years ago with a rapid rise in allelic frequency [336] Possession of the HbE trait appears to protect against the development of severe malaria [349].

The thalassemias, both alpha and beta are found in high frequencies in Thailand, northern Thailand is generally recognised to have one of the highest frequencies of α-thalassemia in the world [350] and some estimations of the frequency of β-thalassaemia in Northern Thailand are as high as 10% [348] The initial evidence supporting malaria protection by both forms of thalassemia was derived from population genetic studies. Globally, the thalassaemias are the commonest single gene disorders thus far described. Overall, gene frequencies >0.10 are the norm in tropical populations, whereas frequencies are somewhat lower in the subtropics and rare in the temperate zones.

In a series of classic studies conducted in the 1960s, a cline (or gradient) in the population frequencies of β-thalassemia in Sardinia that correlated with altitude [351]. Although malaria was no longer endemic in Sardinia when these studies were conducted, historically, the incidence of malaria was known to have correlated closely with altitude. The favoured hypothesis was that the cline represented selection for the thalassaemic β-globin gene under pressure from malaria.

Support for this hypothesis has since come from the Pacific. While the gene frequency for beta thalassaemia followed a similar correlation with altitude in Papua New Guinea [352], it was the data for α-thalassemia collected from communities throughout Melanesia that was perhaps the more dramatic.

These data showed that α-thalassaemia was found in all malaria-exposed populations and at gene frequencies that were proportional to the incidence of malaria based on historical reports.
α-thalassemia has also been shown to be protective against severe malaria [353] and β-thalassaemia has been shown to be associated with lower parasite densities in children with β-thalassaemia trait in Liberia compared with infected controls [354].

6.3.1.4 Endemic dRTA in NE Thailand

Distal RTA is endemic in NE Thailand and is a cause of serious morbidity and mortality [306]. A large proportion of this burden is due to the G701D mutation: one study in NE Thailand found that 7 of 12 paediatric patients (5 of 8 families) with dRTA had the G701D mutation, and further screening of first-degree relatives found the G701D mutation in 16 out of 25 subjects [193]. The only study of its kind showed a gene frequency of >0.7% for G701D in NE Thailand [192].

6.3.2 Founder effect

Individuals with the G701D mutation invariably carry the so-called 'Memphis' polymorphism K56E [63, 315], demonstrating a 'founder effect' and suggesting that the mutation originated from a single index case, and that it has undergone positive evolutionary selection. These observations have led previous authors to speculate that AE1-associated dRTA may also be protective against malaria [63, 315].

6.3.3 Similarity to SAO

This is similar to SAO, another AE1 mutation (in this case a deletion of residues 400-408). Patients with SAO are obligate heterozygotes, as homozygosity is presumably being fatal *in utero*. SAO is endemic in malarial

areas of PNG [355]; while there is no difference in the rates of peripheral parasitaemia, there is a strong protective effect against cerebral malaria [260]. SAO is also linked with the Memphis polymorphism [356] mentioned earlier, again suggesting a founder effect. SAO erythrocytes are susceptible to parasite invasion [264], in contrast to earlier reports [263]. Studies of SAO red cells have shown a temperature-dependent monovalent cation leak [258], reminiscent of the cation leaks seen in HSt red cells; as have SAO AE1 expressing Xenopus oocytes (H.Guizouarn unpublished observation).

6.3.4 Red cell cation leaks in Thalassaemias and Haemoglobinopathies

Indeed, increased membrane cation permeability of red cells from thalassemic patients has been reported, both in β-thalassemia [357] and α-thalassemia [358]. The mechanism for this is not clear, although it has been suggested that it may be due to precipitating haemoglobin subunits [359] and/or hemichromes [360] interacting with the membrane. Interestingly, it has been noted that red cells from patients with thalassemia major undergo large changes in cation contents when the blood collected from them is allowed to stand for a few hours before examination [357].

There are no reports of increased red cell membrane cation permeability in HbE, but it is well documented in another haemoglobinopathy, sickle cell disease. In sickle cell disease, deoxygenation induced sickling also induces a red cell membrane cation leak, which is inhibitable by stilbene compounds (which inhibit AE1) [361]. Whether HbE red cell membranes are cation leaky as well is, at the moment unknown.

6.3.5 Hypothesis - Do red cell cation leaks protect against severe malaria?

In it possible that the cation leak that we have found in the G701D mutant could be related to malaria resistance? In other words, could having a cation leaky AE1 molecule at the red cell membrane be advantageous in the event of malaria infection?

The malaria parasite undergoes its asexual cell cycle (schizogony) in the human erythrocyte with a periodicity of approximately 48 hours. A single parasite invades an erythrocyte, develops as a ring form, then as a trophozoite, undergoes cell division to produce 8-32 daughter merozoites before cell lysis occurs at 48 hours, releasing the merozoites to infect more erythrocytes. Over this period, the parasite induces a number of anion and cation permeabilities in the erythrocyte membrane known as new permeability pathways (NPPs).

Due to these NPPs, the intracellular Na^+ and K^+ concentrations reverse, to eventually approximate the Na^+/K^+ ratio of the extracellular milieu, with the erythrocyte expanding as it gains more Na^+ and water (Figure 6-5). This renders the schizont osmotically fragile-so much so, in fact, that models of the same process occurring in uninfected erythrocytes predict osmotic cell lysis when the relative cell volume reaches the lytic ratio of 1.8 at 44 hours post infection [362].

However recent work has shown that at approximately 48 hours the falciparum-infected schizont undergoes an explosive lysis, which propels the merozoites into contact with uninfected erythrocytes [363]. Just before lysis the schizont exhibits a characteristic ‘flower’ appearance, as parasite proteases digest the erythrocyte cell membranes and cytoskeleton [364], presumably preparing the already osmotically stressed cell for explosive rupture (Figure 6-6 C-D). The parasite appears to delay early osmotic lysis until the red cell is sufficiently weakened by proteolysis for efficient explosive lysis to occur, by consuming haemoglobin in excess of its synthetic requirements, secreting the breakdown products and preventing oxidative damage from the released heme, to compensate for the cell volume increase [365]. That it expends so much metabolic effort to ensure this late explosive lysis underlines its importance to the parasite. This reconciles the observation that although merozoites are known to have a myosin motor complex, they are not motile until they are in contact with an erythrocyte to invade [366]. Explosive lysis would provide the dispersing force for merozoites to reach uninfected red cells. As Glushakova has suggested [363], explosive lysis may

be necessary for adequate dispersion and infection by the parasite when the lysing schizont is surrounded by other infected erythrocytes, such as occurs in the cerebral microcirculation in cerebral malaria, where the chances of merozoites ejected by non-explosive lysis coming into contact with non-infected erythrocytes is much reduced.

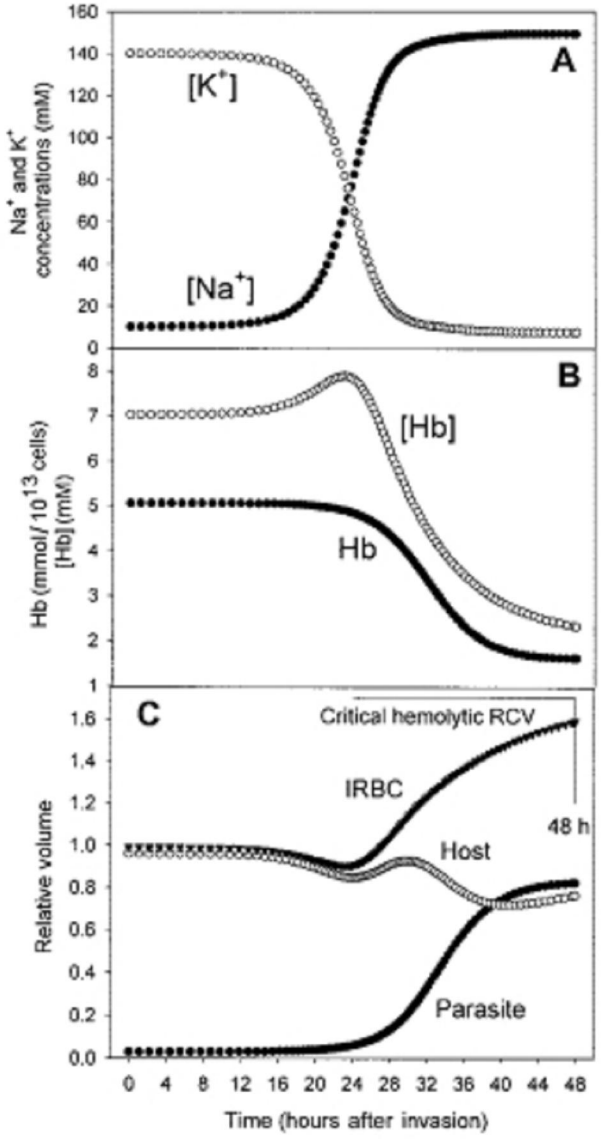

Figure 6-5 Predicted changes in selected homeostatic variables of P falciparum–infected red cells during the asexual reproduction cycle of the parasite.

The panels show the predicted changes in (A) host cell Na^+ and K^+ concentrations and (B) Hb content (Hb) and concentration ([Hb]); Hb content is expressed per 10^{13} cells, the approximate number of cells contained in 1 liter of normal, uninfected human red cells. (C) Relative cell volume of IRBCs (▼) and relative host (○) and parasite (●) volumes; all volumes are expressed relative to RBC volume at the time of invasion. The horizontal top line in panel C indicates the mean critical haemolytic RCV, and the vertical right hand line indicates the 48-hour end of the asexual cycle.

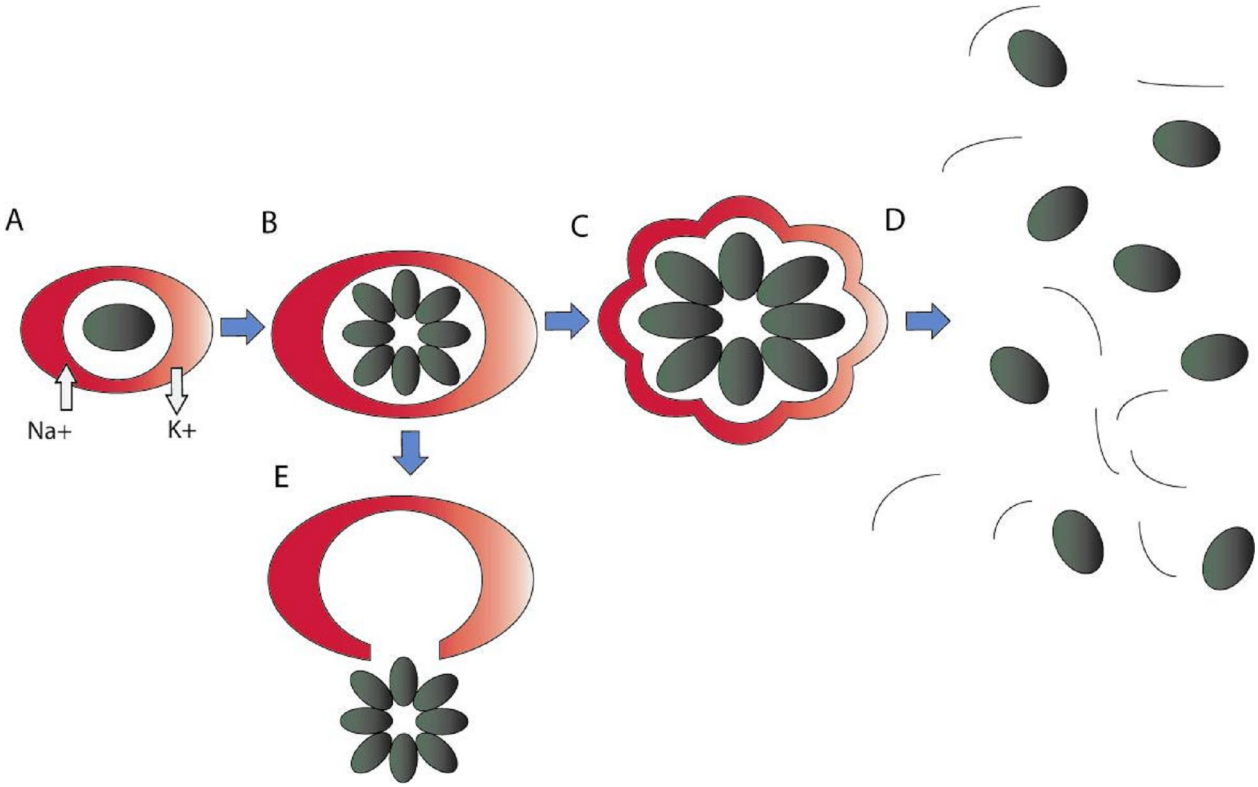

Figure 6-6 A cartoon of the proposed events in malarial asexual reproduction in infected erythrocytes

(A-B) As the infected erythrocyte (A) develops NPPs, the intracellular Na^+ and K^+ concentrations reverse, to eventually approximate the Na^+/K^+ ratio of the extracellular milieu, with the erythrocyte expanding as it gains more Na^+ and water (B).

(C-D) Just before lysis the schizont exhibits a characteristic 'flower' appearance (C), as parasite proteases digest the erythrocyte cell membranes and cytoskeleton, presumably preparing the already osmotically stressed cell for explosive rupture (D).

(E) Cation leaky red cells are predisposed to earlier osmotic lysis, pre-empting explosive lysis, thus reducing the dispersal of merozoites and thus the parasites virulence.

If ‘cation leaky’ erythrocytes were infected and their cation leak predisposed them to earlier osmotic lysis, late explosive lysis would be less likely to occur and so occur less frequently, thereby reducing parasite’s virulence (Figure 6-6 E). This would be particularly important in the microcirculation, where reduced explosive lysis would mean that dense (infected) erythrocyte sequestration would become self-limiting (as has been observed in vitro [367]). This could explain the strong protective effect that SAO (with its cation leaky red cells) exhibits against cerebral malaria [260], and would predict a similar effect for G701D carriers.

6.4 Alternative speculative mechanisms

6.4.1 Accelerated Red Cell ‘Apoptosis’

An alternative mechanism could arise from the observation of apoptotic-like cell death in erythrocytes where old or damaged erythrocytes display cell shrinkage, cell membrane blebbing and phosphatidylserine asymmetry-all features of apoptosis in nucleated cells, which precede erythrocyte endocytosis by macrophages.

Hyperosmotic shock opens non-selective cation permeabilities in the cell membrane [368], as does oxidative stress [369]. Calcium as well as monovalent cations can move through these new pathways[368, 369] (as it can in cation leaky SAO red cells [258]), and activate Ca^{2+} sensitive K^+ Gardos channels and the increasing Ca^{2+} concentration can activate erythrocyte scramblase [370], leading to the breakdown of phosphatidylserine symmetry [371]. The loss of K^+ from the cell in itself appears to play a part in this apoptosis like cell death, as cell shrinkage and phosphatidylserine exposure is blunted if the extracellular K^+ is increased, or the Gardos channel is inhibited (e.g. with clotrimazole) [372].

If the cation leaky AE1 leaks Ca^{2+}, as it may do in SAO, or even if it just transports monovalent cations, then it could plausibly accelerate these

processes. Falciparum infection of the erythrocyte induces apoptotic like changes on the cell [373], and whilst it is not clear whether the parasite benefits from this, or whether it is a native defence response, it will contribute to earlier cell clearance [374], especially if the erythrocyte has a pre-existing cation leak.

6.4.2 ATP depletion

Similarly, it is known that cation leaky SAO red cells, if stored in the cold, can exhaust their intracellular ATP due to the cation leak being larger at low temperatures and the Na^+/K^+ pump up-regulating in an attempt to compensate until it uses all of the available ATP [258].

Malaria infected erythrocytes also develop large permeabilities to monovalent cations, and in a similar way, the Na^+/K^+ pump depletes intracellular ATP in an attempt to compensate for this, and starts to decline in activity because of this at about 36 hours post invasion [362, 375].

Erythrocytes are susceptible to apoptosis-like cell death when ATP-depleted [376] (which may be the reason that phosphate deficiency can lead to anaemia) and this might, therefore, provide another avenue for early clearance of malaria infected erythrocytes in individuals with cation leaky red cells.

This is supported by the observation that P.Falciparum parasites can grow normally in erythrocytes that have the Na^+/K^+ pump inhibited by ouabain, and thus lose potassium via the basal cation leak, but do not become ATP deplete [377].

6.4.3 Low intra-erythrocytic potassium inhibiting parasite growth

X-ray microanalysis has shown that the parasite maintains high intra-parasite potassium [378], despite the intra-erythrocytic potassium being low due to the NPP cation permeability. Could lower red cell potassium adversely affect the parasite's growth, perhaps by depriving it of potassium?

Data about the growth of Falciparum parasites in haemoglobin SA erythrocytes might support this idea. Friedman [379] found that parasite growth in haemoglobin SA erythrocytes was normal under an atmosphere of 17% O_2, but the parasites could not grow at 3% O_2. The parasites could, however, grow normally in SA haemoglobin at 3% O_2 tension if the culture medium contained high K^+ concentrations. The parasitised erythrocytes grown in the usual culture medium at low oxygen tension sickled and lost K^+. The parasitised erythrocytes still sickled in high K^+ medium, but the erythrocyte K^+ remained normal.

Recent work with novel pharmacological agents has shown that agents that can cause loss of intra-parasitic potassium have anti-plasmodium activity, without causing haemolysis of the parasitised red cell [380].

6.5 High sodium/low potassium erythrocyte

6.5.1.1 Animal resistance

If the cationic milieu were important in ameliorating the efficiency of the plasmodium asexual cell cycle, then one would predict that red cells that are low in potassium and high in sodium for other reasons would also be inherently difficult for the parasite to reproduce in. Malaria affects other animal species, there are primate malarias, rodent malarias, avian rolarias and even saurine malarias, but these only occur in animals with high sodium

erythrocytes, there are no malarias in animals with high sodium and low potassium erythrocytes, such as dogs, cats, cows and horses [381].

6.5.1.2 Babesia

However, canine erythrocytes can be infected with Babesia [382], a protozoal intra-erythrocyte parasite that produces far fewer membrane permeabilities than plasmodium does [383], compatible with the concept that the low sodium cell cannot tolerate the greater NPPs induced by plasmodium.

6.5.2 Possible further avenues of investigation

If this hypothesis is correct, then the internal cationic state of the erythrocyte is of vital importance to the asexual cell cycle of plasmodium, and this implies that manipulation of this milieu might offer avenues for pharmacotherapy.

Experimental compounds, which induce cation leaks in normal erythrocytes [384] should have a similar effect on schizonts that we predict with G701D and SAO. This might offer avenues for development of novel pharmacotherapy if the effect could be reproduced non-toxically in-vivo.

Currently, there are 4 classes of anti-malarial drugs, quinoline derivatives, antifolates, artemisinin derivatives and antimicrobials. All act on the parasite, and with the exception of the artesemisin derivatives, parasite resistance is a growing problem. The prospect of a new class of drug, which acts to make the red cell membrane ‘cation leaky’, is attractive for a number of reasons, not least the possibilities afforded for combination therapy, a crucial therapeutic strategy against the development of plasmodial drug resistance.

7. Appendix 1: Further experience with the Furosemide and Fludrocortisone test

The physiology investigations day unit has been running urinary acidification tests using the furosemide and fludrocortisone protocol since 2007, shortly after I performed the measurements detailed in Chapter 3.

In that time, 47 patients have been tested using the furosemide and fludrocortisone protocol (detailed below), which was based on the work detailed in Chapter 3. Of the 47 patients tested, 17 had positive tests (i.e. failed to acidify their urine to a pH of less than 5.3) and a further 6 had positive tests that were confirmed with a follow up ammonium chloride test. 24 patients had negative tests, with normal urinary acidification. The difference between the average values (± s.e.m.) for the positive and negative tests is summarised graphically (Figure 7-1 A). The pattern of the negative results average results is similar to the equivalent in chapter 3, with the threshold pH being surpassed on average at 3 hours, and returning to baseline between 4-5 hours. This pattern is not seen with the positive results. Of those that had a follow up ammonium chloride test, the same negative result was obtained; the average values are detailed below (Figure 7-1 B).

7.1 Protocol for the furosemide and fludrocortisone test

- The patient should be weighed and a baseline urine pH taken

- The patient should be given 40 mg of furosemide and 1mg of fludrocortisone. The patient is at liberty to eat and drink as they like.

- Urinary testing should start 1 hour after the dosing with furosemide and fludrocortisone and carry on hourly after this until the last sample, which should be 4-6 hours after dosing with NH_4Cl started.

- All urinary pH testing should be done with the pH electrode meter as soon as the urine specimen is collected. As before the electrode pH meter needs to be calibrated against the supplied buffers before use each day that it is used.

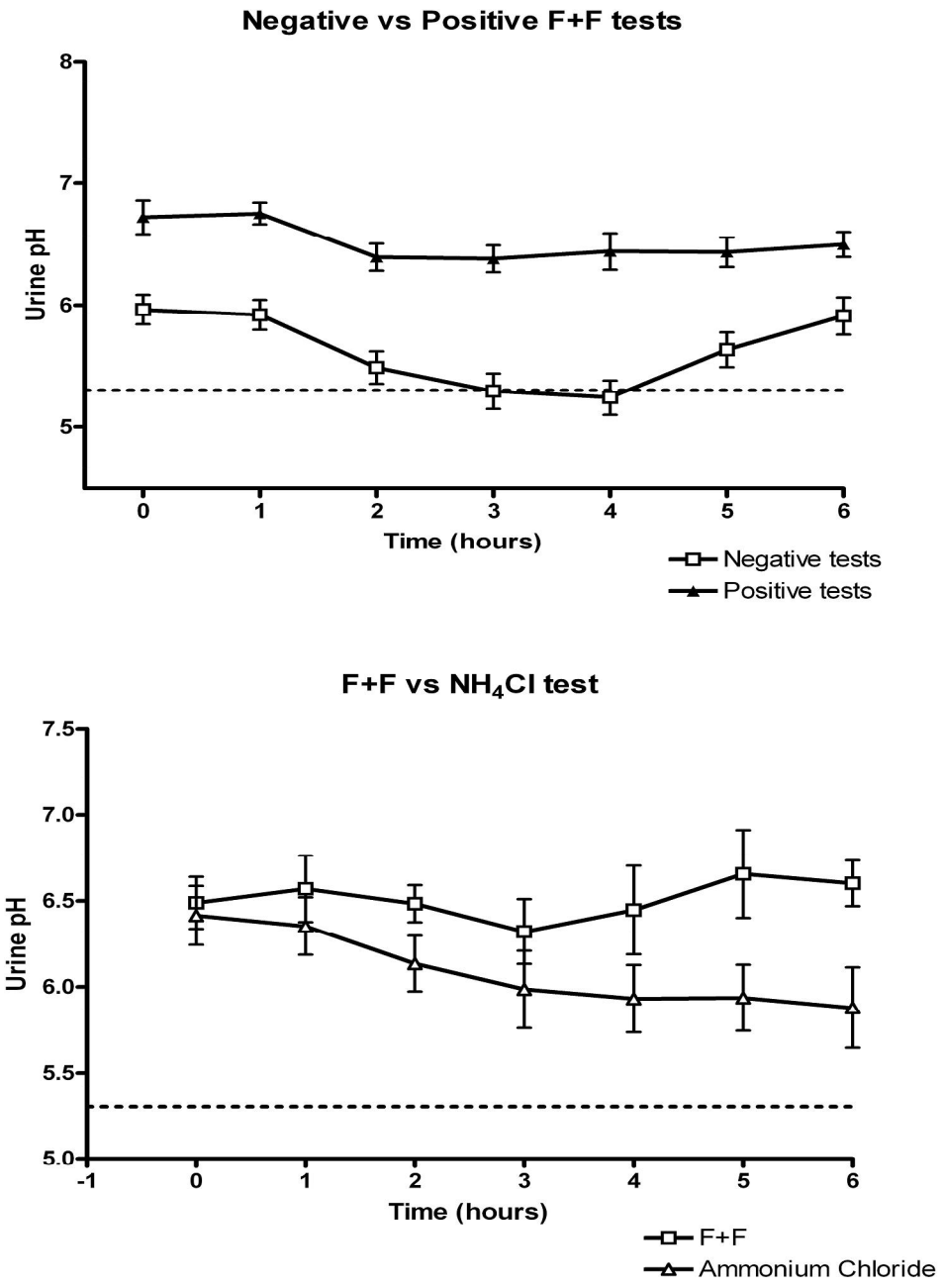

Figure 7-1 Composite graph of urinary pH data for patients routinely receiving urinary acidification testing.

The top graph shows the different average urinary pHs (± s.e.m.) for those with positive and negative results with the F+F test. The bottom graph shows the difference between urinary pH with the F+F and NH_4Cl test in those who underwent both tests.

8. Appendix 2: Potassium Excretion in AE1 and non-AE1 dRTA patients

In the experiments detailed in Chapter 3, I studied patients with dRTA, and some of these had hereditary dRTA caused by AE1 mutations. Unfortunately, only one such patient completed both tests, but two others also completed the ammonium chloride test. All three patients had the R589H mutation, two of the patients being siblings.

The data is summarised in the figure (see Figure 8-1), where the one AE1 dRTA patient (Figure 8-1 A) has a very large potassium excretion (particularly at the 2 hour peak) with the furosemide and fludrocortisone test, compared to the other dRTA patients with the same test.

In the ammonium chloride test, potassium excretion was highest at 4 hours in the three patients with AE1 associated dRTA (Figure 8-1C), which was the time of peak acidification. In contrast, the non-AE1 associated dRTA patients had their lowest potassium excretion at this time, with the only uniformly high excretion being at the start of the test (Figure 8-1D).

Although the numbers of subjects mean that the differences observed between these two groups are statistically not significant, the pattern seen in the furosemide and fludrocortisone test is the pattern one would expect if mutant AE1 caused an increased potassium permeability of the apical α-intercalated cell membrane (either directly, or via the activation of another transporter), mediating potassium loss from the α-intercalated cell when the luminal is at its most electronegative.

It is harder to try and interpret the differences in potassium excretion data in the ammonium chloride test-it is not immediately obvious why a theoretical increase in apical cation permeability would cause increased potassium loss when urinary acidification is increasing; this observation needs to be repeated before meriting further investigation.

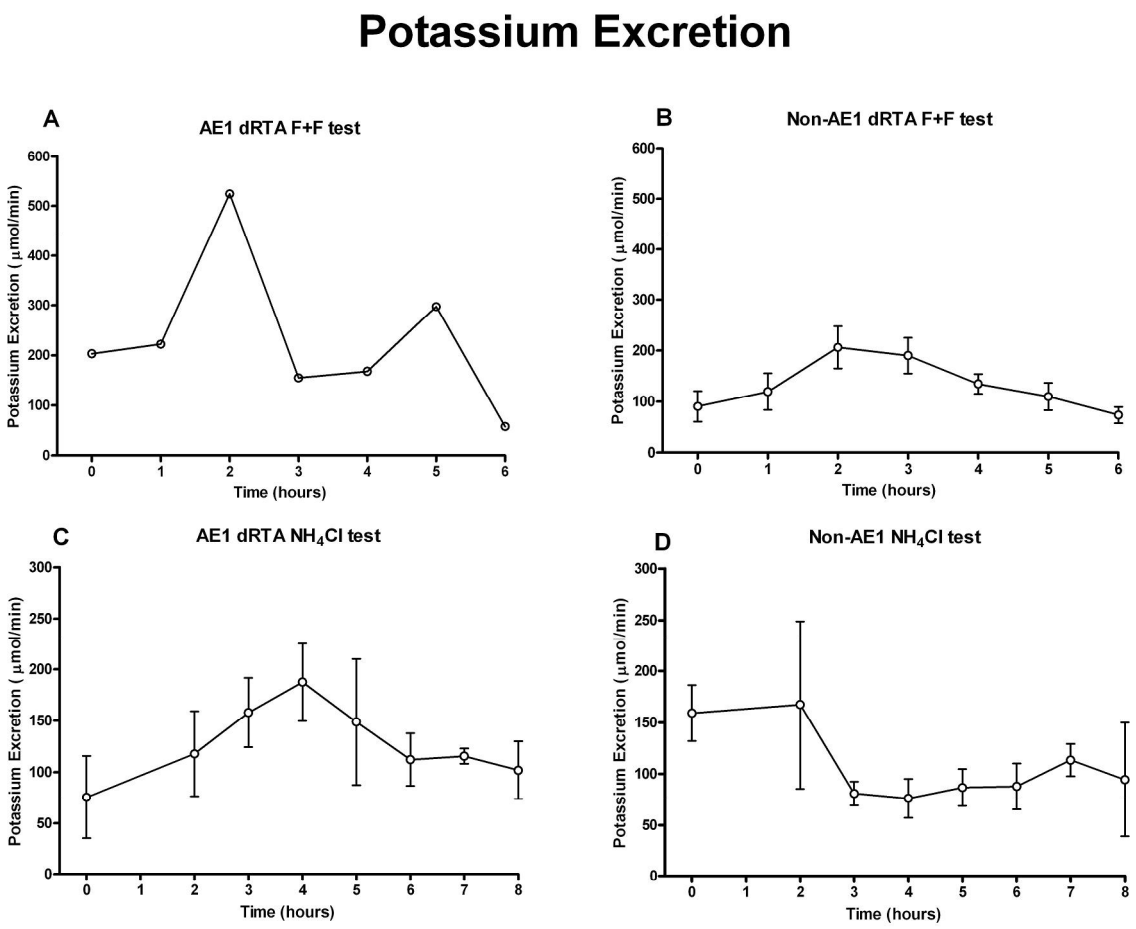

Figure 8-1 Graphs showing potassium excretion.

Graphs show those dRTA patients with AE1 mutations (A and C) and those without (B and D), using both the F+F (A and B) and NH_4Cl (C and D) tests.

9. References

1. Bruce, L.J., et al., *Familial distal renal tubular acidosis is associated with mutations in the red cell anion exchanger (Band 3, AE1) gene.* J Clin Invest, 1997. **100**(7): p. 1693-707.
2. Karet, F.E., et al., *Mutations in the gene encoding B1 subunit of H+-ATPase cause renal tubular acidosis with sensorineural deafness.* Nat Genet, 1999. **21**(1): p. 84-90.
3. Shearn, M.A. and W.H. Tu, *Latent renal tubular acidosis in Sjogren's syndrome.* Ann Rheum Dis, 1968. **27**(1): p. 27-32.
4. Tu, W.H. and M.A. Shearn, *Systemic lupus erythematosus and latent renal tubular dysfunction.* Ann Intern Med, 1967. **67**(1): p. 100-9.
5. Pasternack, A., et al., *Renal acidification and hypergammaglobulinemia. A study of rheumatoid arthritis.* Acta Med Scand, 1970. **187**(1-2): p. 123-7.
6. Mason, A.M. and P.L. Golding, *Renal tubular acidosis and autoimmune thyroid disease.* Lancet, 1970. **2**(7683): p. 1104-7.
7. Golding, P.L. and A.S. Mason, *Renal tubular acidosis and autoimmune liver disease.* Gut, 1971. **12**(2): p. 153-7.
8. McCurdy, D.K., G.G. Cornwell, 3rd, and V.J. DePratti, *Hyperglobulinemic renal tubular acidosis. Report of two cases.* Ann Intern Med, 1967. **67**(1): p. 110-7.
9. Boddy, A.V., et al., *Ifosfamide nephrotoxicity: limited influence of metabolism and mode of administration during repeated therapy in paediatrics.* Eur J Cancer, 1996. **32A**(7): p. 1179-84.
10. Batlle, D.C., S. Sabatini, and N.A. Kurtzman, *On the mechanism of toluene-induced renal tubular acidosis.* Nephron, 1988. **49**(3): p. 210-8.
11. Boton, R., M. Gaviria, and D.C. Batlle, *Prevalence, pathogenesis, and treatment of renal dysfunction associated with chronic lithium therapy.* Am J Kidney Dis, 1987. **10**(5): p. 329-45.
12. McCurdy, D.K., M. Frederic, and J.R. Elkinton, *Renal tubular acidosis due to amphotericin B.* N Engl J Med, 1968. **278**(3): p. 124-30.

13. Butler, A.M., J.L. Wilson, and S. Farber, *Dehydration and acidosis with calcification at renal tubules.* Jounal of Pediatrics, 1936. **8**: p. 489.
14. Goossens, J.P., et al., *Incomplete renal tubular acidosis in sickle cell disease.* Clin Chim Acta, 1972. **41**: p. 149-56.
15. Wilson, D.R. and A.A. Siddiqui, *Renal tubular acidosis after kidney transplantation. Natural history and significance.* Ann Intern Med, 1973. **79**(3): p. 352-61.
16. Heering, P., et al., *Distal tubular acidosis induced by FK506.* Clin Transplant, 1998. **12**(5): p. 465-71.
17. vd Heijden, A.J., et al., *Acute tubular dysfunction in infants with obstructive uropathy.* Acta Paediatr Scand, 1985. **74**(4): p. 589-94.
18. Shear, L., H.L. Bonkowsky, and G.J. Gabuzda, *Renal tubular acidosis in cirrhosis. A determinant of susceptibility to recurrent hepatic precoma.* N Engl J Med, 1969. **280**(1): p. 1-7.
19. Gahl, W.A., J.G. Thoene, and J.A. Schneider, *Cystinosis.* N Engl J Med, 2002. **347**(2): p. 111-21.
20. Golberg, L., et al., *A clinical and biochemical study of galactosaemia; a possible explanation of the nature of the biochemical lesion.* Arch Dis Child, 1956. **31**(158): p. 254-64.
21. Morris, R.C., Jr., *An experimental renal acidification defect in patients with hereditary fructose intolerance. I. Its resemblance to renal tubular acidosis.* J Clin Invest, 1968. **47**(6): p. 1389-98.
22. Hodgson, S.V., et al., *A balanced de novo X/autosome translocation in a girl with manifestations of Lowe syndrome.* Am J Med Genet, 1986. **23**(3): p. 837-47.
23. Matsuo, N., et al., *Proximal renal tubular acidosis in a child with type 1 glycogen storage disease.* Acta Paediatr Scand, 1986. **75**(2): p. 332-5.
24. Wiebers, D.O., et al., *Renal stones in Wilson's disease.* Am J Med, 1979. **67**(2): p. 249-54.
25. Rochman, J., et al., *ASdult Fanconi's syndrome with renal tubular acidosis in association with renal amyloidosis: occurrence in a patient with chronic lymphocytic leukemia.* Arch Intern Med, 1980. **140**(10): p. 1361-3.

26. Messiaen, T., et al., *Adult Fanconi syndrome secondary to light chain gammopathy. Clinicopathologic heterogeneity and unusual features in 11 patients.* Medicine (Baltimore), 2000. **79**(3): p. 135-54.
27. Morris, A.A., S.V. Baudouin, and M.H. Snow, *Renal tubular acidosis and hypophosphataemia after treatment with nucleoside reverse transcriptase inhibitors.* Aids, 2001. **15**(1): p. 140-1.
28. Skinner, R., *Chronic ifosfamide nephrotoxicity in children.* Med Pediatr Oncol, 2003. **41**(3): p. 190-7.
29. Rocher, L.L. and R.L. Tannen, *The clinical spectrum of renal tubular acidosis.* Annu Rev Med, 1986. **37**: p. 319-31.
30. Hu, P.Y., et al., *A splice junction mutation in intron 2 of the carbonic anhydrase II gene of osteopetrosis patients from Arabic countries.* Hum Mutat, 1992. **1**(4): p. 288-92.
31. Sly, W.S., et al., *Carbonic anhydrase II deficiency in 12 families with the autosomal recessive syndrome of osteopetrosis with renal tubular acidosis and cerebral calcification.* N Engl J Med, 1985. **313**(3): p. 139-45.
32. Fathallah, D.M., et al., *Carbonic anhydrase II (CA II) deficiency in Maghrebian patients: evidence for founder effect and genomic recombination at the CA II locus.* Hum Genet, 1997. **99**(5): p. 634-7.
33. DuBose, T.D., Jr. and D.W. Good, *Chronic hyperkalemia impairs ammonium transport and accumulation in the inner medulla of the rat.* J Clin Invest, 1992. **90**(4): p. 1443-9.
34. Lightwood, R., Arch Dis Child, 1936. **10**: p. 205.
35. Lightwood, R., W.W. Payne, and J.A. Black, *Infantile renal acidosis.* Pediatrics, 1953. **12**(6): p. 628-44.
36. Stapleton, T., *Idiopathic renal acidosis in an infant with excessive loss of bicarbonate in the urine.* Lancet, 1949. **1**(6556): p. 683-5.
37. Stapleton, T., *The response of idiopathic renal acidosis to oral sodium lactate.* Acta Paediatr, 1954. **43**(1): p. 49-63.
38. Buchanan, E.U. and G.M. Komrower, *The prognosis of idiopathic renal acidosis in infancy with observations on urine acidification and ammonia production in children.* Arch Dis Child, 1958. **33**(172): p. 532-5.

39. Albright, F. and E.C. Reifenstein, *The Parathyroid Glands and Metabolic Bone Disease*. 1948. p. 393.
40. Pines, K.L. and G.H. Mudge, *Renal tubular acidosis with osteomalacia; report of 3 cases.* Am J Med, 1951. **11**(3): p. 302-11.
41. Wrong, O. and H.E. Davies, *The excretion of acid in renal disease.* Q J Med, 1959. **28**(110): p. 259-313.
42. Rodriguez-Soriano, J. and C.M. Edelmann, Jr., *Renal tubular acidosis.* Annu Rev Med, 1969. **20**: p. 363-82.
43. Morris, R.C., Jr. and E. McSherry, *Symposium on acid-base homeostasis. Renal acidosis.* Kidney Int, 1972. **1**(5): p. 322-40.
44. Albright, F., et al., *Ostcomalacia and late rickets.* Medicine, 1946. **25**.
45. Begun, A. and E. Munster, Z. exp.Path. Ther, 1919. **20**.
46. Linder, G.C., QJM, 1927. **20**.
47. Salvesen, H.A., Acta med. scand., 1928. **69**.
48. Schwartz, W.B., R.L. Jenson, and A.S. Relman, *Acidification of the urine and increased ammonium excretion without change in acid-base equilibrium: sodium reabsorption as a stimulus to the acidifying process.* J Clin Invest, 1955. **34**(5): p. 673-80.
49. Soriano, J.R., H. Boichis, and C.M. Edelmann, Jr., *Bicarbonate reabsorption and hydrogen ion excretion in children with renal tubular acidosis.* J Pediatr, 1967. **71**(6): p. 802-13.
50. Buckalew, V.M., Jr., et al., *Incomplete renal tubular acidosis. Physiologic studies in three patients with a defect in lowering urine pH.* Am J Med, 1968. **45**(1): p. 32-42.
51. Gyory, A.Z. and K.D. Edwards, *Effect of mersalyl, ethacrynic acid and sodium sulphate infusion on urinary acidification in hereditary renal tubular acidosis.* Med J Aust, 1971. **2**(19): p. 940-5.
52. Halperin, M.L., et al., *Studies on the pathogenesis of type I (distal) renal tubular acidosis as revealed by the urinary PCO2 tensions.* J Clin Invest, 1974. **53**(3): p. 669-77.
53. Poy, R.K. and O. Wrong, *The urinary pCO2 in renal disease.* Clin Sci, 1960. **19**: p. 631-9.

54. Fillastre, J.P., R. Ardaillou, and G. Richet, *[Urinary pH and P CO2 in response to an increased alkaline load during chronic renal insufficiency].* Nephron, 1969. **6**(2): p. 91-101.
55. Batlle, D.C., *Segmental characterization of defects in collecting tubule acidification.* Kidney Int, 1986. **30**(4): p. 546-54.
56. Smulders, Y.M., et al., *Renal tubular acidosis. Pathophysiology and diagnosis.* Arch Intern Med, 1996. **156**(15): p. 1629-36.
57. Rastogi, S.P., et al., *Effect of furosemide on urinary acidification in distal renal tubular acidosis.* J Lab Clin Med, 1984. **104**(2): p. 271-82.
58. Weger, W., et al., *Prevalence and characterization of renal tubular acidosis in patients with osteopenia and osteoporosis and in non-porotic controls.* Nephrol Dial Transplant, 2000. **15**(7): p. 975-80.
59. Milne, M.D., S.W. Stanbury, and A.E. Thomson, *Observations on the Fanconi syndrome and renal hyperchloraemic acidosis in the adult.* Q J Med, 1952. **21**(81): p. 61-82.
60. Reynolds, T.B., *Observations on the pathogenesis of renal tubular acidosis.* Am J Med, 1958. **25**(4): p. 503-15.
61. Gill, J.R., Jr., N.H. Bell, and F.C. Bartter, *Impaired conservation of sodium and potassium in renal tubular acidosis and its correction by buffer anions.* Clin Sci, 1967. **33**(3): p. 577-92.
62. Wrong, O.M., T.G. Feest, and A.G. MacIver, *Immune-related potassium-losing interstitial nephritis: a comparison with distal renal tubular acidosis.* Q J Med, 1993. **86**(8): p. 513-34.
63. Bruce, L.J., et al., *Band 3 mutations, renal tubular acidosis and South-East Asian ovalocytosis in Malaysia and Papua New Guinea: loss of up to 95% band 3 transport in red cells.* Biochem J, 2000. **350 Pt 1**: p. 41-51.
64. Sartorius, O.W., et al., *The Renal Regulation of Acid-Base Balance in Man. Iv. the Nature of the Renal Compensations in Ammonium Chloride Acidosis.* J Clin Invest, 1949. **28**(3): p. 423-39.
65. Stokes, J.B., *Sodium and potassium transport by the collecting duct.* Kidney Int, 1990. **38**(4): p. 679-86.
66. Sebastian, A., E. McSherry, and R.C. Morris, Jr., *Renal potassium wasting in renal tubular acidosis (RTA): its occurrence in types 1 and 2*

RTA despite sustained correction of systemic acidosis. J Clin Invest, 1971. **50**(3): p. 667-78.

67. Sebastian, A., E. McSherry, and R.C. Morris, Jr., *Impaired renal conservation of sodium and chloride during sustained correction of systemic acidosis in patients with type 1, classic renal tubular acidosis.* J Clin Invest, 1976. **58**(2): p. 454-69.
68. Kurtzman, N.A., *Disorders of distal acidification.* Kidney Int, 1990. **38**(4): p. 720-7.
69. Sabatini, S. and N.A. Kurtzman, *Pathophysiology of the renal tubular acidoses.* Semin Nephrol, 1991. **11**(2): p. 202-11.
70. Dafnis, E., et al., *Vanadate causes hypokalemic distal renal tubular acidosis.* Am J Physiol, 1992. **262**(3 Pt 2): p. F449-53.
71. Kraut, J.A., et al., *Detection and localization of H+-K+-ATPase isoforms in human kidney.* Am J Physiol Renal Physiol, 2001. **281**(4): p. F763-8.
72. Batlle, D., et al., *Distal renal tubular acidosis and the potassium enigma.* Semin Nephrol, 2006. **26**(6): p. 471-8.
73. Bernstein, B.A. and J.R. Clapp, *Micropuncture study of bicarbonate reabsorption by the dog nephron.* Am J Physiol, 1968. **214**(2): p. 251-7.
74. Kurtzman, N.A., *Regulation of renal bicarbonate reabsorption by extracellular volume.* J Clin Invest, 1970. **49**(3): p. 586-95.
75. Malnic, G., M. De Mello Aires, and G. Giebisch, *Micropuncture study of renal tubular hydrogen ion transport in the rat.* Am J Physiol, 1972. **222**(1): p. 147-58.
76. McKinney, T.D. and M.B. Burg, *Bicarbonate transport by rabbit cortical collecting tubules. Effect of acid and alkali loads in vivo on transport in vitro.* J Clin Invest, 1977. **60**(3): p. 766-8.
77. Atkins, J.L. and M.B. Burg, *Bicarbonate transport by isolated perfused rat collecting ducts.* Am J Physiol, 1985. **249**(4 Pt 2): p. F485-9.
78. Lombard, W.E., J.P. Kokko, and H.R. Jacobson, *Bicarbonate transport in cortical and outer medullary collecting tubules.* Am J Physiol, 1983. **244**(3): p. F289-96.
79. McKinney, T.D. and K.K. Davidson, *Bicarbonate transport in collecting tubules from outer stripe of outer medulla of rabbit kidneys.* Am J Physiol, 1987. **253**(5 Pt 2): p. F816-22.

80. Stetson, D.L., et al., *A double-membrane model for urinary bicarbonate secretion.* Am J Physiol, 1985. **249**(4 Pt 2): p. F546-52.
81. Stetson, D.L. and P.R. Steinmetz, *Alpha and beta types of carbonic anhydrase-rich cells in turtle bladder.* Am J Physiol, 1985. **249**(4 Pt 2): p. F553-65.
82. Evan, A.P., et al., *Postnatal maturation of rabbit renal collecting duct. II. Morphological observations.* Am J Physiol, 1991. **261**(1 Pt 2): p. F91-107.
83. Madsen, K.M. and C.C. Tisher, *Structural-functional relationship along the distal nephron.* Am J Physiol, 1986. **250**(6 Pt 3): p. F1-15.
84. Schuster, V.L. and J.B. Stokes, *Chloride transport by the cortical and outer medullary collecting duct.* Am J Physiol, 1987. **253**(2 Pt 2): p. F203-12.
85. Nelson, R.D., et al., *Selectively amplified expression of an isoform of the vacuolar H(+)-ATPase 56-kilodalton subunit in renal intercalated cells.* Proc Natl Acad Sci U S A, 1992. **89**(8): p. 3541-5.
86. Alper, S.L., et al., *Subtypes of intercalated cells in rat kidney collecting duct defined by antibodies against erythroid band 3 and renal vacuolar H+-ATPase.* Proc Natl Acad Sci U S A, 1989. **86**(14): p. 5429-33.
87. Bastani, B., et al., *Expression and distribution of renal vacuolar proton-translocating adenosine triphosphatase in response to chronic acid and alkali loads in the rat.* J Clin Invest, 1991. **88**(1): p. 126-36.
88. Brown, D., S. Hirsch, and S. Gluck, *Localization of a proton-pumping ATPase in rat kidney.* J Clin Invest, 1988. **82**(6): p. 2114-26.
89. Brown, D., S. Hirsch, and S. Gluck, *An H+-ATPase in opposite plasma membrane domains in kidney epithelial cell subpopulations.* Nature, 1988. **331**(6157): p. 622-4.
90. Verlander, J.W., et al., *Ultrastructural localization of H+ATPase in rabbit cortical collecting duct.* J Am Soc Nephrol, 1994. **4**(8): p. 1546-57.
91. Hays, S.R. and R.J. Alpern, *Apical and basolateral membrane H+ extrusion mechanisms in inner stripe of rabbit outer medullary collecting duct.* Am J Physiol, 1990. **259**(4 Pt 2): p. F628-35.

92. Stone, D.K., et al., *Anion dependence of rabbit medullary collecting duct acidification.* J Clin Invest, 1983. **71**(5): p. 1505-8.
93. Zeidel, M.L., P. Silva, and J.L. Seifter, *Intracellular pH regulation in rabbit renal medullary collecting duct cells. Role of chloride-bicarbonate exchange.* J Clin Invest, 1986. **77**(5): p. 1682-8.
94. Janoshazi, A., et al., *Relation between the anion exchange protein in kidney medullary collecting duct cells and red cell band 3.* J Membr Biol, 1988. **103**(2): p. 181-9.
95. Schwartz, G.J., J. Barasch, and Q. Al-Awqati, *Plasticity of functional epithelial polarity.* Nature, 1985. **318**(6044): p. 368-71.
96. Emmons, C. and I. Kurtz, *Functional characterization of three intercalated cell subtypes in the rabbit outer cortical collecting duct.* J Clin Invest, 1994. **93**(1): p. 417-23.
97. Schuster, V.L., *Cyclic adenosine monophosphate-stimulated bicarbonate secretion in rabbit cortical collecting tubules.* J Clin Invest, 1985. **75**(6): p. 2056-64.
98. Royaux, I.E., et al., *Pendrin, encoded by the Pendred syndrome gene, resides in the apical region of renal intercalated cells and mediates bicarbonate secretion.* Proc Natl Acad Sci U S A, 2001. **98**(7): p. 4221-6.
99. Soleimani, M., et al., *Pendrin: an apical Cl-/OH-/HCO3- exchanger in the kidney cortex.* Am J Physiol Renal Physiol, 2001. **280**(2): p. F356-64.
100. Kim, Y.H., et al., *Immunocytochemical localization of pendrin in intercalated cell subtypes in rat and mouse kidney.* Am J Physiol Renal Physiol, 2002. **283**(4): p. F744-54.
101. Fejes-Toth, G. and A. Naray-Fejes-Toth, *Isolated principal and intercalated cells: hormone responsiveness and Na+-K+-ATPase activity.* Am J Physiol, 1989. **256**(4 Pt 2): p. F742-50.
102. Fejes-Toth, G. and A. Naray-Fejes-Toth, *Differentiation of renal beta-intercalated cells to alpha-intercalated and principal cells in culture.* Proc Natl Acad Sci U S A, 1992. **89**(12): p. 5487-91.

103. Schwartz, G.J., et al., *Acid incubation reverses the polarity of intercalated cell transporters, an effect mediated by hensin.* J Clin Invest, 2002. **109**(1): p. 89-99.
104. Weiner, I.D. and L.L. Hamm, *Regulation of Cl-/HCO3- exchange in the rabbit cortical collecting tubule.* J Clin Invest, 1991. **87**(5): p. 1553-8.
105. Fairbanks, G., T.L. Steck, and D.F. Wallach, *Electrophoretic analysis of the major polypeptides of the human erythrocyte membrane.* Biochemistry, 1971. **10**(13): p. 2606-17.
106. Ho, M.K. and G. Guidotti, *A membrane protein from human erythrocytes involved in anion exchange.* J Biol Chem, 1975. **250**(2): p. 675-83.
107. Kopito, R.R. and H.F. Lodish, *Primary structure and transmembrane orientation of the murine anion exchange protein.* Nature, 1985. **316**(6025): p. 234-8.
108. Tanner, M.J., P.G. Martin, and S. High, *The complete amino acid sequence of the human erythrocyte membrane anion-transport protein deduced from the cDNA sequence.* Biochem J, 1988. **256**(3): p. 703-12.
109. Papageorgiou, P., et al., *AE anion exchangers in atrial tumor cells.* Am J Physiol Heart Circ Physiol, 2001. **280**(3): p. H937-45.
110. Alper, S.L., et al., *Cloning and characterization of a murine band 3-related cDNA from kidney and from a lymphoid cell line.* J Biol Chem, 1988. **263**(32): p. 17092-9.
111. Huber, S., et al., *Expression of rat kidney anion exchanger 1 in type A intercalated cells in metabolic acidosis and alkalosis.* Am J Physiol, 1999. **277**(6 Pt 2): p. F841-9.
112. Swenson, E.R., et al., *In vivo quantitation of carbonic anhydrase and band 3 protein contributions to pulmonary gas exchange.* J Appl Physiol, 1993. **74**(2): p. 838-48.
113. Peters, L.L., et al., *Anion exchanger 1 (band 3) is required to prevent erythrocyte membrane surface loss but not to form the membrane skeleton.* Cell, 1996. **86**(6): p. 917-27.

114. Weinstein, A.M., *A mathematical model of the outer medullary collecting duct of the rat.* Am J Physiol Renal Physiol, 2000. **279**(1): p. F24-45.
115. Jennings, M.L., *Proton fluxes associated with erythrocyte membrane anion exchange.* J Membr Biol, 1976. **28**(2-3): p. 187-205.
116. Akel, A., et al., *Enhanced suicidal death of erythrocytes from gene-targeted mice lacking the Cl-/HCO(3)(-) exchanger AE1.* Am J Physiol Cell Physiol, 2007. **292**(5): p. C1759-67.
117. Jarolim, P., et al., *Mutations of conserved arginines in the membrane domain of erythroid band 3 lead to a decrease in membrane-associated band 3 and to the phenotype of hereditary spherocytosis.* Blood, 1995. **85**(3): p. 634-40.
118. Schofield, A.E., D.M. Reardon, and M.J. Tanner, *Defective anion transport activity of the abnormal band 3 in hereditary ovalocytic red blood cells.* Nature, 1992. **355**(6363): p. 836-8.
119. Bennett, V. and P.J. Stenbuck, *Association between ankyrin and the cytoplasmic domain of band 3 isolated from the human erythrocyte membrane.* J Biol Chem, 1980. **255**(13): p. 6424-32.
120. Low, P.S., *Structure and function of the cytoplasmic domain of band 3: center of erythrocyte membrane-peripheral protein interactions.* Biochim Biophys Acta, 1986. **864**(2): p. 145-67.
121. Low, P.S., et al., *Contribution of the band 3-ankyrin interaction to erythrocyte membrane mechanical stability.* Blood, 1991. **77**(7): p. 1581-6.
122. An, X.L., et al., *Modulation of band 3-ankyrin interaction by protein 4.1. Functional implications in regulation of erythrocyte membrane mechanical properties.* J Biol Chem, 1996. **271**(52): p. 33187-91.
123. Pasternack, G.R., et al., *Interactions between protein 4.1 and band 3. An alternative binding site for an element of the membrane skeleton.* J Biol Chem, 1985. **260**(6): p. 3676-83.
124. Cohen, C.M., E. Dotimas, and C. Korsgren, *Human erythrocyte membrane protein band 4.2 (pallidin).* Semin Hematol, 1993. **30**(2): p. 119-37.

125. Rybicki, A.C., et al., *Increased rotational mobility and extractability of band 3 from protein 4.2-deficient erythrocyte membranes: evidence of a role for protein 4.2 in strengthening the band 3-cytoskeleton linkage.* Blood, 1996. **88**(7): p. 2745-53.
126. Rogalski, A.A., T.L. Steck, and A. Waseem, *Association of glyceraldehyde-3-phosphate dehydrogenase with the plasma membrane of the intact human red blood cell.* J Biol Chem, 1989. **264**(11): p. 6438-46.
127. Jenkins, J.D., D.P. Madden, and T.L. Steck, *Association of phosphofructokinase and aldolase with the membrane of the intact erythrocyte.* J Biol Chem, 1984. **259**(15): p. 9374-8.
128. Murthy, S.N., et al., *The aldolase-binding site of the human erythrocyte membrane is at the NH2 terminus of band 3.* J Biol Chem, 1981. **256**(21): p. 11203-8.
129. Walder, J.A., et al., *The interaction of hemoglobin with the cytoplasmic domain of band 3 of the human erythrocyte membrane.* J Biol Chem, 1984. **259**(16): p. 10238-46.
130. Waugh, S.M. and P.S. Low, *Hemichrome binding to band 3: nucleation of Heinz bodies on the erythrocyte membrane.* Biochemistry, 1985. **24**(1): p. 34-9.
131. Harrison, M.L., et al., *Phosphorylation of human erythrocyte band 3 by endogenous p72syk.* J Biol Chem, 1994. **269**(2): p. 955-9.
132. Low, P.S., P. Rathinavelu, and M.L. Harrison, *Regulation of glycolysis via reversible enzyme binding to the membrane protein, band 3.* J Biol Chem, 1993. **268**(20): p. 14627-31.
133. Malik, S., M. Sami, and A. Watts, *A role for band 4.2 in human erythrocyte band 3 mediated anion transport.* Biochemistry, 1993. **32**(38): p. 10078-84.
134. Kannan, R., J. Yuan, and P.S. Low, *Isolation and partial characterization of antibody- and globin-enriched complexes from membranes of dense human erythrocytes.* Biochem J, 1991. **278 (Pt 1)**: p. 57-62.

135. Vince, J.W. and R.A. Reithmeier, *Carbonic anhydrase II binds to the carboxyl terminus of human band 3, the erythrocyte C1-/HCO3- exchanger.* J Biol Chem, 1998. **273**(43): p. 28430-7.
136. Vince, J.W. and R.A. Reithmeier, *Identification of the carbonic anhydrase II binding site in the Cl(-)/HCO(3)(-) anion exchanger AE1.* Biochemistry, 2000. **39**(18): p. 5527-33.
137. Low, P.S., et al., *The role of hemoglobin denaturation and band 3 clustering in red blood cell aging.* Science, 1985. **227**(4686): p. 531-3.
138. Turrini, F., et al., *Clustering of integral membrane proteins of the human erythrocyte membrane stimulates autologous IgG binding, complement deposition, and phagocytosis.* J Biol Chem, 1991. **266**(35): p. 23611-7.
139. Zhang, D., et al., *Crystallographic structure and functional interpretation of the cytoplasmic domain of erythrocyte membrane band 3.* Blood, 2000. **96**(9): p. 2925-33.
140. Low, P.S., et al., *Characterization of the reversible conformational equilibrium of the cytoplasmic domain of erythrocyte membrane band 3.* J Biol Chem, 1984. **259**(21): p. 13070-6.
141. Schofield, A.E., et al., *Basis of unique red cell membrane properties in hereditary ovalocytosis.* J Mol Biol, 1992. **223**(4): p. 949-58.
142. Wang, D.N., *Band 3 protein: structure, flexibility and function.* FEBS Lett, 1994. **346**(1): p. 26-31.
143. Wang, D.N., et al., *Two-dimensional structure of the membrane domain of human band 3, the anion transport protein of the erythrocyte membrane.* Embo J, 1993. **12**(6): p. 2233-9.
144. Wang, D.N., et al., *Three-dimensional map of the dimeric membrane domain of the human erythrocyte anion exchanger, Band 3.* Embo J, 1994. **13**(14): p. 3230-5.
145. Tang, X.B., et al., *Topology of the region surrounding Glu681 of human AE1 protein, the erythrocyte anion exchanger.* J Biol Chem, 1998. **273**(35): p. 22545-53.
146. Popov, M., J. Li, and R.A. Reithmeier, *Transmembrane folding of the human erythrocyte anion exchanger (AE1, Band 3) determined by*

scanning and insertional N-glycosylation mutagenesis. Biochem J, 1999. **339 (Pt 2)**: p. 269-79.

147. Popov, M., et al., *Mapping the ends of transmembrane segments in a polytopic membrane protein. Scanning N-glycosylation mutagenesis of extracytosolic loops in the anion exchanger, band 3.* J Biol Chem, 1997. **272**(29): p. 18325-32.
148. Cobb, C.E. and A.H. Beth, *Identification of the eosinyl-5-maleimide reaction site on the human erythrocyte anion-exchange protein: overlap with the reaction sites of other chemical probes.* Biochemistry, 1990. **29**(36): p. 8283-90.
149. Cobb, C.E., et al., *Effects of diethyl ether on membrane lipid ordering and on rotational dynamics of the anion exchange protein in intact human erythrocytes: correlations with anion exchange function.* Biochemistry, 1990. **29**(48): p. 10799-806.
150. Okubo, K., et al., *Red blood cell band 3. Lysine 539 and lysine 851 react with the same H2DIDS (4,4'-diisothiocyanodihydrostilbene-2,2'-disulfonic acid) molecule.* J Biol Chem, 1994. **269**(3): p. 1918-26.
151. Jennings, M.L. and J.S. Smith, *Anion-proton cotransport through the human red blood cell band 3 protein. Role of glutamate 681.* J Biol Chem, 1992. **267**(20): p. 13964-71.
152. Fujinaga, J., X.B. Tang, and J.R. Casey, *Topology of the membrane domain of human erythrocyte anion exchange protein, AE1.* J Biol Chem, 1999. **274**(10): p. 6626-33.
153. Kuma, H., et al., *Topology of the anion exchange protein AE1: the controversial sidedness of lysine 743.* Biochemistry, 2002. **41**(10): p. 3380-8.
154. Erickson, H.K., *Cytoplasmic disposition of aspartate 821 in anion exchanger from human erythrocytes.* Biochemistry, 1997. **36**(33): p. 9958-67.
155. Wainwright, S.D., W.J. Mawby, and M.J. Tanner, *The membrane domain of the human erythrocyte anion transport protein. Epitope mapping of a monoclonal antibody defines the location of a cytoplasmic loop near the C-terminus of the protein.* Biochem J, 1990. **272**(1): p. 265-8.

156. Jennings, M.L. and S. Al-Rhaiyel, *Modification of a carboxyl group that appears to cross the permeability barrier in the red blood cell anion transporter.* J Gen Physiol, 1988. **92**(2): p. 161-78.
157. Jennings, M.L. and M.P. Anderson, *Chemical modification and labeling of glutamate residues at the stilbenedisulfonate site of human red blood cell band 3 protein.* J Biol Chem, 1987. **262**(4): p. 1691-7.
158. Jennings, M.L., *Rapid electrogenic sulfate-chloride exchange mediated by chemically modified band 3 in human erythrocytes.* J Gen Physiol, 1995. **105**(1): p. 21-47.
159. Chernova, M.N., et al., *Electrogenic sulfate/chloride exchange in Xenopus oocytes mediated by murine AE1 E699Q.* J Gen Physiol, 1997. **109**(3): p. 345-60.
160. Sekler, I., R.S. Lo, and R.R. Kopito, *A conserved glutamate is responsible for ion selectivity and pH dependence of the mammalian anion exchangers AE1 and AE2.* J Biol Chem, 1995. **270**(48): p. 28751-8.
161. Muller-Berger, S., et al., *Roles of histidine 752 and glutamate 699 in the pH dependence of mouse band 3 protein-mediated anion transport.* Biochemistry, 1995. **34**(29): p. 9325-32.
162. Liu, S.Q. and P.A. Knauf, *Lys-430, site of irreversible inhibition of band 3 Cl- flux by eosin-5-maleimide, is not at the transport site.* Am J Physiol, 1993. **264**(5 Pt 1): p. C1155-64.
163. Liu, D., S.D. Kennedy, and P.A. Knauf, *35Cl nuclear magnetic resonance line broadening shows that eosin-5-maleimide does not block the external anion access channel of band 3.* Biophys J, 1995. **69**(2): p. 399-408.
164. Passow, H., et al., *Exploration of the functional significance of the stilbene disulfonate binding site in mouse band 3 by site-directed mutagenesis.* Biophys J, 1992. **62**(1): p. 98-100.
165. Pan, R.J. and R.J. Cherry, *Evidence that eosin-5-maleimide binds close to the anion transport site of human erythrocyte band 3: a fluorescence quenching study.* Biochemistry, 1995. **34**(14): p. 4880-8.

166. Izuhara, K., K. Okubo, and N. Hamasaki, *Conformational change of band 3 protein induced by diethyl pyrocarbonate modification in human erythrocyte ghosts.* Biochemistry, 1989. **28**(11): p. 4725-8.
167. Muller-Berger, S., et al., *Inhibition of mouse erythroid band 3-mediated chloride transport by site-directed mutagenesis of histidine residues and its reversal by second site mutation of Lys 558, the locus of covalent H2DIDS binding.* Biochemistry, 1995. **34**(29): p. 9315-24.
168. Jin, X.R., et al., *Histidine-834 of human erythrocyte band 3 has an essential role in the conformational changes that occur during the band 3-mediated anion exchange.* Biochemistry, 2003. **42**(44): p. 12927-32.
169. Falke, J.J. and S.I. Chan, *Molecular mechanisms of band 3 inhibitors. 2. Channel blockers.* Biochemistry, 1986. **25**(24): p. 7895-8.
170. Bahar, S., et al., *Persistence of external chloride and DIDS binding after chemical modification of Glu-681 in human band 3.* Am J Physiol, 1999. **277**(4 Pt 1): p. C791-9.
171. Tang, X.B., et al., *Identification of residues lining the translocation pore of human AE1, plasma membrane anion exchange protein.* J Biol Chem, 1999. **274**(6): p. 3557-64.
172. Zhu, Q. and J.R. Casey, *The substrate anion selectivity filter in the human erythrocyte Cl-/HCO3- exchange protein, AE1.* J Biol Chem, 2004. **279**(22): p. 23565-73.
173. Ruf, R., et al., *Confirmation of the ATP6B1 gene as responsible for distal renal tubular acidosis.* Pediatr Nephrol, 2003. **18**(2): p. 105-9.
174. Smith, A.N., et al., *Mutations in ATP6N1B, encoding a new kidney vacuolar proton pump 116-kD subunit, cause recessive distal renal tubular acidosis with preserved hearing.* Nat Genet, 2000. **26**(1): p. 71-5.
175. Stover, E.H., et al., *Novel ATP6V1B1 and ATP6V0A4 mutations in autosomal recessive distal renal tubular acidosis with new evidence for hearing loss.* J Med Genet, 2002. **39**(11): p. 796-803.
176. Karet, F.E., et al., *Mutations in the chloride-bicarbonate exchanger gene AE1 cause autosomal dominant but not autosomal recessive distal renal tubular acidosis.* Proc Natl Acad Sci U S A, 1998. **95**(11): p. 6337-42.

177. Sritippayawan, S., et al., *A de novo R589C mutation of anion exchanger 1 causing distal renal tubular acidosis.* Pediatr Nephrol, 2003. **18**(7): p. 644-8.
178. Weber, S., et al., *Atypical distal renal tubular acidosis confirmed by mutation analysis.* Pediatr Nephrol, 2000. **15**(3-4): p. 201-4.
179. Ribeiro, M.L., et al., *Severe hereditary spherocytosis and distal renal tubular acidosis associated with the total absence of band 3.* Blood, 2000. **96**(4): p. 1602-4.
180. Tanphaichitr, V.S., et al., *Novel AE1 mutations in recessive distal renal tubular acidosis. Loss-of-function is rescued by glycophorin A.* J Clin Invest, 1998. **102**(12): p. 2173-9.
181. Vasuvattakul, S., et al., *Autosomal recessive distal renal tubular acidosis associated with Southeast Asian ovalocytosis.* Kidney Int, 1999. **56**(5): p. 1674-82.
182. Canfield, W.M., et al., *Localization of the signal for rapid internalization of the bovine cation-independent mannose 6-phosphate/insulin-like growth factor-II receptor to amino acids 24-29 of the cytoplasmic tail.* J Biol Chem, 1991. **266**(9): p. 5682-8.
183. Distel, B., et al., *Basolateral sorting of the cation-dependent mannose 6-phosphate receptor in Madin-Darby canine kidney cells. Identification of a basolateral determinant unrelated to clathrin-coated pit localization signals.* J Biol Chem, 1998. **273**(1): p. 186-93.
184. Lin, S., H.Y. Naim, and M.G. Roth, *Tyrosine-dependent basolateral sorting signals are distinct from tyrosine-dependent internalization signals.* J Biol Chem, 1997. **272**(42): p. 26300-5.
185. Matter, K. and I. Mellman, *Mechanisms of cell polarity: sorting and transport in epithelial cells.* Curr Opin Cell Biol, 1994. **6**(4): p. 545-54.
186. Bonifacino, J.S. and E.C. Dell'Angelica, *Molecular bases for the recognition of tyrosine-based sorting signals.* J Cell Biol, 1999. **145**(5): p. 923-6.
187. Folsch, H., et al., *A novel clathrin adaptor complex mediates basolateral targeting in polarized epithelial cells.* Cell, 1999. **99**(2): p. 189-98.

188. Toye, A.M., G. Banting, and M.J. Tanner, *Regions of human kidney anion exchanger 1 (kAE1) required for basolateral targeting of kAE1 in polarised kidney cells: mis-targeting explains dominant renal tubular acidosis (dRTA).* J Cell Sci, 2004. **117**(Pt 8): p. 1399-410.
189. Devonald, M.A., et al., *Non-polarized targeting of AE1 causes autosomal dominant distal renal tubular acidosis.* Nat Genet, 2003. **33**(2): p. 125-7.
190. Cordat, E., J. Li, and R.A. Reithmeier, *Carboxyl-terminal truncations of human anion exchanger impair its trafficking to the plasma membrane.* Traffic, 2003. **4**(9): p. 642-51.
191. Jarolim, P., et al., *Autosomal dominant distal renal tubular acidosis is associated in three families with heterozygosity for the R589H mutation in the AE1 (band 3) Cl-/HCO3- exchanger.* J Biol Chem, 1998. **273**(11): p. 6380-8.
192. Yenchitsomanus, P.T., et al., *Anion exchanger 1 mutations associated with distal renal tubular acidosis in the Thai population.* J Hum Genet, 2003. **48**(9): p. 451-6.
193. Yenchitsomanus, P.T., et al., *Autosomal recessive distal renal tubular acidosis caused by G701D mutation of anion exchanger 1 gene.* Am J Kidney Dis, 2002. **40**(1): p. 21-9.
194. Cheidde, L., et al., *A novel mutation in the anion exchanger 1 gene is associated with familial distal renal tubular acidosis and nephrocalcinosis.* Pediatrics, 2003. **112**(6 Pt 1): p. 1361-7.
195. Rungroj, N., et al., *A novel missense mutation in AE1 causing autosomal dominant distal renal tubular acidosis retains normal transport function but is mistargeted in polarized epithelial cells.* J Biol Chem, 2004. **279**(14): p. 13833-8.
196. Sritippayawan, S., et al., *Novel compound heterozygous SLC4A1 mutations in Thai patients with autosomal recessive distal renal tubular acidosis.* Am J Kidney Dis, 2004. **44**(1): p. 64-70.
197. Quilty, J.A., E. Cordat, and R.A. Reithmeier, *Impaired trafficking of human kidney anion exchanger (kAE1) caused by hetero-oligomer formation with a truncated mutant associated with distal renal tubular acidosis.* Biochem J, 2002. **368**(Pt 3): p. 895-903.

198. Quilty, J.A., J. Li, and R.A. Reithmeier, *Impaired trafficking of distal renal tubular acidosis mutants of the human kidney anion exchanger kAE1.* Am J Physiol Renal Physiol, 2002. **282**(5): p. F810-20.
199. Cordat, E., et al., *Dominant and recessive distal renal tubular acidosis mutations of kidney anion exchanger 1 induce distinct trafficking defects in MDCK cells.* Traffic, 2006. **7**(2): p. 117-28.
200. Toye, A.M., et al., *Band 3 Walton, a C-terminal deletion associated with distal renal tubular acidosis, is expressed in the red cell membrane but retained internally in kidney cells.* Blood, 2002. **99**(1): p. 342-7.
201. Toye, A.M., *Defective kidney anion-exchanger 1 (AE1, Band 3) trafficking in dominant distal renal tubular acidosis (dRTA).* Biochem Soc Symp, 2005(72): p. 47-63.
202. Kittanakom, S., et al., *Trafficking defects of a novel autosomal recessive distal renal tubular acidosis mutant (S773P) of the human kidney anion exchanger (kAE1).* J Biol Chem, 2004. **279**(39): p. 40960-71.
203. Cordat, E. and R.A. Reithmeier, *Expression and interaction of two compound heterozygous distal renal tubular acidosis mutants of kidney anion exchanger 1 in epithelial cells.* Am J Physiol Renal Physiol, 2006. **291**(6): p. F1354-61.
204. Chu, H. and P.S. Low, *Mapping of glycolytic enzyme-binding sites on human erythrocyte band 3.* Biochem J, 2006. **400**(1): p. 143-51.
205. De Rosa, M.C., et al., *Allosteric properties of hemoglobin and the plasma membrane of the erythrocyte: new insights in gas transport and metabolic modulation.* IUBMB Life, 2008. **60**(2): p. 87-93.
206. Zhang, Y., et al., *Human erythrocyte membrane band 3 protein influences hemoglobin cooperativity. Possible effect on oxygen transport.* J Biol Chem, 2003. **278**(41): p. 39565-71.
207. Bruce, L.J., et al., *Changes in the blood group Wright antigens are associated with a mutation at amino acid 658 in human erythrocyte band 3: a site of interaction between band 3 and glycophorin A under certain conditions.* Blood, 1995. **85**(2): p. 541-7.

208. Telen, M.J. and J.A. Chasis, *Relationship of the human erythrocyte Wrb antigen to an interaction between glycophorin A and band 3.* Blood, 1990. **76**(4): p. 842-8.
209. Groves, J.D. and M.J. Tanner, *Glycophorin A facilitates the expression of human band 3-mediated anion transport in Xenopus oocytes.* J Biol Chem, 1992. **267**(31): p. 22163-70.
210. Young, M.T., et al., *Red-cell glycophorin A-band 3 interactions associated with the movement of band 3 to the cell surface.* Biochem J, 2000. **350 Pt 1**: p. 53-60.
211. Tanner, M.J., *The structure and function of band 3 (AE1): recent developments (review).* Mol Membr Biol, 1997. **14**(4): p. 155-65.
212. Bruce, L.J., et al., *Altered band 3 structure and function in glycophorin A- and B-deficient (MkMk) red blood cells.* Blood, 1994. **84**(3): p. 916-22.
213. Dahr, W., et al., *The Dantu erythrocyte phenotype of the NE variety. I. Dodecylsulfate polyacrylamide gel electrophoretic studies.* Blut, 1987. **55**(1): p. 19-31.
214. Russ, W.P. and D.M. Engelman, *TOXCAT: a measure of transmembrane helix association in a biological membrane.* Proc Natl Acad Sci U S A, 1999. **96**(3): p. 863-8.
215. Young, M.T. and M.J. Tanner, *Distinct regions of human glycophorin A enhance human red cell anion exchanger (band 3; AE1) transport function and surface trafficking.* J Biol Chem, 2003. **278**(35): p. 32954-61.
216. Chetrite, G. and R. Cassoly, *Affinity of hemoglobin for the cytoplasmic fragment of human erythrocyte membrane band 3. Equilibrium measurements at physiological pH using matrix-bound proteins: the effects of ionic strength, deoxygenation and of 2,3-diphosphoglycerate.* J Mol Biol, 1985. **185**(3): p. 639-44.
217. Waugh, S.M., J.A. Walder, and P.S. Low, *Partial characterization of the copolymerization reaction of erythrocyte membrane band 3 with hemichromes.* Biochemistry, 1987. **26**(6): p. 1777-83.
218. Rettig, M.P., et al., *Evaluation of biochemical changes during in vivo erythrocyte senescence in the dog.* Blood, 1999. **93**(1): p. 376-84.

219. Willardson, B.M., et al., *Localization of the ankyrin-binding site on erythrocyte membrane protein, band 3.* J Biol Chem, 1989. **264**(27): p. 15893-9.
220. Van Dort, H.M., R. Moriyama, and P.S. Low, *Effect of band 3 subunit equilibrium on the kinetics and affinity of ankyrin binding to erythrocyte membrane vesicles.* J Biol Chem, 1998. **273**(24): p. 14819-26.
221. Casey, J.R. and R.A. Reithmeier, *Analysis of the oligomeric state of Band 3, the anion transport protein of the human erythrocyte membrane, by size exclusion high performance liquid chromatography. Oligomeric stability and origin of heterogeneity.* J Biol Chem, 1991. **266**(24): p. 15726-37.
222. Workman, R.F. and P.S. Low, *Biochemical analysis of potential sites for protein 4.1-mediated anchoring of the spectrin-actin skeleton to the erythrocyte membrane.* J Biol Chem, 1998. **273**(11): p. 6171-6.
223. Rybicki, A.C., S. Musto, and R.S. Schwartz, *Identification of a band-3 binding site near the N-terminus of erythrocyte membrane protein 4.2.* Biochem J, 1995. **309 (Pt 2)**: p. 677-81.
224. Marini, A.M., et al., *The Rh (rhesus) blood group polypeptides are related to NH4+ transporters.* Trends Biochem Sci, 1997. **22**(12): p. 460-1.
225. Gross, S.S., *Vascular biology. Targeted delivery of nitric oxide.* Nature, 2001. **409**(6820): p. 577-8.
226. Pawloski, J.R., D.T. Hess, and J.S. Stamler, *Export by red blood cells of nitric oxide bioactivity.* Nature, 2001. **409**(6820): p. 622-6.
227. Brown, E.J. and W.A. Frazier, *Integrin-associated protein (CD47) and its ligands.* Trends Cell Biol, 2001. **11**(3): p. 130-5.
228. Brittain, J.E., et al., *Activation of sickle red blood cell adhesion via integrin-associated protein/CD47-induced signal transduction.* J Clin Invest, 2001. **107**(12): p. 1555-62.
229. Bruce, L.J., et al., *Absence of CD47 in protein 4.2-deficient hereditary spherocytosis in man: an interaction between the Rh complex and the band 3 complex.* Blood, 2002. **100**(5): p. 1878-85.

230. Ridgwell, K., M.J. Tanner, and D.J. Anstee, *The Rhesus (D) polypeptide is linked to the human erythrocyte cytoskeleton.* FEBS Lett, 1984. **174**(1): p. 7-10.
231. Vanlair, C.F. and J.B. Masius, *De la microcythemie.* Bull Acad R Med Belg, 1871(5): p. 515-613.
232. Alloisio, N., et al., *Hereditary spherocytosis with band 3 deficiency. Association with a nonsense mutation of the band 3 gene (allele Lyon), and aggravation by a low-expression allele occurring in trans (allele Genas).* Blood, 1996. **88**(3): p. 1062-9.
233. Alloisio, N., et al., *Modulation of clinical expression and band 3 deficiency in hereditary spherocytosis.* Blood, 1997. **90**(1): p. 414-20.
234. Dhermy, D., et al., *Heterogenous band 3 deficiency in hereditary spherocytosis related to different band 3 gene defects.* Br J Haematol, 1997. **98**(1): p. 32-40.
235. Jarolim, P., et al., *Characterization of 13 novel band 3 gene defects in hereditary spherocytosis with band 3 deficiency.* Blood, 1996. **88**(11): p. 4366-74.
236. Jarolim, P., et al., *Duplication of 10 nucleotides in the erythroid band 3 (AE1) gene in a kindred with hereditary spherocytosis and band 3 protein deficiency (band 3PRAGUE).* J Clin Invest, 1994. **93**(1): p. 121-30.
237. Jenkins, P.B., et al., *A nonsense mutation in the erythrocyte band 3 gene associated with decreased mRNA accumulation in a kindred with dominant hereditary spherocytosis.* J Clin Invest, 1996. **97**(2): p. 373-80.
238. Perrotta, S., et al., *The N-terminal 11 amino acids of human erythrocyte band 3 are critical for aldolase binding and protein phosphorylation: implications for band 3 function.* Blood, 2005. **106**(13): p. 4359-66.
239. Toye, A.M., et al., *Band 3 Courcouronnes (Ser667Phe): a trafficking mutant differentially rescued by wild-type band 3 and glycophorin A.* Blood, 2008. **111**(11): p. 5380-9.

240. Zarkowsky, H.S., et al., *Congenital hemolytic anemia with high sodium, low potassium red cells. I. Studies of membrane permeability.* N Engl J Med, 1968. **278**(11): p. 573-81.
241. Dalla Venezia, N., et al., *Homozygous 4.1(-) hereditary elliptocytosis associated with a point mutation in the downstream initiation codon of protein 4.1 gene.* J Clin Invest, 1992. **90**(5): p. 1713-7.
242. Stewart, G.W., *Hemolytic disease due to membrane ion channel disorders.* Curr Opin Hematol, 2004. **11**(4): p. 244-50.
243. Bruce, L.J., et al., *Monovalent cation leaks in human red cells caused by single amino-acid substitutions in the transport domain of the band 3 chloride-bicarbonate exchanger, AE1.* Nat Genet, 2005. **37**(11): p. 1258-63.
244. Liu, S.C., et al., *The homozygous state for the band 3 protein mutation in Southeast Asian Ovalocytosis may be lethal.* Blood, 1994. **84**(10): p. 3590-1.
245. Genton, B., et al., *Ovalocytosis and cerebral malaria.* Nature, 1995. **378**(6557): p. 564-5.
246. Booth, P.B., et al., *Selective depression of blood group antigens associated with hereditary ovalocytosis among melanesians.* Vox Sang, 1977. **32**(2): p. 99-110.
247. Cattani, J.A., et al., *Hereditary ovalocytosis and reduced susceptibility to malaria in Papua New Guinea.* Trans R Soc Trop Med Hyg, 1987. **81**(5): p. 705-9.
248. Amato, D. and P.B. Booth, *Hereditary ovalocytosis in Melanesians. 1977.* P N G Med J, 2005. **48**(1-2): p. 102-8.
249. Fix, A.G., A.S. Baer, and L.E. Lie-Injo, *The mode of inheritance of ovalocytosis/elliptocytosis in Malaysian Orang Asli families.* Hum Genet, 1982. **61**(3): p. 250-3.
250. Honig, G.R., P.S. Lacson, and H.S. Maurer, *A new familial disorder withh abnormal erythrocyte morphology and increased permeability of the erythrocytes to sodium and potassium.* Pediatr Res, 1971(5): p. 159-166.
251. Coetzer, T.L., et al., *Southeast Asian ovalocytosis in a South African kindred with hemolytic anemia.* Blood, 1996. **87**(4): p. 1656-7.

252. Schischmanoff, P.O., et al., *Southeast Asian ovalocytosis in White persons.* Hemoglobin, 1999. **23**(1): p. 47-56.
253. O'Donnell, A., et al., *Red cell morphology and malaria anaemia in children with Southeast-Asian ovalocytosis band 3 in Papua New Guinea.* Br J Haematol, 1998. **101**(3): p. 407-12.
254. Mohandas, N., et al., *Rigid membranes of Malayan ovalocytes: a likely genetic barrier against malaria.* Blood, 1984. **63**(6): p. 1385-92.
255. Mohandas, N., et al., *Molecular basis for membrane rigidity of hereditary ovalocytosis. A novel mechanism involving the cytoplasmic domain of band 3.* J Clin Invest, 1992. **89**(2): p. 686-92.
256. Kidson, C., et al., *Ovalocytic erythrocytes from Melanesians are resistant to invasion by malaria parasites in culture.* Proc Natl Acad Sci U S A, 1981. **78**(9): p. 5829-32.
257. Saul, A., et al., *Decreased membrane deformability in Melanesian ovalocytes from Papua New Guinea.* J Cell Biol, 1984. **98**(4): p. 1348-54.
258. Bruce, L.J., et al., *South-east asian ovalocytic (SAO) erythrocytes have a cold sensitive cation leak: implications for in vitro studies on stored SAO red cells.* Biochim Biophys Acta, 1999. **1416**(1-2): p. 258-70.
259. Mgone, C.S., et al., *Occurrence of the erythrocyte band 3 (AE1) gene deletion in relation to malaria endemicity in Papua New Guinea.* Trans R Soc Trop Med Hyg, 1996. **90**(3): p. 228-31.
260. Allen, S.J., et al., *Prevention of cerebral malaria in children in Papua New Guinea by southeast Asian ovalocytosis band 3.* Am J Trop Med Hyg, 1999. **60**(6): p. 1056-60.
261. Castelino, D., et al., *Ovalocytosis in Papua New Guinea -- dominantly inherited resistance to malaria.* Southeast Asian J Trop Med Public Health, 1981. **12**(4): p. 549-55.
262. Foo, L.C., et al., *Ovalocytosis protects against severe malaria parasitemia in the Malayan aborigines.* Am J Trop Med Hyg, 1992. **47**(3): p. 271-5.
263. Hadley, T., et al., *Resistance of Melanesian elliptocytes (ovalocytes) to invasion by Plasmodium knowlesi and Plasmodium falciparum malaria parasites in vitro.* J Clin Invest, 1983. **71**(3): p. 780-2.

264. Dluzewski, A.R., et al., *Invasion of hereditary ovalocytes by Plasmodium falciparum in vitro and its relation to intracellular ATP concentration.* Mol Biochem Parasitol, 1992. **55**(1-2): p. 1-7.
265. Garcia-Romeu, F., A.R. Cossins, and R. Motais, *Cell volume regulation by trout erythrocytes: characteristics of the transport systems activated by hypotonic swelling.* J Physiol, 1991. **440**: p. 547-67.
266. Roy, G. and C. Malo, *Activation of amino acid diffusion by a volume increase in cultured kidney (MDCK) cells.* J Membr Biol, 1992. **130**(1): p. 83-90.
267. Kirk, K., J.C. Ellory, and J.D. Young, *Transport of organic substrates via a volume-activated channel.* J Biol Chem, 1992. **267**(33): p. 23475-8.
268. Strange, K., et al., *Mechanism and regulation of swelling-activated inositol efflux in brain glial cells.* Am J Physiol, 1993. **265**(1 Pt 1): p. C244-56.
269. Goldstein, L. and S.R. Brill, *Volume-activated taurine efflux from skate erythrocytes: possible band 3 involvement.* Am J Physiol, 1991. **260**(5 Pt 2): p. R1014-20.
270. Motais, R., et al., *Regulation of Na+/H+ exchange and pH in erythrocytes of fish.* Comp Biochem Physiol Comp Physiol, 1992. **102**(4): p. 597-602.
271. Motais, R., H. Guizouarn, and F. Garcia-Romeu, *Red cell volume regulation: the pivotal role of ionic strength in controlling swelling-dependent transport systems.* Biochim Biophys Acta, 1991. **1075**(2): p. 169-80.
272. Banderali, U. and G. Roy, *Anion channels for amino acids in MDCK cells.* Am J Physiol, 1992. **263**(6 Pt 1): p. C1200-7.
273. Fievet, B., et al., *Expression of band 3 anion exchanger induces chloride current and taurine transport: structure-function analysis.* Embo J, 1995. **14**(21): p. 5158-69.
274. Guizouarn, H. and R. Motais, *Swelling activation of transport pathways in erythrocytes: effects of Cl-, ionic strength, and volume changes.* Am J Physiol, 1999. **276**(1 Pt 1): p. C210-20.

275. Guizouarn, H., et al., *Multiple transport functions of a red blood cell anion exchanger, tAE1: its role in cell volume regulation.* J Physiol, 2001. **535**(Pt 2): p. 497-506.
276. Martial, S., et al., *Consequences of point mutations in trout anion exchanger 1 (tAE1) transmembrane domains: evidence that tAE1 can behave as a chloride channel.* J Cell Physiol, 2006. **207**(3): p. 829-35.
277. Martial, S., et al., *Importance of several cysteine residues for the chloride conductance of trout anion exchanger 1 (tAE1).* J Cell Physiol, 2007. **213**(1): p. 70-8.
278. Stewart, G.W., et al., *Isolation of cDNA coding for an ubiquitous membrane protein deficient in high Na+, low K+ stomatocytic erythrocytes.* Blood, 1992. **79**(6): p. 1593-601.
279. Rix, M., et al., *[Congenital stomatocytosis with hemolytic anemia--with abnormal cation permeability and defective membrane proteins].* Ugeskr Laeger, 1991. **153**(10): p. 724-6.
280. Morle, L., et al., *Reduction of membrane band 7 and activation of volume stimulated (K+, Cl-)-cotransport in a case of congenital stomatocytosis.* Br J Haematol, 1989. **71**(1): p. 141-6.
281. Oski, F.A., et al., *Congenital hemolytic anemia with high-sodium, low-potassium red cells. Studies of three generations of a family with a new variant.* N Engl J Med, 1969. **280**(17): p. 909-16.
282. Wiley, J.S., et al., *Hereditary stomatocytosis: association of low 2,3-diphosphoglycerate with increased cation pumping by the red cell.* Br J Haematol, 1979. **41**(1): p. 133-41.
283. Mentzer, W.C., Jr., et al., *Hereditary stomatocytosis: membrane and metabolism studies.* Blood, 1975. **46**(5): p. 659-69.
284. Guizouarn, H., et al., *Point mutations involved in red cell stomatocytosis convert the electroneutral anion exchanger 1 to a nonselective cation conductance.* Blood, 2007. **110**(6): p. 2158-65.
285. Morris, R.C., Jr. and A. Sebastian, *Alkali therapy in renal tubular acidosis: who needs it?* J Am Soc Nephrol, 2002. **13**(8): p. 2186-8.
286. McSherry, E., A. Sebastian, and R.C. Morris, Jr., *Renal tubular acidosis in infants: the several kinds, including bicarbonate-wasting, classic renal tubular acidosis.* J Clin Invest, 1972. **51**(3): p. 499-514.

287. Walter, S.J., et al., *Assessment of Urinary Acidification.* Kidney International, 1997. **52**: p. 2092.
288. Kamynina, E. and O. Staub, *Concerted action of ENaC, Nedd4-2, and Sgk1 in transepithelial Na(+) transport.* Am J Physiol Renal Physiol, 2002. **283**(3): p. F377-87.
289. Coutry, N., et al., *Time course of sodium-induced Na(+)-K(+)-ATPase recruitment in rabbit cortical collecting tubule.* Am J Physiol, 1992. **263**(1 Pt 1): p. C61-8.
290. Khadouri, C., et al., *Short-term effect of aldosterone on NEM-sensitive ATPase in rat collecting tubule.* Am J Physiol, 1989. **257**(2 Pt 2): p. F177-81.
291. Stone, D.K., et al., *Mineralocorticoid modulation of rabbit medullary collecting duct acidification. A sodium-independent effect.* J Clin Invest, 1983. **72**(1): p. 77-83.
292. Winter, C., et al., *Nongenomic stimulation of vacuolar H+-ATPases in intercalated renal tubule cells by aldosterone.* Proc Natl Acad Sci U S A, 2004. **101**(8): p. 2636-41.
293. Sen, S., et al., *Pathophysiological effects of albumin dialysis in acute-on-chronic liver failure: a randomized controlled study.* Liver Transpl, 2004. **10**(9): p. 1109-19.
294. Arruda, J.A. and N.A. Kurtzman, *Mechanisms and classification of deranged distal urinary acidification.* Am J Physiol, 1980. **239**(6): p. F515-23.
295. Knauf, P.A. and P. Pal, *Band 3 mediated transport*, in *Red cell membrane transport in health and disease*, B. I. and E. C., Editors. 2003, Springer: Berlin. p. 253-302.
296. Laing, C.M., et al., *Renal tubular acidosis: developments in our understanding of the molecular basis.* Int J Biochem Cell Biol, 2005. **37**(6): p. 1151-61.
297. Guizouarn, H., et al., *Point mutations involved in red cell stomatocytosis convert the electroneutral anion exchanger 1 to a non-selective cation conductance.* Blood, 2007.

298. Groves, J.D., L. Wang, and M.J. Tanner, *Functional reassembly of the anion transport domain of human red cell band 3 (AE1) from multiple and non-complementary fragments.* FEBS Lett, 1998. **433**(3): p. 223-7.
299. Tanford, C., *Simple model for the chemical potential change of a transported ion in active transport.* Proc Natl Acad Sci U S A, 1982. **79**(9): p. 2882-4.
300. DeFelice, L.J. and T. Goswami, *Transporters as channels.* Annu Rev Physiol, 2007. **69**: p. 87-112.
301. Gadsby, D.C., *Ion transport: spot the difference.* Nature, 2004. **427**(6977): p. 795-7.
302. Pimplikar, S.W. and R.A. Reithmeier, *Affinity chromatography of Band 3, the anion transport protein of erythrocyte membranes.* J Biol Chem, 1986. **261**(21): p. 9770-8.
303. Khositseth, S., et al., *Distal renal tubular acidosis associated with anion exchanger 1 mutations in children in Thailand.* Am J Kidney Dis, 2007. **49**(6): p. 841-850 e1.
304. Woda, C.B., et al., *Flow-dependent K+ secretion in the cortical collecting duct is mediated by a maxi-K channel.* Am J Physiol Renal Physiol, 2001. **280**(5): p. F786-93.
305. Bailey, M.A., et al., *Maxi-K channels contribute to urinary potassium excretion in the ROMK-deficient mouse model of Type II Bartter's syndrome and in adaptation to a high-K diet.* Kidney Int, 2006. **70**(1): p. 51-9.
306. Nilwarangkur, S., et al., *Endemic primary distal renal tubular acidosis in Thailand.* Q J Med, 1990. **74**(275): p. 289-301.
307. Nimmannit, S., et al., *Pathogenesis of sudden unexplained nocturnal death (lai tai) and endemic distal renal tubular acidosis.* Lancet, 1991. **338**(8772): p. 930-2.
308. Nademanee, K., et al., *Arrhythmogenic marker for the sudden unexplained death syndrome in Thai men.* Circulation, 1997. **96**(8): p. 2595-600.
309. Phakdeekitcharoen, B., C. Ruangraksa, and P. Radinahamed, *Hypokalaemia and paralysis in the Thai population.* Nephrol Dial Transplant, 2004. **19**(8): p. 2013-8.

310. Tosukhowong, P., et al., *Hypokalemia, high erythrocyte Na+ and low erythrocyte Na,K-ATPase in relatives of patients dying from sudden unexplained death syndrome in north-east Thailand and in survivors from near-fatal attacks.* Am J Nephrol, 1996. **16**(5): p. 369-74.
311. Walsh, S.B., et al., *Cation transport activity of anion exchanger 1 (AE1) mutations found in inherited distal renal tubular acidosis (dRTA): structure-function implications for AE1.* Am J Physiol Renal Physiol, 2008.
312. Zhu, Q., D.W. Lee, and J.R. Casey, *Novel topology in C-terminal region of the human plasma membrane anion exchanger, AE1.* J Biol Chem, 2003. **278**(5): p. 3112-20.
313. Kawano, Y., et al., *Localization of the pyridoxal phosphate binding site at the COOH-terminal region of erythrocyte band 3 protein.* J Biol Chem, 1988. **263**(17): p. 8232-8.
314. Ramakrishnan, V. and D.D. Busath, *An inverting basket model for AE1 transport.* J Theor Biol, 2002. **215**(2): p. 215-26.
315. Wrong, O., et al., *Band 3 mutations, distal renal tubular acidosis, and Southeast Asian ovalocytosis.* Kidney Int, 2002. **62**(1): p. 10-9.
316. Viljoen, A., A.G. Norden, and F.E. Karet, *Replacing the short ammonium chloride test.* Kidney Int, 2007. **72**(9): p. 1163; author reply 1164.
317. Romero, M.F., et al., *Cloning and characterization of a Na+-driven anion exchanger (NDAE1). A new bicarbonate transporter.* J Biol Chem, 2000. **275**(32): p. 24552-9.
318. Virkki, L.V., et al., *Cloning of a Na+-driven Cl/HCO3 exchanger from squid giant fiber lobe.* Am J Physiol Cell Physiol, 2003. **285**(4): p. C771-80.
319. Zhao, R. and R.A. Reithmeier, *Expression and characterization of the anion transporter homologue YNL275w in Saccharomyces cerevisiae.* Am J Physiol Cell Physiol, 2001. **281**(1): p. C33-45.
320. Frommer, W.B. and N. von Wiren, *Plant biology: Ping-pong with boron.* Nature, 2002. **420**(6913): p. 282-3.
321. Takano, J., et al., *Arabidopsis boron transporter for xylem loading.* Nature, 2002. **420**(6913): p. 337-40.

322. Guizouarn, H., R. Christen, and F. Borgese, *Phylogeny of anion exchangers: could trout AE1 conductive properties be shared by other members of the gene family?* Biochim Biophys Acta, 2005. **1726**(3): p. 244-50.
323. Musch, M.W., et al., *Hypotonic-stimulated taurine efflux in skate erythrocytes: regulation by tyrosine phosphatase activity.* Am J Physiol, 1998. **274**(6 Pt 2): p. R1677-86.
324. Romano, L. and H. Passow, *Characterization of anion transport system in trout red blood cell.* Am J Physiol, 1984. **246**(3 Pt 1): p. C330-8.
325. Kirk, K., *Membrane transport in the malaria-infected erythrocyte.* Physiol Rev, 2001. **81**(2): p. 495-537.
326. Joiner, C.H., *Deoxygenation-induced cation fluxes in sickle cells: II. Inhibition by stilbene disulfonates.* Blood, 1990. **76**(1): p. 212-20.
327. Jones, G.S. and P.A. Knauf, *Mechanism of the increase in cation permeability of human erythrocytes in low-chloride media. Involvement of the anion transport protein capnophorin.* J Gen Physiol, 1985. **86**(5): p. 721-38.
328. Johnson, R.M. and K. Tang, *DIDS inhibition of deformation-induced cation flux in human erythrocytes.* Biochim Biophys Acta, 1993. **1148**(1): p. 7-14.
329. Snow, R.W., et al., *The global distribution of clinical episodes of Plasmodium falciparum malaria.* Nature, 2005. **434**(7030): p. 214-7.
330. Lederberg, J., *J. B. S. Haldane (1949) on infectious disease and evolution.* Genetics, 1999. **153**(1): p. 1-3.
331. Ackerman, H., et al., *A comparison of case-control and family-based association methods: the example of sickle-cell and malaria.* Ann Hum Genet, 2005. **69**(Pt 5): p. 559-65.
332. Hill, A.V., et al., *Common west African HLA antigens are associated with protection from severe malaria.* Nature, 1991. **352**(6336): p. 595-600.
333. Agarwal, A., et al., *Hemoglobin C associated with protection from severe malaria in the Dogon of Mali, a West African population with a low prevalence of hemoglobin S.* Blood, 2000. **96**(7): p. 2358-63.

334. Modiano, D., et al., *Haemoglobin C protects against clinical Plasmodium falciparum malaria.* Nature, 2001. **414**(6861): p. 305-8.
335. Chotivanich, K., et al., *Hemoglobin E: a balanced polymorphism protective against high parasitemias and thus severe P falciparum malaria.* Blood, 2002. **100**(4): p. 1172-6.
336. Ohashi, J., et al., *Extended linkage disequilibrium surrounding the hemoglobin E variant due to malarial selection.* Am J Hum Genet, 2004. **74**(6): p. 1198-208.
337. Flint, J., et al., *High frequencies of alpha-thalassaemia are the result of natural selection by malaria.* Nature, 1986. **321**(6072): p. 744-50.
338. Williams, T.N., et al., *High incidence of malaria in alpha-thalassaemic children.* Nature, 1996. **383**(6600): p. 522-5.
339. Bienzle, U., et al., *Glucose-6-phosphate dehydrogenase and malaria. Greater resistance of females heterozygous for enzyme deficiency and of males with non-deficient variant.* Lancet, 1972. **1**(7742): p. 107-10.
340. Ganczakowski, M., et al., *Multiple glucose 6-phosphate dehydrogenase-deficient variants correlate with malaria endemicity in the Vanuatu archipelago (southwestern Pacific).* Am J Hum Genet, 1995. **56**(1): p. 294-301.
341. Ruwende, C. and A. Hill, *Glucose-6-phosphate dehydrogenase deficiency and malaria.* J Mol Med, 1998. **76**(8): p. 581-8.
342. Sabeti, P.C., et al., *Detecting recent positive selection in the human genome from haplotype structure.* Nature, 2002. **419**(6909): p. 832-7.
343. Tishkoff, S.A., et al., *Haplotype diversity and linkage disequilibrium at human G6PD: recent origin of alleles that confer malarial resistance.* Science, 2001. **293**(5529): p. 455-62.
344. Chitnis, C.E. and L.H. Miller, *Identification of the erythrocyte binding domains of Plasmodium vivax and Plasmodium knowlesi proteins involved in erythrocyte invasion.* J Exp Med, 1994. **180**(2): p. 497-506.
345. Hamblin, M.T. and A. Di Rienzo, *Detection of the signature of natural selection in humans: evidence from the Duffy blood group locus.* Am J Hum Genet, 2000. **66**(5): p. 1669-79.

346. Miller, L.H., et al., *The resistance factor to Plasmodium vivax in blacks. The Duffy-blood-group genotype, FyFy.* N Engl J Med, 1976. **295**(6): p. 302-4.
347. Thimasarn, K., et al., *Epidemiology of Malaria in Thailand.* J Travel Med, 1995. **2**(2): p. 59-65.
348. Flatz, G., C. Pik, and S. Sringam, *Haemoglobin E and beta-thalassaemia: their distribution in Thailand.* Ann Hum Genet, 1965. **29**(2): p. 151-70.
349. Hutagalung, R., et al., *Influence of hemoglobin E trait on the severity of Falciparum malaria.* J Infect Dis, 1999. **179**(1): p. 283-6.
350. Fucharoen, S. and P. Winichagoon, *Hemoglobinopathies in Southeast Asia: molecular biology and clinical medicine.* Hemoglobin, 1997. **21**(4): p. 299-319.
351. Siniscalco, M.B., L; Latte, B; Motulski, AG, *Favism and thalassaemia in Sardinia and their relationship to malaria.* Nature, 1961(190): p. 1179.
352. Hill, A.V., et al., *Beta thalassemia in Melanesia: association with malaria and characterization of a common variant (IVS-1 nt 5 G----C).* Blood, 1988. **72**(1): p. 9-14.
353. Mockenhaupt, F.P., et al., *Alpha(+)-thalassemia protects African children from severe malaria.* Blood, 2004. **104**(7): p. 2003-6.
354. Willcox, M., A. Bjorkman, and J. Brohult, *Falciparum malaria and beta-thalassaemia trait in northern Liberia.* Ann Trop Med Parasitol, 1983. **77**(4): p. 335-47.
355. Serjeantson, S., et al., *Malaria and hereditary ovalocytosis.* Hum Genet, 1977. **37**(2): p. 161-7.
356. Jarolim, P., et al., *Deletion in erythrocyte band 3 gene in malaria-resistant Southeast Asian ovalocytosis.* Proc Natl Acad Sci U S A, 1991. **88**(24): p. 11022-6.
357. Cividalli, G., H. Locker, and A. Russell, *Increased permeability of erythrocyte membrane in thalassemia.* Blood, 1971. **37**(6): p. 716-24.
358. Wiley, J.S., *Increased erythrocyte cation permeability in thalassemia and conditions of marrow stress.* J Clin Invest, 1981. **67**(4): p. 917-22.

359. Yataganas, X. and P. Fessas, *The pattern of hemoglobin precipitation in thalassemia and its significance.* Ann N Y Acad Sci, 1969. **165**(1): p. 270-87.
360. Rachmilewitz, E.A., *Formation of hemichromes from oxidized hemoglobin subunits.* Ann N Y Acad Sci, 1969. **165**(1): p. 171-84.
361. Joiner, C.H., O.S. Platt, and S.E.t. Lux, *Cation depletion by the sodium pump in red cells with pathologic cation leaks. Sickle cells and xerocytes.* J Clin Invest, 1986. **78**(6): p. 1487-96.
362. Staines, H.M., J.C. Ellory, and K. Kirk, *Perturbation of the pump-leak balance for Na(+) and K(+) in malaria-infected erythrocytes.* Am J Physiol Cell Physiol, 2001. **280**(6): p. C1576-87.
363. Glushakova, S., et al., *Membrane transformation during malaria parasite release from human red blood cells.* Curr Biol, 2005. **15**(18): p. 1645-50.
364. Salmon, B.L., A. Oksman, and D.E. Goldberg, *Malaria parasite exit from the host erythrocyte: a two-step process requiring extraerythrocytic proteolysis.* Proc Natl Acad Sci U S A, 2001. **98**(1): p. 271-6.
365. Lew, V.L., T. Tiffert, and H. Ginsburg, *Excess hemoglobin digestion and the osmotic stability of Plasmodium falciparum-infected red blood cells.* Blood, 2003. **101**(10): p. 4189-94.
366. Jones, M.L., E.L. Kitson, and J.C. Rayner, *Plasmodium falciparum erythrocyte invasion: a conserved myosin associated complex.* Mol Biochem Parasitol, 2006. **147**(1): p. 74-84.
367. Trager, W. and J.B. Jensen, *Human malaria parasites in continuous culture.* Science, 1976. **193**(4254): p. 673-5.
368. Huber, S.M., N. Gamper, and F. Lang, *Chloride conductance and volume-regulatory nonselective cation conductance in human red blood cell ghosts.* Pflugers Arch, 2001. **441**(4): p. 551-8.
369. Duranton, C., S.M. Huber, and F. Lang, *Oxidation induces a Cl(-)-dependent cation conductance in human red blood cells.* J Physiol, 2002. **539**(Pt 3): p. 847-55.

370. Zhou, Q., et al., *Normal hemostasis but defective hematopoietic response to growth factors in mice deficient in phospholipid scramblase 1.* Blood, 2002. **99**(11): p. 4030-8.
371. Lang, K.S., et al., *Cation channels trigger apoptotic death of erythrocytes.* Cell Death Differ, 2003. **10**(2): p. 249-56.
372. Lang, P.A., et al., *Blunted apoptosis of erythrocytes from taurine transporter deficient mice.* Cell Physiol Biochem, 2003. **13**(6): p. 337-46.
373. Brand, V.B., et al., *Dependence of Plasmodium falciparum in vitro growth on the cation permeability of the human host erythrocyte.* Cell Physiol Biochem, 2003. **13**(6): p. 347-56.
374. Lang, K.S., et al., *Mechanisms of suicidal erythrocyte death.* Cell Physiol Biochem, 2005. **15**(5): p. 195-202.
375. Kirk, K., et al., *Transport of diverse substrates into malaria-infected erythrocytes via a pathway showing functional characteristics of a chloride channel.* J Biol Chem, 1994. **269**(5): p. 3339-47.
376. Birka, C., et al., *Enhanced susceptibility to erythrocyte "apoptosis" following phosphate depletion.* Pflugers Arch, 2004. **448**(5): p. 471-7.
377. Ginsburg, H., et al., *Effects of red blood cell potassium and hypertonicity on the growth of Plasmodium falciparum in culture.* Z Parasitenkd, 1986. **72**(2): p. 185-99.
378. Lee, P., et al., *X-ray microanalysis of Plasmodium falciparum and infected red blood cells: effects of qinghaosu and chloroquine on potassium, sodium, and phosphorus composition.* Am J Trop Med Hyg, 1988. **39**(2): p. 157-65.
379. Friedman, M.J., *Erythrocytic mechanism of sickle cell resistance to malaria.* Proc Natl Acad Sci U S A, 1978. **75**(4): p. 1994-7.
380. Efron, L., et al., *Direct interaction of dermaseptin S4 aminoheptanoyl derivative with intraerythrocytic malaria parasite leading to increased specific antiparasitic activity in culture.* J Biol Chem, 2002. **277**(27): p. 24067-72.
381. Garnham, P.C.C., *Malaria parasites and other Haemosporidia*. 1966, Oxford: Blackwell Scientific Publications. xviii, 1114p.

382. Guitian, F.J., A.T. Camacho, and S.R. Telford, 3rd, *Case-control study of canine infection by a newly recognised Babesia microti-like piroplasm.* Prev Vet Med, 2003. **61**(2): p. 137-45.
383. Alkhalil, A., D.A. Hill, and S.A. Desai, *Babesia and plasmodia increase host erythrocyte permeability through distinct mechanisms.* Cell Microbiol, 2007. **9**(4): p. 851-60.
384. Ellory, J.C., et al., *Abnormal permeability pathways in human red blood cells.* Blood Cells Mol Dis, 2007. **39**(1): p. 1-6.